

Wearable Haptic Interfaces for Telerobotics

Présentée le 28 octobre 2021

Faculté des sciences et techniques de l'ingénieur
Laboratoire de systèmes intelligents
Programme doctoral en robotique, contrôle et systèmes intelligents

pour l'obtention du grade de Docteur ès Sciences

par

Vivek RAMACHANDRAN

Acceptée sur proposition du jury

Prof. D. Kyritsis, président du jury
Prof. D. Floreano, directeur de thèse
Prof. L. Marchal-Crespo, rapporteuse
Prof. J. Rossiter, rapporteur
Prof. A. Ijspeert, rapporteur

If you are free, you need to free somebody else.
If you have some power, then your job is to empower somebody else.
— Toni Morrison

To my parents and my sister ...

Acknowledgements

“Yet another moment to pause, to look back, and to recapitulate.”

This is how the Acknowledgements section begins in my father’s PhD thesis that he defended in 1986. It so poignantly captures how I have been feeling these past few months as I recall and relive several memories with family, friends, and colleagues. All of these memories when woven together form an exquisite tapestry five-years in the making that is my PhD. My friends have heard me say that, “I am an amalgam of the people that I have rubbed shoulders with” and so, this thesis is a testament to those people, who have made an unmistakable, permanent impression on my life.

I would like to begin by paying tribute to my parents, Usha and Kavil Ramachandran, whose past 30 years have been dedicated to ensuring that my sister, Radhika, and I have had the best possible quality of life that they could afford to give us at any given time. Growing up in academic spaces is a rare privilege and to have had the opportunity to do that on two entirely different campuses is a rarer one. Acha, you will always be my benchmark when it comes to standing up for one’s own principles and Amma, you are the one who taught me how being vulnerable makes one courageous, not weak. Rad, I could not have asked for a more fiercer, caring, and loving sister, who has watched over me over tribulation after tribulation. My parents and my sister were the first people to imbue in me the values of honesty, care, and empathy. These are the values that I centre even today, and in moments of confusion, they have been my guiding light. No amount of words will do justice to the impact that they have had on my life. Their voices provided me with incomparable relief during the most trying periods of my PhD. To Achan, Amma, Rad, I owe you everything.

My extended family - my parents’ siblings and my cousins have nourished me with so much affection and they have taught me so much from their life experiences. In particular, my uncle, Suku Vasudevan was pivotal in fostering my interest in the sciences and encouraging me to question the world critically.

Dearest friends from school - Shoumik, Aishwarya, Ashwini, Sanjana, Pranav, and Darshani have been a perennial force of nature. The rock-solid support that you have given me during my lifetime and especially, during the PhD has been unconditional and I count my blessings for being part of such a loving group of people.

My undergrad was a gruelling process - I learnt many life lessons, but it was arduous. However, there were a few gems, like Mithika, Safvan, and Amrutha who shone so bright that their sparkle mesmerized me and my lasting-friendships with them were crucial for the last five years.

I am being rhetorical and also genuine when I ask: How can I begin to thank what my master's advisor, Prof. Carmel Majidi has done for me? The experience of having him as a mentor and fraternal figure has shaped the way I approach research even today. During my first years in Lausanne, he was always a reference point for me when I was in a quandary about work. The opportunity to work in his Soft Machines Lab (SML) was so immensely positive. The people I became friends with in SML, especially James and Steven, have continued to be an important part of my life and our friendships forged over hours-long conversations across time zones.

I built so many beautiful relationships at Carnegie Mellon University! It was truly one of the happiest periods of my life! While I am no longer in touch with many of the wonderful people from that period, I still cherish the memories I have of them. Yet, there are a few people, including Evan, Rachel, and Deepa, whose regular correspondence served as a tether to that joyful period and in many ways, helped me during the early months of my time in Lausanne, when I had difficulties creating a life for myself in this new place, where the language was unfamiliar to me. I am especially grateful to Ruta, who taught me the importance of building a support structure wherever I went. She is truly my kindred spirit - without her presence, this PhD would not be what it is.

Now comes the hard part - my time in Lausanne. In all honesty, writing this section is probably harder than any other section of the thesis, but the part about the people in Lausanne - I feel overwhelmed. Each person that I have met here has in some way or the other played a crucial part in contributing to my life as a PhD student.

Foremost, I would like to thank my thesis director, Prof. Dario Floreano. Thank you so much for the opportunity to become part of your Laboratory of Intelligent Systems's (LIS) family. Under your tutelage, I have learned to be a critical researcher, to question the foundational aspects of any scientific problem and to relentlessly approach

Acknowledgements

challenges with a mindset to derive solutions. I am most grateful though for having learned how to distill my thoughts and communicate them as clearly and succinctly as possible. This is a lifelong gift that you have given me and I am extremely grateful for it.

I would like to thank my thesis committee members, Prof. Dimitrios Kyristis, Prof. Laura Marchal-Crespo, Prof. Auke Jan Ijspeert, and Prof. Jonathan Rossiter. Each of them have been inspirational to me, not only in terms of their research, which has undoubtedly shaped my work, but also their values and principles that dictate their actions that reach beyond the confines of academia. Having them preside over my thesis defense was a profound honour.

I would like to thank Michelle Wälti, our lab's administrative assistant, one of the "chief engineers" responsible for the lab functioning as a well-oiled machine. I am deeply indebted to Michelle for being a bulwark of strength at multiple times during my PhD and giving me reassurance when I needed it the most.

Corinne Lebet, the administrative assistant of my doctoral program EDRS, and personally, my confidant in the doctoral school. When I was a student representative, Corinne's presence in EDRS gave me relief - a word that tends to not get its due in terms of how significant it is. Only Corinne knows the numerous times that I have delighted in joy and vented in frustration during my time as a representative and afterwards too. I will say this much - SoScience Day would not have been a reality without her.

Just as Corinne's presence was a relief for me in EDRS, so was Sandra Roux in the doctoral school EDOC. Certainly, Sandra is fantastic at what she does, but personally, she has been a trustworthy friend and her emotional understanding of what was happening during my PhD is not something that I take for granted.

The research I carried out during my PhD would have been several times harder had I not received the timely advice from post-docs both in my lab and outside. Foremost amongst them are Prof. Jun Shintake, Prof. Amy Wu, Dr Ronan Hinchet, Dr. Alice Tonazzini, Prof. Stefano Mintchev, and Dr. Julien Lecoœur, who helped me conceptualize multiple projects and bring them to fruition by assuaging my fears and giving me guidance throughout their time at EPFL and afterwards as well.

To Carine, one of the first, true friends I made in Lausanne, I have learnt so much from you. You showed me, a naive first-year PhD, the ropes when I first got to LIS and over the years, we developed a strong friendship, one that I take pride in each day. This

friendship is meant to last and we both know it!

Dear Olex, my PhD literally would not have been complete without your presence in the lab. Thank you for being patient with me and filtering through my muddled thoughts to give me concrete support for each of my projects.

My PhD siblings - Fabian, Enrico, Valentin, Roeltje, Enrica, Davide, and Alex. You have seen me through the best and the worst times of my PhD. What I love the most about you is how you always check in on me without prompting, giving reassurance time and again that you are there for me and that you will always be there for me. Through you, I made your friends/partners, Carine, Sophie, Joanna, Eva, and Sophie as some of my closest friends. In all sincerity, you are the primary reason why I was able to survive last year's lockdown. I fondly remember the numerous discussions (some serious, but mostly hilarious and silly) we have had on our hikes, game nights, late-nights at the lab, and chilling by the "toilet seat" and by the lake. Yet, these words do not do justice to the depth of our relationship and possibly, they never will. But that does not matter though, does it? I love you all so so so very much! :)

There are many many many more LIS family members that I have not mentioned by name who are close to my heart. I have an immense amount of love for you and my hope is that we will always cross paths during our lifetimes.

I have scores and scores of friends from many of the labs at EPFL, but especially at BIOROB, RRL, and FLEXLAB. I would like to pay tribute to some people in particular who played such a key role in my personal growth. Laura and Kamilo, thank you for making me feel welcome in your life, for every Friday night we spent at Chez Xu, for our road trip in Colombia, for the multiple weekends we spent together at yours putting together a doll house (!) and for so many many more memories that I have shared with you. Robin, our relationship has blossomed over these past few years and the long chats we have had have profoundly affected me. I eagerly await your return to Switzerland every year to pick up where we left off! Chiara, you are an incredible person and I keep wondering how lucky I am to have met you. Our friendship gave me the comfort and space that I needed to explore and introspect aspects of my identity that I have become more in touch with. Ece, you are one of the coolest people I know who was always ready to meet and delve into topics about life with such a unique perspective provided we had a cup of tea in hand! Frederike, ever since we met, I feel like we are PhD mates from the start to end, maybe it has a little to do with the fact that we both started and are ending the PhD at the same time! You are a kind, caring, and insightful friend and I enjoy your company so much! Matt, thank you

Acknowledgements

for being a part of my PhD life - our conversations about academia, research, life as an immigrant, and your resolve to be a better version of yourself are ingrained in mind.

My tenure as a PhD student representative was one of the most invigorating experiences at EPFL. Being able to highlight the grievances of PhD colleagues and formulate solutions to them with a cohort of the most inspiring people was so liberating. Thank you to all of you, but in particular to Arnaud, Margaux, Leo, Kaitlin, and Gabriel.

To my friend and mentor, Siara, to say that it was fortuitous that we met feels insufficient. You have had a transformative impact on my life and I say that without any hesitation. Working with you on *Make It Awkward* saved me multiple times. Since we met, you have been my constant cheerleader and I do not know how best to express my gratitude. It made me so happy that both of us defended our PhDs days apart! This piece of text is merely the beginning of a lengthy novel that I could write about how much your affection and support has bolstered me.

To the wonderful team members of the Hackahealth association, being a part of your family allowed me to grow as a leader and a team player simultaneously. The core values of Hackahealth and the labour that our association invests in all our activities have uplifted me on days when my motivation was faltering. A special thank you to dear Iselin, whom I became extremely close to through Hackahealth. You who have been a true friend, who has stood with me through thick and thin and your presence in my life has left an indelible impression. You inspire me every single day!

My “Pittsburgh-Lausanne” friends, Mike and Yomei (and your beautiful bird, Tesla), we became friends through such a fun coincidence. Our tango classes, numerous Sunday discussions over chai, and multiple jam sessions are dear to my heart. Your absence in Lausanne left a large void that I have been struggling to fill. Our friendship will outlast borders :)

Lna and Ibrahim, my cuties! Thank you for being such patient and loving people. Our many dinners, concerts, Lavaux hikes, and general shenanigans make me tear up in joy. While it breaks my heart to know that you two will be moving from Switzerland soon, I take comfort in the fact that we will always be in touch with each other. Vulcan salute to you two ;)

Helena, my fastest friend! I think one of the reasons that we became such close friends was because of how alike we are (in the good and not-so-good ways ;) However, the reason that our friendship has continued to grow is because of our natural rapport,

our shared principles, and our desire to do more for the people around us.

Rhythmima, you are one of the last people I met on my PhD journey. These past few months that I have spent with you might have breezed by quickly, but they did so with such a whirlwind of exquisite fragrances. I cherish you deeply.

This section has been very emotionally difficult for me to write as I have tried to treat it as a tribute to the people who made this PhD possible. I might have failed, but I knew that this was likely to happen. Yet, I am not unhappy. Actually, I am elated because at the end of this section I realize that the people that I am grateful towards already know this and that I will always be grateful to them.

Lausanne, 30 Juillet 2021

Vivek Ramachandran

Abstract

Telerobotics is the process by which human operators control the movement of robots to achieve specific tasks. However, conventional control interfaces, such as joysticks and remote controllers, are not intuitive to use for novice users. Training to use these interfaces requires a considerable amount of training. Wearable control interfaces are more inclusive because they allow humans to control the movement of robots with their own body movements through intuitive gestures without the need for excessive training. Haptic devices integrated in these interfaces can help users learn to teleoperate robots by applying forces to the parts of the body where corrective action is needed. Typically, these devices require the use of bulky actuators that can hinder natural user mobility and induce fatigue over prolonged usage. This thesis presents a framework in which users can successfully learn to teleoperate robots using fabric-based wearable haptic interfaces composed of electroadhesive clutches and free of actuators.

Key words: Wearable robotics, Haptics, Electroadhesion

Résumé

La télérobotique est le processus par lequel les opérateurs humains contrôlent le mouvement des robots pour réaliser des tâches spécifiques. Cependant, les interfaces de commande classiques, telles que les joysticks et les télécommandes, ne sont pas intuitives pour les utilisateurs novices. L'apprentissage de l'utilisation de ces interfaces nécessite une formation considérable. Les interfaces de commande portables sont plus inclusives car elles permettent aux humains de contrôler le mouvement des robots avec les mouvements de leur propre corps par des gestes intuitifs sans avoir besoin d'une formation excessive. Les dispositifs haptiques intégrés à ces interfaces peuvent aider les utilisateurs à apprendre à téléopérer les robots en appliquant des forces sur les parties du corps où une action corrective est nécessaire. En général, ces dispositifs nécessitent l'utilisation d'actionneurs encombrants qui peuvent entraver la mobilité naturelle de l'utilisateur et induire de la fatigue lors d'une utilisation prolongée. Cette thèse présente un cadre dans lequel les utilisateurs peuvent apprendre avec succès à téléopérer des robots en utilisant des interfaces haptiques portables basées sur le tissu, composées d'embrayages électro-adhésifs et exemptes d'actionneurs.

Mots clefs : Robotique portable, Haptique, Electroadhésion

Contents

Acknowledgements	i
Abstract (English/Français/Deutsch)	vii
List of figures	xv
List of tables	xvii
1 Introduction	1
1.1 Designing wearable interfaces for telerobotics	2
1.1.1 Morphological considerations	2
1.1.2 Physiological considerations	4
1.1.3 Cognitive considerations	4
1.2 From Robots to Humans: Sensory Feedback	5
1.2.1 Visual Feedback	5
1.2.2 Auditory Feedback	6
1.2.3 Haptic Feedback	7
1.3 Thesis Outline	12
2 The design and development of an all-fabric haptic device	17
2.1 Introduction	17
2.2 Methods	19
2.2.1 Structure, working principle, and fabrication	19
2.2.2 Electromechanical characterisation	24
2.3 Results	27
2.3.1 Holding force characteristics	27
2.3.2 Charging and discharging characteristics	29
2.3.3 Preliminary demonstration of haptic device	30
2.4 Conclusions	31

3	A fabric-based elbow haptic sleeve for motor training	35
3.1	Introduction	35
3.2	Methods	38
3.2.1	Design of the electroadhesive haptic sleeve	38
3.2.2	Motor learning to teleoperate a drone	45
3.2.3	Simulation framework for drone teleoperation	48
3.2.4	Human subject study	49
3.2.5	Statistics	50
3.3	Results	50
3.3.1	Acquisition and retention of motor skills	50
3.3.2	Transfer of motor skills	52
3.3.3	Subjective assessment of drone teleoperation and sleeve comfort	55
3.4	Conclusion	56
4	Multi-joint wearable haptic sleeve for telerobotics with reduced visual feed-back	59
4.1	Introduction	59
4.2	Methods	62
4.2.1	Wearable haptic sleeve	63
4.2.2	Simulation environment	65
4.2.3	Human subject study	66
4.3	Results	67
4.3.1	Performance analysis of obstacle avoidance	68
4.3.2	Questionnaire responses	69
4.4	Conclusions	71
5	Conclusions	77
5.1	Future research avenues	80
5.2	Final thoughts	83
A	Clutch holding force derivation	85
B	Capacitor charging and discharging	87
C	Mechanics of the clutched-spring	91
D	Fabrication method for multi-layered all-fabric clutch	95
E	Tensile test characteristics of fabric clutches	97

CONTENTS

Bibliography	115
Curriculum Vitae	117

List of Figures

1.1	Robotics in everyday life requires human involvement.	3
2.1	Structure and working principle of the fabric clutch.	20
2.2	Fabrication of the fabric clutch	21
2.3	Maximum clutch holding force capacity as a response to an applied voltage	28
2.4	Demonstration of haptic device with single clutch pair	31
3.1	Wearable haptic system to train users for motor activities	40
3.2	Cross-sectional view of one electroadhesive clutch.	41
3.3	Forearm and upper arm attachments straps.	42
3.4	Different views of the foam-padded fabric elbow joint attachment. . .	43
3.5	Experimental pipeline for motor learning	47
3.6	Results from the motor learning human subject study for path following and waypoint navigation.	53
3.7	Subject responses to questionnaires filled after experimental phases. .	54
4.1	Experimental setup of the elbow and wrist haptic sleeve.	61
4.2	Performance analysis of drone wall collisions for left and right walls. .	63
4.3	Variance in drone position relative to the walls over the experimental phases.	73
4.4	Questionnaire responses pertaining to drone teleoperation and user comfort.	74
4.5	Subject responses to NASA-TLX workload questionnaire.	75
5.1	Experimental setup of the hand, wrist, and elbow haptic sleeve.	84
A.1	Generation of Maxwell stress in capacitors.	86
B.1	Capacitor charging and discharging using a customized H-bridge. . . .	88
B.2	Clutch plate discharge characteristics.	89

LIST OF FIGURES

C.1 Kinematics of the haptic device.	92
D.1 Fabrication process to develop the haptic device with two clutch pairs.	96
E.1 Holding force measurements for a pair of clutch plates.	98



List of Tables

3.1 Comparison of existing textile-based haptic devices and the one presented in this study.	37
--	----

1 Introduction

Robots are becoming a quotidian presence in our surroundings, both domestic and non-domestic [146]. They can help humans perform tasks that may be otherwise difficult for humans to perform due to a variety of physical limitations. Indeed, robots are used to inspect industrial zones, such as nuclear power plants and chemical factories that may be potentially hazardous for humans [41, 109]. They are used for Search-and-Rescue operations to help first responders look for and aid survivors. They are also used for both construction and maintenance of large infrastructure projects, such as buildings, bridges, and pipelines [19, 154]. Robots have enabled automated assembly lines across a number of manufacturing industries, thereby reducing the number of industrial casualties [62]. Their application in terrains that are physically difficult for humans to access, such as in space and underwater, have accelerated exploratory scientific research in these respective domains [32, 74, 45]. Robots are useful for tasks that require high precision manipulation, such as cell growth, drug delivery, and minimally invasive surgery [23, 9, 43]. In the fields of healthcare and rehabilitation, robots can provide a better quality of life to people with disabilities by reducing some of the challenges they face in performing activities of daily living [26]. The ubiquity of robotics in these different fields of application are illustrated in Figure 1.1.

While robot autonomy is a burgeoning area of research, presently, human operators are still needed to control distally - located robots for most tasks [47]. This form of robot control is called robotic teleoperation or telerobotics [112]. The successful completion of a telerobotic task is incumbent upon the operator's level of expertise in

controlling the robot. This includes the operator's proficiency with using control interfaces, such as joysticks to communicate with the robot. Professional teleoperators, who are able to control robots effectively using these conventional controllers, require a considerable amount of training to use them [19, 21]. However, these interfaces are not intuitive for novice users. Indeed, the complexity of learning to use conventional control interfaces can be very mentally demanding. Furthermore, these interfaces do not directly provide much feedback about the robot's state to the operator. The lack of feedback from the interfaces can cause operators to hesitate, commit errors, and detrimentally affect their performance [109, 50]. The growing popularity of robotics amongst non-professional teleoperators mandates more intuitive interfaces [18]. New types of control interfaces will not only broaden the scope of teleoperation to a larger population, but also increase the application of robots to a wider variety of domains. In recent years, researchers have developed wearable interfaces that map natural human body movements to robot movements with the specific intent of making them more intuitive and natural for users to use. These interfaces are designed by prioritising both functionality and comfort [14]. The following section describes the most important considerations that developers must account for when designing wearable interfaces.

1.1 Designing wearable interfaces for telerobotics

1.1.1 Morphological considerations

Human body morphology varies considerably from person to person. Thus, designing a “one-size-fits-all” wearable interface can be challenging. To mitigate this challenge, these interfaces can be broken down into multiple modular components. The size and location of these components on the human body can then be determined using anthropometric data sets pertaining to mass and length proportions that are available in the literature. However, a majority of these data sets are based on measurements of people who are considered normatively able-bodied, more often of men. To account for these shortcomings, researchers should make independent anthropometric measurements with a more diverse population.

Introduction



Figure 1.1 – Robotics in everyday life requires human involvement. (A) Underwater applications [74] (B) Minimally invasive surgery [43] (C) Space exploration [45] (D) Infrastructure maintenance and inspection [154] (E) Wearables for rehabilitation [26]

1.1.2 Physiological considerations

User comfort is paramount, especially if users are expected to use the interface over a prolonged period of time. Human physiology serves as a guide in informing design choices that reduce user discomfort. This includes the knowledge of human anatomical pressure sensitivity [153] to locate proper anchoring points for the interface components and skin strain field mapping [64] to prevent slippage between the interface and the skin.

It is imperative to ensure that the components of the wearable interface are not bulky and are not unintentionally obtrusive to natural human mobility. There are a number of wearable telerobotic interfaces that are both bulky and hinder human movement and yet, they are functionally effective [171, 135, 76]. However, these types of wearable interfaces can cause users a considerable amount of discomfort over time by inducing fatigue over prolonged usage and are even potentially injurious to naive users [126]. To address this concern, researchers have been developing soft exoskeletons using compliant materials that match the inherent flexibility of human bodies [65, 80, 160, 125, 3].

In addition to size and weight considerations for portability, these interfaces should be breathable. Wearables that use textiles to directly interface with the human body are considerably better than hard plastics and soft rubbers in this regard. However, researchers should be conscious about choosing fabrics that do not cause skin rashes or dye-induced allergic reactions.

1.1.3 Cognitive considerations

Another important design consideration is cognitive workload. During teleoperation, users need information about the robot's state and its interaction with the environment. If this information is not provided coherently, this can make the task strenuous for the user to perform. Wearable interfaces can facilitate bidirectional communication i.e., the interface maps body movements to robot commands and, relays information from the robot to the teleoperator via sensory feedback, namely visual, auditory, and haptic feedback. This information is relayed through a combination of

sensory feedback channels as opposed to concentrating it through one channel alone to prevent cognitive overload. Distributing the information over multiple channels also facilitates an immersive experience for users.

1.2 From Robots to Humans: Sensory Feedback

All telerobotic tasks require users to expend some combination of motor and cognitive effort. To perform these tasks well, users require information about the state of the robot and its interaction with the environment. This information can be communicated through different modes of sensory feedback, such as vision (eyes), audition (ears), and haptics. Haptic feedback can be subdivided into two branches - tactile/cutaneous feedback (skin) and kinesthetic/proprioceptive feedback (joints, muscles, and connective tissues) [49]. In the context of wearable telerobotics, sensory feedback serves two related purposes - improving task performance and increasing operator immersiveness.

1.2.1 Visual Feedback

In almost all cases of teleoperation, vision is the most important sensory modality used to gather information about a robot's position relative to its environment [103]. This information is vital for navigating through space and manipulating objects. It also helps operators to distinguish various visually identifiable features of objects, such as colour, shape, and size, particularly if those objects are not within immediate reach of the robot or already in contact with it. In situations where teleoperated robots interact physically with other humans in its vicinity, visual feedback may be essential in recognising gestures for communication.

There are three types of visual displays that are commonly used to render visual feedback: Desktop Displays, Projection Displays, and Head-Mounted Displays.

Typically, Desktop Displays are two-dimensional computer screens fixed in place, whereas Projection Displays are large screens, which may encircle the operator. Both Desktop Displays and Projection Displays can render three-dimensional images to the operator with varying fields of view. While these two types of displays can provide

stereoscopic vision and permit freedom of movement, they do not isolate operators from their real surroundings and hence, cannot completely immerse the operator in the robot's environment. Head-Mounted Displays or HMDs are portable displays that sit on a user's head and are commonly used as visual displays for virtual reality applications. HMDs are used because they are usually lightweight, compact, and provide stereoscopic vision in First-Person View. For teleoperation, HMDs can track the movement of the operator's head and couple that movement with that of the camera mounted on the robot. Additionally, HMDs can provide operators better immersion in the robot's environment by removing the operator's physical environment from their field of view [156, 148, 100, 22]. However, long-term usage of HMDs can result in health problems, including fatigue and double vision [145]. Additionally, temporal lag in relaying visual feedback from the robot to the operator can be disorienting and lead to loss of balance and motion sickness [72].

1.2.2 Auditory Feedback

Audition is an important sense used by humans, and compared to vision, it has several unique properties. Audition is omnidirectional i.e., when sound is emitted by a source, it propagates through the surrounding atmosphere, which can then be captured by a receiver in the vicinity of the source irrespective of their orientation, unlike vision where the receiver must be directly facing the source of visual information [63]. Moreover, audition is not dependent on illumination, allowing robots to carry on functioning despite poor lighting or visual occlusions [164, 46, 143]. In addition, audition is affected to a much smaller degree by the presence of obstacles, enabling navigation and obstacle avoidance by localizing the robot's position relative to other objects in its proximity [63, 163, 58]. Therefore, the auditory system can provide spatial clues about the robot's surroundings even in the absence of the vision system. Auditory feedback also serves as a warning mechanism by making operators aware of the presence of other objects or individuals within the robot's vicinity [169, 70, 58, 133]. Auditory feedback serves a critical role in enhancing the sense of realism and the feeling of immersion in the robot's environment [69, 10, 111, 57, 11, 73, 81].

Like visual displays, auditory displays can be categorized into two - fixed (or stationary) displays, such as loudspeakers, and head-mounted displays, such as head-

phones. Both types of displays can provide either the same information to both ears (monophonic) or different information (stereophonic), with the latter resembling the functionality of the human auditory system. While three-dimensional sound can be simulated more easily using loudspeakers, headphones can change the feedback by tracking the operator's head orientation, thereby isolating them from their real environments and enhancing the feeling of immersion in the robot's environment. Loudspeakers are better suited when used in conjunction with visual projection displays, where both the stationary displays are independent of the user's position. Compared to loudspeakers, headphones may cause discomfort over long-term use and are in general, more invasive. However, headphones are much better equipped at eliminating reverberation and background noise to help clearly identify the source of a sound [82, 82, 55, 24]. Headphones belong to the class of binaural audio rendering systems that can simulate the experience of the robot by spatialising the sound in the robot's vicinity [44]. Sound spatialization refers to a set of methods by which sound can be localized to a specific point in a space relative to the listener. For teleoperation, sound spatialization is vital to aid operators in robot navigation and obstacle avoidance by directing the robot-mounted cameras to face the source of sound [86, 89, 162].

While there are numerous advantages to using auditory feedback, there are some issues that continue to hamper its effectiveness. For instance, poor sound quality can be a detrimental factor on performance. To avert this problem, psycho-acoustic models of human aural perception can be used to test an auditory display's sensory pleasantness [182]. Latency in sound rendering can also be a major performance determining factor – quick feedback can enhance user engagement and subsequently, refine their control over the robot [180]. Another aspect to consider is the rendering of simultaneous sounds. Humans can perform selective listening, but attending to multiple sounds can result in increased stress and mental workload, and often, the amount of information that can be gathered from simultaneous sounds is limited [53].

1.2.3 Haptic Feedback

Although visual and auditory feedback can provide a lot of information about the robot's environment to help users navigate and avoid obstacles, only haptic feedback

can truly simulate the robot's physical interaction with its environment [116, 31]. Haptic feedback can encode a variety of information about the robot's interaction, including inertia and viscosity. Unlike visual and auditory feedback that have specific sensory receptors (eyes and ears, respectively), haptic feedback can be perceived as tactile or kinesthetic feedback at different parts of the body due to the ubiquity of haptic sensory receptors across the body. This is a crucial advantage for teleoperation because haptic feedback can be provided to the part of the body where corrective action is needed [8, 67]. Therefore, haptic feedback can be very powerful in aiding teleoperation performance, particularly for accuracy and timing tasks [101, 107, 54].

The sensory receptors in humans that perceive haptic stimuli are located in different parts of the body and have varying degrees of sensitivity [39, 56]. Kinesthetic sensory receptors are located in tendons and joints and perceive movements or tension in muscles, whereas tactile sensory receptors in the skin can sense temperature, pressure, and skin stretch. All haptic displays are designed to target specific kinesthetic or tactile receptors. For instance, in a telerobotic task involving object manipulation, a kinesthetic haptic display would render the grasping force of the manipulated object, whereas tactile haptic displays would render the object's texture [115, 157, 83, 2].

Haptic interfaces can be categorised into two types – Desktop Haptic interfaces and Wearable Haptic interfaces. A desktop haptic interface is typically composed of a robotic end effector arm with one end fixed and a sphere or a stylus at the other, free end. Operators can manipulate the stylus with their hand and often, this is the only point of contact between the operator and the display. The robotic arm has multiple degrees of freedom to allow operators movement in free space without any constraints when haptic feedback is not provided. There are force and position sensors on the robotic end effector to track the movement of the operator's hand, which determine the magnitude and direction of forces that are applied by the stylus on the operator. Since operators physically handle only the stylus, it should be capable of rendering both cutaneous and proprioceptive feedback. Typically, these displays have commonly been used to train operators in performing specific tasks such as path following and object manipulation. This is important for applications, such as telesurgery, where surgeons are provided feedback about different object stiffnesses and textures, such as tools and/or organs [31, 35, 113].

Introduction

The advent of virtual reality applications has led to an increased demand for whole-body haptic feedback rendering. Desktop haptic interfaces mandate operators to remain in a specific place during teleoperation, whereas wearable haptic interfaces often provide freedom to move. Moreover, desktop haptic interfaces have a single point of contact to render both kinesthetic and tactile feedback, whereas wearable haptic displays can provide feedback to various parts of the body independent of each other [66, 129, 110]. Existing wearable haptic interfaces often provide kinesthetic feedback with actuators, such as electromagnetic motors [111], motor-driven cables [159, 141], and they provide tactile feedback using vibration motors [123], pneumatic actuators [165, 161], and electrostimulation [118]. These new interfaces are not only capable of matching the functionalities of desktop haptic displays, but can also facilitate new paradigms of teleoperation with regard to movement mapping between the operator and the robot [140, 142].

For all types of haptic displays, the common challenges for teleoperation pertain to realism. Realism is primarily affected by the sheer difficulty in rendering stiffness and texture of objects because often, the sensors on the robots cannot measure these quantities with high enough fidelity. Another source of concern that affects realism is the rate at which haptic feedback is provided. A high feedback rate can provide a more realistic experience for the operator, but may be computationally expensive, whereas a low refresh rate could deteriorate the sensation of immersion. A related issue is latency between different types of displays, which is caused by either long delays between the actions of the operator and the corresponding movements of the robot or an asynchronization between haptic and visual displays. The latter case can induce a lot of confusion for the operator because haptic interactions for humans are largely dependent on hand-eye coordination. Finally, safety is another important consideration that needs to be taken into account, particularly with wearable haptic displays, with which operators can handle heavy machinery via the robot. Since these machines can exert large forces, there is a risk of operators harming themselves and fail safe protocols must be enforced to avert these situations [102].

Haptic-training for motor learning applications

Motor learning is defined as “*a set of [internal] processes associated with practice or experience leading to relatively permanent changes in the capability for responding*” according to Richard Schmidt in his seminal work on the subject [150]. Hence, learners practice the motor task repeatedly till they are able to perform the task with a certain level of proficiency. For several motor tasks, haptic feedback is used as a teaching aid to help learners improve their performance. The function of this haptic aid is to provide feedback regarding the learner’s movements and movement outcomes. This feedback is meant to supplement the intrinsic sensory information gathered by the learner. As described in Schmidt’s definition, motor learning is said to have taken place if the performance improvement is permanent. Therefore, the quality of haptic feedback provided to train learners is evaluated by testing its effectiveness in fostering skill retention by observing relatively permanent gains in motor task performance. One of the main goals of practice is to enhance the learner’s error detection capability i.e., the learner becomes more skilled for a given motor activity if they are able to detect and analyze their errors, and amend them when the task is being carried out. When feedback is provided to correct movement errors, it tends to direct learners towards the goal movement. This is particularly true in the case of “haptic guidance” based feedback, where the learner is physically guided to carry out the prescribed movement patterns. For trajectory-tracking tasks in particular, this form of guidance is enabled by a haptic system that applied forces to the learner’s body to ensure that they do not deviate from the trajectory [1]. However, a significant problem arises as result of excessive support provided by this guidance-based haptic feedback. The haptic guidance provides short term improvement in skilled performance which are much lower after the retention interval. Indeed, when the guidance based-haptic feedback is removed during the skill retention test, their performance markedly deteriorates [147]. The learner becomes so dependent on the external support that they treat the augmented source of information as the primary, instead of relying more on their intrinsic sensory feedback to carry out the movements. One of the main reasons for this over-dependence on guidance is that the user carries out the task almost as a passive entity, unaware of potential errors they might have committed [40]. This has also been referred to as the “Guidance Hypothesis” [150]. To avoid the learner developing such dependency effects, a popular alternative to the guidance-based

haptic training is “error amplification” [121]. Broadly speaking, error amplification as the name suggests involves purposefully amplifying the learner’s errors during training, forcing the learner to be more vigilant and forceful in correcting for these amplified errors. The merits of this approach are supported by studies which show that learning through the modification of movement patterns, is an error informed process [176]. Compared to guidance-based feedback, amplifying errors results in relatively permanent retention of skilled performance due to the learner playing an active role in detecting and correcting their errors. The key limitation, however, is that error amplification requires a considerable amount of practice and therefore, induces latencies. Furthermore, it is postulated that error amplification is not a suitable method for complete novices and in fact, it is method better suited to learners with a certain skill level in performing the task [104]. To bypass some of these challenges posed by guidance-based feedback and error-amplification, another approach is explored in the past that provides guidance to learners only in so far as to make them cognizant of their errors, and then, allowing the learners to correct those errors by themselves. This approach is characterized by the presence of a “forbidden” region that dissuades users from committing movement errors. This forbidden region is perceived by the learner when they deviate from the region in which free movement is permitted. Rosenberg made one of the most significant contributions towards developing this mode of feedback [144]. He created rigid virtual fixtures i.e., virtual surfaces simulated to serve as hard constraints, to help learners navigate in that space by interacting with them. Subsequently, several studies extended this concept to create spatially varying, viscous force fields for user assistance [1]. Like error amplification, this method of creating a forbidden region emphasizes the active participation of the learner in error detection during practice, improves task performance, and fosters longer term skill retention. At the same time, this method is more suitable for complete novices and does not cause practice-related latencies. The work presented in this thesis is situated in the conceptualization, creation, and testing of wearable haptic systems that can provide haptic feedback that can create this type of forbidden region. The haptic system is used to train learners in motor tasks, specifically tasks that are relevant to the field of robotic teleoperation.

1.3 Thesis Outline

This thesis describes the development of new types of wearable haptic interfaces and their application to telerobotic tasks. The haptic interfaces take into account the different design criteria proposed in Section 1.1. Each of the interfaces are characterised for their electromechanical properties. The interfaces are used to train novice users in teleoperating drones in simulated environments for different types of tasks under different conditions of visual feedback. For each drone telerobotic task, the motor learning characteristics are observed, analysed and reported.

Publication Note: The material presented in the summary list is adapted from abstracts of the publications mentioned in each section.

Chapter 2, **The design and development of an all-fabric haptic device**

This chapter describes the development of a lightweight, textile fabricated, haptic device consisting of an electrostatic adhesive clutch, which can constrain body movement when activated at low power (~ 1 mW). The clutch electrodes are composite structures, prepared by coating copper-plated polyester fabric with thin films of high- κ dielectric ink. When voltage is applied across a pair of overlapping electrodes, the charge separation created between the overlapped surfaces gives rise to adhesive forces that resist tensile loads along the electrode surface. The clutch is arranged in parallel with a sheet of knitted fabric, which exhibits low-stiffness spring-like characteristics, thus decreasing load resistance when the clutch is deactivated. Mechanical tests are carried out to assess the dependency on scaling and loading rate at different voltages. The load-bearing capacity of the device is experimentally shown to sustain a 1 kg load for a clutch pair with $120 \times 70 \text{ mm}^2$ dielectric overlap, when activated at 400 V. This chapter presents current-dependent charging and discharging times that can be as low as 15 ms. To exemplify its pertinence in wearable applications, the device is used as an elbow joint constraint, exhibiting its conformability to curvatures and suitability for skin-mounted applications.

The main contributions of Chapter 2 are:

- The first all-fabric electroadhesive clutch to be developed for wearable applica-

tions.

- The design, working principle, and fabrication technique used for the clutch.
- The characterisation of the clutch's electromechanical properties.
- Preliminary demonstrations to indicate the feasibility of the clutch for haptic applications.

Chapter 3, **A fabric-based elbow haptic sleeve for motor training**

People learn motor activities best when they are conscious of their errors and make a concerted effort to correct them. While haptic interfaces can facilitate motor training, existing interfaces are often bulky and do not always ensure post-training skill retention. This chapter describes a programmable haptic sleeve composed of textile-based electroadhesive clutches for skill acquisition and retention. The functionality of the sleeve is shown in a motor learning study where users control a drone's movement using elbow joint rotation. Haptic feedback is used to restrain elbow motion and make users aware of their errors. This helps users consciously learn to avoid errors from occurring. While all subjects exhibit similar performance during the baseline phase of motor learning, those subjects who receive haptic feedback from the haptic sleeve commit 23.5 % fewer errors than subjects in the control group during the evaluation phase. The results show that the sleeve helps users retain and transfer motor skills better than visual feedback alone. This work shows the potential for fabric-based haptic interfaces as a training aid for motor tasks in the fields of rehabilitation and teleoperation.

The main contributions of Chapter 3 are:

- The improvement of the earlier all-fabric electroadhesive clutches to increase holding force capacity.
- The creation of a fabric-based elbow-joint wearable haptic sleeve composed of electroadhesive clutches and anchoring body attachments.
- The successful demonstration of the haptic sleeve as a teaching aid for novice users to learn drone path following.

- The observed ability of users to transfer motor skills to related tasks, such as waypoint navigation.

Chapter 4, **Multi-joint wearable haptic sleeve for telerobotics with reduced visual feedback**

Teleoperators rely on both visual and haptic feedback to perform drone teleoperation tasks, such as obstacle avoidance. Haptic feedback becomes essential when visual feedback is compromised, either due to visual occlusions or poor depth perception. However, haptic interfaces, are often bulky because they require heavy actuators to provide force feedback. As mentioned in previous chapters, this bulkiness reduces user mobility and makes these interfaces unsuitable for prolonged use. This chapter proposes a wearable haptic sleeve that encompasses the wrist and elbow joints of a human arm. The two joint rotations control the motion of a drone in a simulated environment along a horizontal plane. The sleeve is composed of modular electroadhesive clutches that block the joint movement when the drone is in the vicinity of an obstacle. The clutches are lightweight (27 g), require low power (~ 1 mW) to operate, and can be mounted on the user without affecting the user's mobility. A motor learning subject study is conducted to navigate a drone through a hole in a wall where the depth perception of visual feedback is compromised. The results of the study show that subjects trained with the wearable haptic sleeve learn the drone obstacle avoidance task and retain the necessary motor skills after haptic training, compared to subjects who receive only visual feedback and are unable to learn the motor task.

The main contributions of Chapter 4 are:

- An updated version of the wearable haptic sleeve is developed to encompass both the elbow and the wrist joints with new body anchoring attachments.
- The different electroadhesive clutches are capable of blocking the joint movements independently.
- An qualitative and quantitative evaluation of user interaction with the device for wrist extension and flexion is carried out.
- A user study is conducted that successfully exhibits the haptic sleeve's ability to

Introduction

aid users in learning obstacle avoidance tasks under reduced visual feedback.

2 The design and development of an all-fabric haptic device

The first chapter describes the design and fabrication of the all-fabric wearable electroadhesive clutch. The clutch is used as the fundamental building block in developing a wearable haptic interface that is used to train users for telerobotic tasks. The wearable interface provides haptic feedback using the clutches to correct erroneous body movement in the context of the task by blocking specific joint movements.

Publication Note: The work presented in this chapter is adapted from:

V. Ramachandran, J. Shintake and D. Floreano, "All-Fabric Wearable Electroadhesive Clutch", in *Advanced Materials Technologies*, vol. 4, no. 2, Feb. 2018, doi: 10.1002/admt.201800313.

2.1 Introduction

In the field of wearables, the provision of haptic feedback has successfully been shown to supplement the information gathered by the human body's intrinsic sensory mechanisms for applications ranging from rehabilitation to teleoperation [1, 52]. In fact, with the introduction of new wearable interfaces to control distally-located robots, haptic feedback to the whole body could help users learn to control robots better than they might with conventional hand-held controllers that have limited physical

points of contact with the human skin [139, 122]. One approach is to provide haptic feedback produced by devices that generate mechanical impedance, such as brakes and clutches [144, 56]. Such haptic devices are characterised by guides that transmit impedance that can constrain user movement and prevent them from committing errors. Unlike powered wearable orthotics, which require bulky actuators [36, 48], these types of wearable impedance-based haptic devices can be developed exclusively using soft materials. Indeed, in recent years there has been a greater emphasis to incorporate human skin-like elastic materials in wearable systems for improved biomechanical compatibility [173]. In soft matter engineering, the predominant materials used are silicone-based elastomers because they can deform under light mechanical loading and distribute the load to avoid high stress concentrations [92]. However, a key limitation of such elastomers is that they are non-porous. This makes them unsuitable for direct skin-mounted applications because of potential health risks caused by skin occlusion and sweat build-up. One way to address this issue is to use textiles that allow the skin to breathe through their intrinsic porous texture [117].

To provide impedance-based haptic feedback using textiles, stiffness tuning technologies can be used. Several stiffness-tuning technologies are explored in the literature that examine their functionality when used in conjunction with textiles [93, 166]. In addition to flexibility, lightness, and breathability, the haptic device needs to respond rapidly and match the compliance of the human body. The variable stiffness technologies that satisfy most of these requirements include, layer/particle jamming [166, 25, 77, 13, 42], phase changeable materials [167, 137, 152, 155], or electrostatic adhesion [33]. Jamming technologies suffer from the need for bulky auxiliary equipment to remove air and regulate air pressure and are therefore, unsuitable from the standpoint of portability. Material phase change, often a thermal process, consumes significant amount of power and takes a long time to respond due to slow heat dissipation. Electrostatic adhesion, or electroadhesion, exploits the characteristics of capacitors, such as low power consumption and short response time, and require only lightweight and portable electronic components. Therefore, electroadhesion may be more suitable for the development of impedance-based haptic devices using textiles.

Electroadhesion has mostly been used in the field of robotics for gripping, perching and wall-climbing applications [158, 51, 128, 106, 105]. In most instances, a combina-

tion of tacky polymers with moderate conductive and dielectric properties were used to fabricate capacitors [17]. However, the use of intrinsically-adhesive polymers could also result in residual stiction and slow disengagement. This problem is addressed recently in work that focused on the development of an electroadhesive clutch for an ankle prosthesis by using a solid dielectric with a smooth surface [33]. Their device is very effective in controlling the spring engagement of the exoskeleton and returning stored mechanical energy during walking. However, it must be noted that the use of metallised plastic electrodes in their clutches could be unsuitable for textile fabricated devices, arising from materials compatibility issues in the manufacturing process.

2.2 Methods

This section presents the method to develop wearable haptic clutches that are almost entirely fabricated using different types of textiles (Figure 2.1). The advantage of the method proposed here is the employment of stitching, a common textile manufacturing method. Compared to dry or wet adhesives that create chemical bonds to join surfaces, stitches are more resilient to environmental externalities, such as humidity and are more easily mendable in case of damage. The feasibility of the manufacturing process is demonstrated as well as the material architecture that allows for directional stiffness tuning at low power.

2.2.1 Structure, working principle, and fabrication

The haptic device is composed of a pair of electroadhesive clutch plates coupled with knitted and woven fabrics, arranged in the order shown in Figure 2.1. Knitted fabrics are stretchable and woven fabrics are inextensible. The device is designed to have a low-stiffness spring in parallel with the high-holding force clutch. This means that when the clutch is not in operation, the device can comfortably stretch along the human body without exerting a significant restoring force. The assumption here is that the friction between the dielectric surfaces of the clutch plates is negligible. The clutch operates on the same principle governing parallel plate capacitors (see Appendix A). When a voltage is applied across the electrodes, charge separation induces Maxwell stress normal to the electrode plane (Figure 2.1b). This adhesion

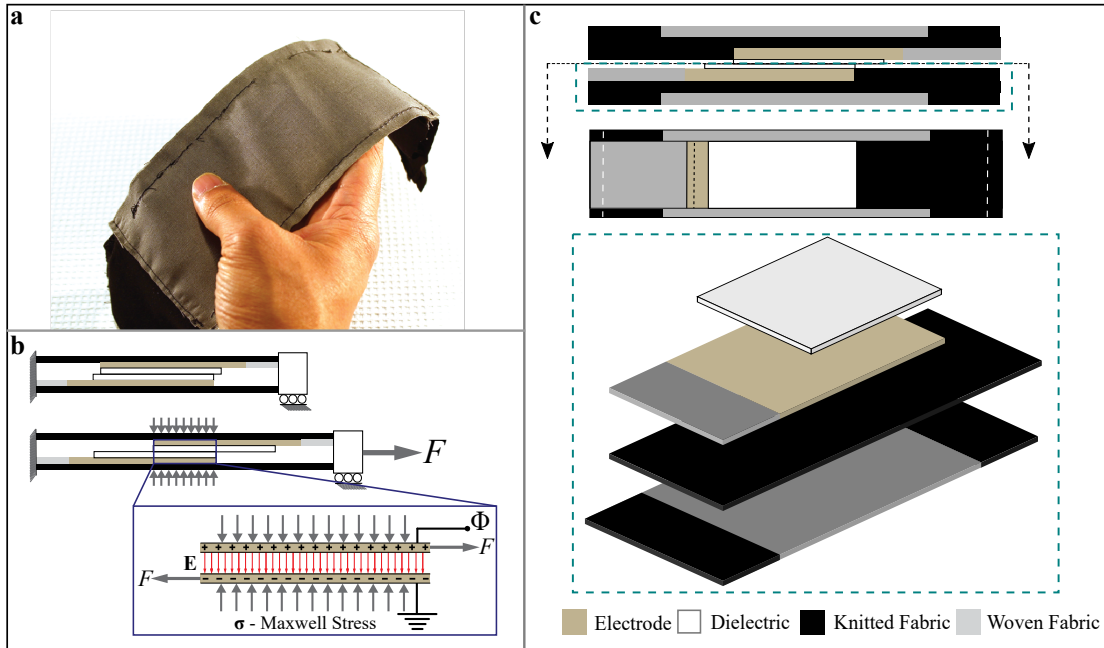


Figure 2.1 – Structure and working principle of the fabric clutch. (a) Encapsulated haptic device with integrated electroadhesive clutch plates. (b) When the haptic device is stretched longitudinally, the dielectric overlap area reduces. To prevent further stretch, a voltage Φ is applied across the electrodes that induces Maxwell stress σ normal to the electrode surface and increases the frictional force. (c) Cross-section and exploded view of the clutch pair components. Fabric components are joined by stitches (dashed, white & black).

The design and development of an all-fabric haptic device

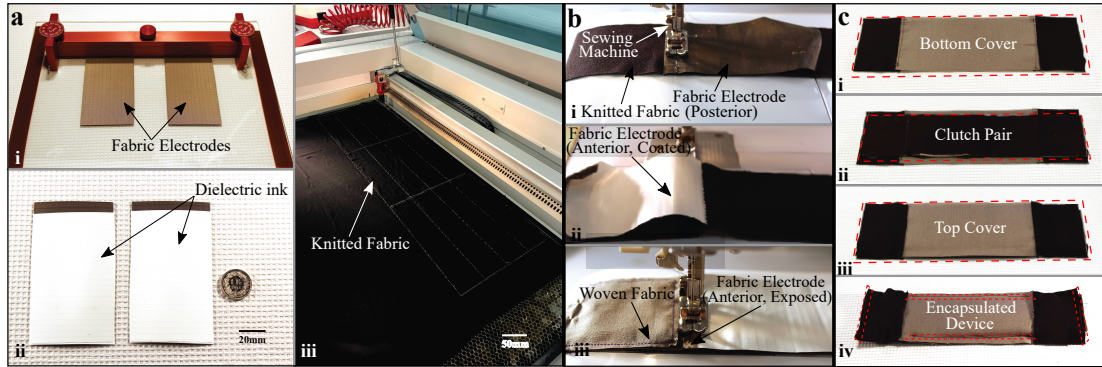


Figure 2.2 – Fabrication of the fabric clutch. (a) Component manufacture of the clutch plates and fabric sheets. (i) Two copper plated polyester fabric electrodes are bonded to a glass substrate. (ii) The electrodes are thin-film coated with a dielectric ink. A portion of the electrode is left uncoated to interface with a high voltage power supply. (iii) Knitted fabric is laser cut into rectangular sheets. (b) Assembly of haptic device. (i) The posterior surface of the electrode is stitched onto the knitted substrate along the wider edge of the coated surface. (ii) The electrode is folded to cover the stitched seam and the coated surface is aligned in parallel with the knitted substrate. (iii) The exposed portion of the coated (anterior) electrode face is stitched onto the substrate along with a rectangular laser-cut woven fabric sheet covering the knitted fabric surface between the exposed, anterior electrode portion and the substrate edge. This sample is replicated and aligned such that the coated electrodes are in planar contact and the unconstrained portion of the knitted substrate are longitudinally at opposite ends. (c) Encapsulation in a textile covering. (i) Bottom cover is manufactured by stitching two identical knitted fabric sheets to a single woven fabric sheet. (ii) Clutch pair with overlapping electrodes is placed on top of the bottom cover. (iii) A top cover, identical to the bottom cover, is placed on top of the clutch pair. (iv) The covers are stitched along the longer edges with seams avoiding the clutch pair. The covers and the clutch pair are stitched together along the wider edges to completely encapsulate the device.

increases the maximum shear force required to induce slippage when subjected to a tensile load.

Each clutch plate consists of a conductive woven textile sheet of pre-determined shape, which is thin-film coated with a high- κ dielectric ink and laser-cut knitted and woven fabrics (Figure 2.2a).

The steps involved in the fabrication of the clutch plates are as follows:

- Two 105 mm \times 60 mm sheets of the Nickel on Copper-Plated Polyester Fabric tape (CN-3190, 3M), a woven fabric shielding with acrylic adhesive backing, are bonded to a 127 μ m sheet of Polymethyl methacrylate (PMMA), as shown in Figure 2.2(a)-i.
- 50 μ m layers of dielectric ink (Luxprint 8153, DuPont) are deposited onto the fabric substrates using thin film application (ZUA 2000, Zehntner), leaving only 5 mm \times 60 mm of the fabric exposed.
- The ink is oven-cured at 140 °C for 60 minutes.
- This step is repeated once and the resulting solid dielectric layer is 40 μ m in thickness as shown in Figure 2.2(a)-ii.
- The clutch plates are removed from the PMMA substrate.

The device is comprised of two identical parts, each fabricated by stitching a clutch plate and a piece of woven fabric onto a sheet of knitted fabric, leaving only a portion of the knitted fabric unconstrained (Figure 2.2b). The two parts are aligned to form a clutch pair, such that the dielectric surfaces of the pair are in planar contact and the unconstrained portions of the knitted fabric are at opposite ends (Figure 2.1c). Finally, the entire device is enclosed in a protective textile covering to prevent plate separation perpendicular to the longitudinal axis.

The steps involved in the fabrication of the haptic device are as follows:

- Rectangular sheets of knitted fabric (280 mm \times 60 mm) and woven fabric (60 mm \times 60 mm) are laser cut, as shown in Figure 2.2a-iii, using a commercial CO₂ laser cutter (Speedy 400, Trotec).

The design and development of an all-fabric haptic device

- Using one sheet of knitted fabric as a substrate, the posterior, uncoated surface of one fabric clutch plate was stitched onto it using a commercial sewing machine (H Class E20, Husqvarna Viking), 150 mm from the substrate edge (Figure 2.2b-i).
- The plate is folded backwards to cover the seam (Figure 2.2b-ii), such that the coated surface of the plate is aligned with the longer edge of the knitted fabric substrate.
- The exposed portion of the coated surface is stitched onto the substrate (Figure 2.2b-iii), along with one sheet of the laser cut woven fabric, thereby covering the portion of the knitted fabric surface between the covered seam of the electrode and the substrate edge. As a consequence, only 130 mm × 60 mm of the knitted substrate remains unconstrained.
- The sample is replicated and aligned, such that the coated electrodes are in planar contact and the unconstrained portions of the jersey fabric sheets are at opposite ends.
- The clutch pair is encapsulated by embedding it between two layers of textile covering sheets - each layer consisted of a woven fabric sheet (180 mm × 80 mm) stitched to two identical jersey fabric sheets (60 mm × 80 mm) along its wider edges (Figure 2.2c).
- The covering layers are stitched together along the longer edges without the clutch pair. The two layers along with the clutch pair were stitched together along the wider edges. The total device weighs 23 g.

The fabrication of the device can be modified to incorporate multiple clutch plate pairs that are arranged in parallel to increase the maximum holding force (see Appendix D).

For the plate electrode, the fabric tape is chosen because it can easily be sewn onto other fabrics. While the tape's acrylic adhesive backing provides a weaker, secondary bond to the substrate that could resist shear loading, it can also be delaminated by peeling if the plate needs to be replaced. Luxprint is selected as the dielectric material because it contains barium titanate, a ferroelectric crystal commonly used in solid-state ceramic capacitors [138, 75]. The high dielectric constant ($\kappa = 35$) of barium

titanate increases the charge-carrying capacity of the capacitor, thereby increasing the adhesive force when a voltage is applied. Luxprint is particularly suitable for the fabrication process as well. In its uncured state, it is a free-flowing, viscous fluid that can be oven-cured into thin films on flat substrates using a thin film applicator. In its cured state, the surface is smooth and thus displays low friction. This physical property is important to ensure high surface conformability, which results in stronger adhesion upon clutch activation, and for providing negligible shear resistance when no voltage is applied [33]. The thin dielectric film bonds well to the flexible fabric without cracking, although the dielectric layer thickness decreases by more than half after the sample is cured in the oven. This phenomenon is due to the fact that the solvent present in the dielectric ink, which gives it its fluidic constitution, evaporates during the curing process and that the ink seeps through the numerous air gaps present in the weaves of the fabric.

2.2.2 Electromechanical characterisation

Two sets of experiments are performed in order to characterize the behaviour of the device. In the first set, the mechanical characteristics are measured, such as the dependence of the maximum clutching load on the area of dielectric overlap, the effect of number of clutch plate pairs arranged in parallel, and the rate of loading (displacement-controlled and force-controlled). In the second set, the relevant electrical characteristics are measured, such as capacitor charging and discharging time, and the total power consumption.

When a voltage Φ is applied across the parallel plate capacitor, an electric field is created between the plates and charges begin to flow from one electrode to the other until the potential difference across the capacitor plates equals Φ (Figure 2.1b). The capacitor has a capacitance $C = A\kappa\epsilon_0/x$, where A is the capacitor planar surface area, κ is the dielectric constant, ϵ_0 is the dielectric permittivity of free space, and x is the dielectric thickness. The electric field induces Maxwell stress normal to the electrode plane (see Appendix A). This stress component is responsible for the rapid increase in frictional force along the surface area of the planar electrodes, opposite to the loading direction. For n engaged clutch plate pairs placed parallel to each other, the adhesive

force in-plane is given by:

$$F = \frac{1}{2} \mu \kappa \epsilon_0 n A \left(\frac{\Phi}{x} \right)^2 \quad (2.1)$$

where μ is the coefficient of static friction between the surfaces of the dielectric.

The steps involved in the characterisation of the holding force dependency of the haptic device on different parameters are as follows:

- Each clutch plate is bonded onto 150 mm × 60 mm rectangular sheets of laser cut woven fabric, by iron pressing the woven cloth onto the acrylic adhesive backing of the fabric tape. The melted adhesive creates a strong bond between the plate and the fabric.
- Force-displacement tests of the clutch pairs are conducted with a materials testing machine (Instron 5965). The plates of the pair are fixed to the vices of the tensile tester, such that the dielectric surfaces are in planar contact with each other.
- To test the dependence of maximum holding force on applied voltage, the vertical separation between the vices is adjusted to ensure an overlap area of 50 × 60 mm². Prior to commencing each test, voltage is applied to the clutch electrodes using a high voltage supply (PS 350, Stanford Research Systems).
- The clutch pairs are engaged at 200 V, 300 V, 400 V, and 500 V and loaded under force-controlled conditions (0.1, 1, 10, 100 N s⁻¹) and displacement-controlled conditions (0.1, 1, 10, 100 mm s⁻¹) (see Appendix E).
- The clutch pairs are engaged at 200 V, 300 V, 400 V, and 500 V and loaded under force-controlled conditions (0.1, 1, 10, 100 N s⁻¹) and displacement-controlled conditions (0.1, 1, 100 mm s⁻¹).
- To test the dependence of maximum holding force on area of overlap, tests are carried out for the following areas: 10 cm², 30 cm², 50 cm², while the plates are engaged at 400 V and the vices are loaded at 10 mm s⁻¹.

- To test the effect of number of clutch plate pairs operating in parallel, experiments are carried out using 1, 2, 3, 4, and 5 pairs of clutch plates. Each characterisation study is carried out for 5 trials.

To calculate the charging and discharging times of the capacitor, a customized H-bridge is used with a resistor placed in series with the capacitor to determine the capacitor voltage drop by measuring the branch current (see Appendix B). When a digital signal is sent from a microcontroller to transistors in one branch of the bridge, the high voltage Φ is applied across the capacitive load.

The steps involved in the measurement of the charging and discharging temporal characteristics of the clutches are as follows:

- The clutch plates are interfaced with the H-bridge by soldering wires to the textile electrodes. The H-bridge is customized with four identical transistors (1NK60Z, STMicroelectronics). The H-bridge also consists of a $2\text{ M}\Omega$ resistor placed in series with the capacitive load, to measure the current flow through the individual branches and calculate the voltage drop across the capacitor.
- The transistor of the H-bridge that are closer to the ground potential are denoted as LTs and the transistors closer to the high voltage supply as HTs. Initially, LTs are closed and HTs are kept open.
- When a 5 V digital signal is sent from the microcontroller (Arduino Nano, Arduino LLC) to close the HT of one branch of the bridge and open the LT of the second branch, a high voltage (200 V, 300 V, or 400 V) is applied across the first branch.
- The current flow is measured and stored using a digital oscilloscope (HMO2024, Rohde & Schwarz). The time required for the current to decay to 0.7 % of its peak value is calculated as the charging time.
- Capacitor discharging is instigated by opening the HT of the first branch and closing the LT of the second branch, thus shorting the circuit and reverting to the initial condition. The current flow, voltage drop, and discharge time are

measured in the same manner as the charging phase, using the oscilloscope across the measurement resistor.

Discharge time is shortened even further using the H-bridge by two steps that are performed simultaneously (see Appendix B). One, the HT of the first branch is opened, and the LT of the second branch is closed and two, the HT of the second branch is closed and the LT of the first branch is opened. This should result in the capacitor current and voltage drop peaking in the second branch to twice the peak value recorded in the first branch, before undergoing exponential decay. Based on experimental data collected for discharge through branch short circuiting, the time needed to reduce the voltage to half is determined. The second branch is kept closed for that exact period of time, after which the HT of the second branch is opened and the LT of the first branch is closed, returning to the initial condition. The capacitor discharge time is measured as the sum total of the time required for the current to drop to 0.7 % of the peak value starting from when the first branch was opened.

2.3 Results

2.3.1 Holding force characteristics

As shown in Figure 2.3, the mechanical characteristics of the clutches are observed to be in keeping with expected trends. As Equation (2.1) suggests, the maximum load that the clutch plates can withstand increases in proportion to the dielectric area of overlap and the number of engaged clutch plate pairs (Figures 2.3a,b). The linear dependency on the dielectric area of overlap is especially relevant when the clutch plates are engaged after the device has been stretched by a certain amount. Here, the dielectric area of overlap reduces from its initial value in the rest configuration and consequently, the maximum holding force capacity also reduces. It must be noted that the force is only dependent on the total surface area of dielectric overlap and not the individual dimensions of the clutch plates. Therefore, the device can be designed with plate dimensions and rest configuration dielectric area of overlap that are capable of handling different magnitudes of load. As predicted by Equation (2.1), Figures 2.3c,d also show a quadratic load dependence on the applied voltage. The samples

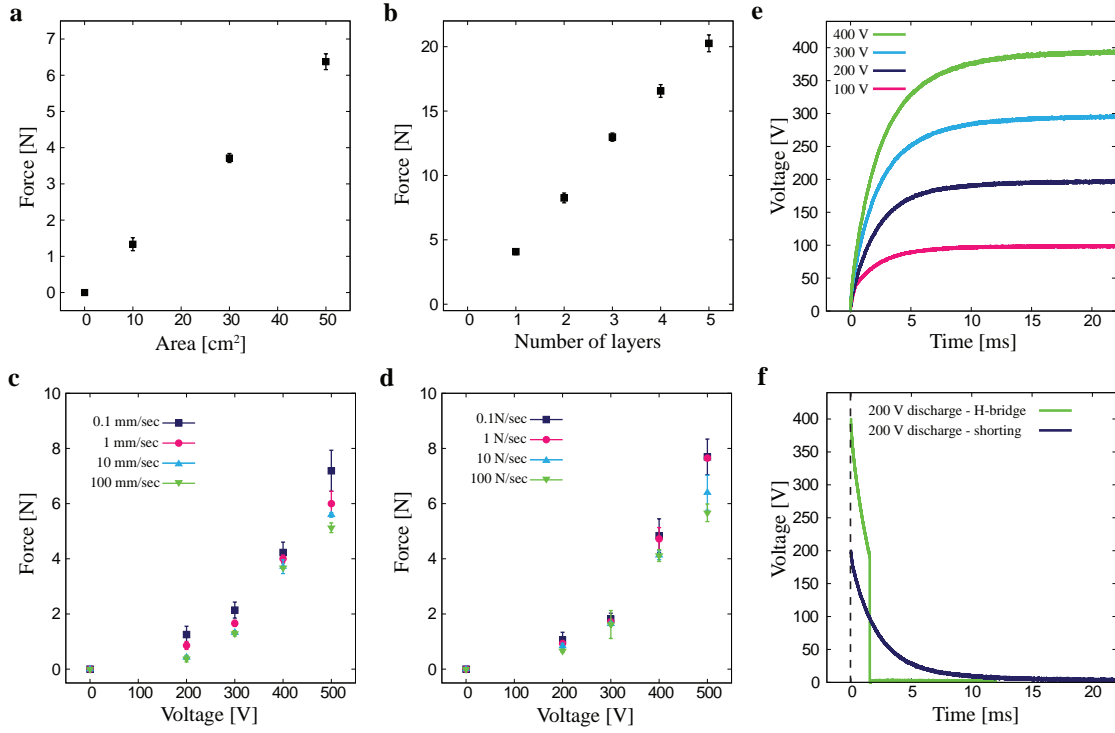


Figure 2.3 – Maximum clutch holding force capacity as a response to an applied voltage for varying (a) area of overlap, (b) number of parallel clutch plate pairs, (c) displacement-controlled loading rate, and (d) force-controlled loading rate. Each clutch plate is bonded to a 150 mm × 60 mm sheet of woven fabric and each clutch pair has an initial dielectric overlap area of 50 × 60 mm². (e) Exponential capacitor charging characteristics of a clutch plate pair at different voltages. (f) Clutch plate discharge characteristics observed at 200 V, both by short circuiting and by reversing the voltage polarity using an H-bridge. The discharge characteristics are measured by observing the voltage drop across the measurement resistor placed in series with the capacitor.

are loaded by defining the rate of loading, either displacement-controlled (mm s^{-1}) or force-controlled (Ns^{-1}). It is worth pointing out that for both sets of tests, the maximum holding force reduces at high rates of loading. The force-controlled tests exhibit a slightly higher variance compared to displacement-controlled tests at high voltages. Unlike displacement-controlled tests that are open-loop processes where the tests are carried out by specifying a fixed displacement rate, force-controlled tests are closed-loop processes where the loading rate depends on the force measured by the load cell of the commercial tensile tester. Therefore, delays in transmitting the measured value from the load cell to the operating software may have contributed to the aforementioned artefact.

2.3.2 Charging and discharging characteristics

The voltage drop across the capacitor increases exponentially from zero to the peak value at steady state (Figure 2.3e). This rise is caused by a corresponding exponential charge build-up on the capacitor electrodes. The charging time is calculated as the time required for the voltage to reach 90 % of its peak value. For instance, a single clutch plate pair with a dielectric overlap area of $50 \times 60 \text{ mm}^2$ takes 13 ms to charge when operated at 200 V.

A consequence of capacitance charge build-up is dielectric space charge. Space charge is caused by the induced polarising electric field that aligns the ionic crystals to oppose the applied electric field [130]. When the capacitor plates are shorted, the charges in the capacitor begin to flow in the opposite direction until the voltage across the electrodes is zero. However, the presence of space charge might cause the plates to retain residual stiction that can have significant consequences when operating haptic devices at high frequency. While the space charge for Luxprint is low [33], the discharging time can be reduced even further by driving current in the opposite direction for a brief period of time to quicken space charge removal (see Appendix B). When operated at 200 V, a clutch pair with a dielectric overlap area of $100 \times 60 \text{ mm}^2$ consumes an average power of 0.9 mW during charging and 1 mW during discharging. By using the H-bridge to drive current in the opposite direction until the capacitor voltage is driven to zero, the discharge time can be reduced from 15 ms to 2 ms, while the clutch pair consumes an average power of 2.7 mW to discharge (see Figure 2.2f).

It is important to state that the dielectric permittivity of the capacitor (clutch) is not constant and varies with applied voltage. This is because the dielectric used, Luxprint 8153 is composed of Barium Titanate, a ferroelectric crystal. Ferroelectric materials undergo field-induced transitions when a field (electric, thermal, stress, gravitational) is applied. As a result, the dielectric permittivity changes when a voltage is applied across the clutch and a constant capacitance, and thereby a constant RC cannot be used. However, this is not a problem for measuring the charging and discharging time of the capacitor because these quantities depend on charge accumulation over time, and this has been quantified experimentally at different voltages in Chapter 2 and Appendix B. The resistance R used for the charge/discharge characteristics is $2\text{ M}\Omega$. When the voltage is set to zero, the capacitance of the clutch is 23.24 nF for an area of overlap of $50 \times 60\text{ mm}^2$.

2.3.3 Preliminary demonstration of haptic device

To validate the capabilities of the haptic device, two demonstrations are carried out using a single clutch pair device that weighed 23 g , with rest configuration dielectric overlap area of $120 \times 70\text{ mm}^2$, and operated at 400 V .

To demonstrate the load bearing capacity of a single clutch pair device, a 1 litre bottle of water weighing 1 kg was attached to a plank of wood using a bowline knot (see Figure 2.3a). A $75\text{ mm} \times 40\text{ mm}$ rectangular piece of Velcro with adhesive backing is attached to one of the surfaces of the plank. The mating Velcro portion of the same dimensions was attached to one end of the haptic device. Initially, the clutch is engaged at 400 V , with a dielectric area overlap of $120 \times 70\text{ mm}^2$. The clutch along with the bottle is lifted to a height of 1 m above the ground and held. Keeping the top end of the device fixed, the clutch is disengaged and the knitted fabric extends downwards under the influence of the attached weight.

To show the device's ability to constrain human body movement, a mannequin arm with a hinge elbow joint is used (Figure 2.3b). The arm is positioned such that the shoulder joint is kept locked but the forearm, weighing 0.8 kg , is free to rotate about the elbow hinge joint. The activated device is capable of supporting the weight of the forearm, thus indicating that it can impart force feedback to block undesirable

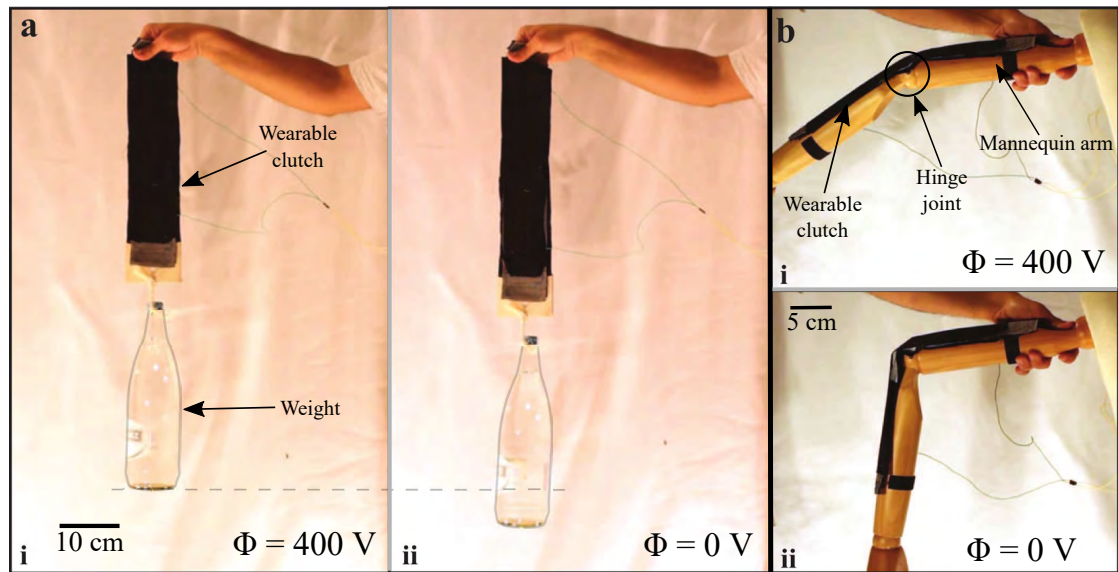


Figure 2.4 – Demonstration of haptic device with single clutch pair having a dielectric overlap area of $120 \times 70 \text{ mm}^2$ and engaged at 400 V for (a) load bearing and (b) skin-mounted applications. (a)-(i) The initially engaged clutch is able to lift a weight of 1 kg. (a)-(ii) Upon disengagement, the knitted fabric stretches like a spring under the influence of the loaded weight. (b)-(i) The engaged clutch is able to constrain the rotation of a mannequin forearm about the elbow hinge joint. (b)-(ii) The disengaged clutch readily allows the forearm rotation without providing comparable resistance to movement

movement. When the device is not in operation, the forearm should rotate under the influence of its own weight and cause the device to stretch longitudinally. Velcro strips are adhered along the 18 mm circumferences of the forearm and upper arm. With respect to the hinge joint, the strips are 12 cm along the forearm and the upper arm each and the clutch was attached along the arm's posterior side. As expected, upon engagement, the rotation is constrained and the forearm is held fixed. When the clutch is disengaged, the forearm is able to rotate freely again.

2.4 Conclusions

In summary, this chapter describes the development of a haptic device consisting of an electroadhesive clutch, fabricated using textiles. When the clutch is not activated, the device is allowed to stretch without providing much resistance to loading. Upon

activation, a voltage is applied across the electrodes of the clutch which increases the resistance to tensile load. The device is lightweight, flexible, and operates at low power. The best reported work on electrostatic clutches is the one developed for the ankle exoskeleton [33]. It is capable of withstanding a shear stress of 17 kPa at 120 V mm^{-1} , the device weighed 26 g, and the net power consumption was 0.6 mW over a period of 30 ms. In comparison, the clutch presented here can sustain a maximum shear stress of 3.5 kPa at the same voltage per unit dielectric thickness, weighs 23 g, and consumes 0.9 mW over a period of 15 ms. The lower shear stress of the fabric clutch can be attributed to the mechanical and electrical properties of the fabric electrode – the presence of air gaps between the weaves of the textile reduces the capacitor's charge carrying capacity and its surface irregularities lower the effective overlap surface area. However, the use of an all-fabric device greatly facilitates material-level compatibility for integration in textile-based wearable systems and streamlines the manufacturing process for rapid fabrication. In addition, the mechanical design of a spring and clutch in parallel is an elegant solution for providing impedance-based haptic feedback. Despite requiring high operating voltages, electrostatic adhesion as a technology is safe provided the power-consumption is low i.e., the current required to charge and discharge the circuit is small ($< 5 \mu\text{A}$).

Given that the holding force increases linearly with the dielectric area of overlap and not the individual dimensions of the clutch plates, it is possible to scale up the device to encompass large parts of the body. For body appendages like fingers where the area to mount the device is small, multiple clutch plate pairs can be stacked to produce sufficient force to provide haptic feedback. Power loss due to leakage through the capacitor is low ($\approx 320 \text{ nA}$). Thus, for larger capacitors, power consumption during charging and discharging will largely depend on Joule heating through the series resistance, which limits the current flow through the circuit. Larger capacitors require more time to charge and discharge, but increasing current flow can reduce the reaction time, at the expense of marginally increasing power consumption.

Despite the numerous advantages of using this technology, there are some limitations that need to be addressed. The application of high voltages to barium titanate results in a decay of its dielectric properties [151, 124, 172]. The same is indicated through anecdotal observations made over a period of a few months, where repeated clutch

charging and discharging led to a deterioration in its holding force. Additionally, barium titanate, like other high- κ dielectrics, also has a low breakdown strength ($\approx 20 \text{ MVm}^{-1}$) that limits the operating range of voltages. One way to address this issue is through the addition of conductive fillers that increases the breakdown strength [37, 168]. Alternatively, multiple clutch plates arranged in parallel can be operated at lower voltages instead of engaging a single clutch plate at a high voltage. Another common problem experienced when loading the engaged clutch plate was arc discharge at the electrode edges, where the dielectric coating was sparse. This can be avoided either by coating both surfaces of the electrode with the dielectric ink or by adhering strips of polyimide tape, which has a higher dielectric strength than Luxprint, along the edges of the electrodes. While the risk of sweat-induced capacitor short circuiting is highly remote, it can be avoided by using commercial waterproof fabrics for the encapsulation.

3 A fabric-based elbow haptic sleeve for motor training

The previous chapter introduces an all-fabric wearable electroadhesive clutch, which would be suitable for providing haptic feedback. This chapter addresses some of the major limitations of the earlier clutch by developing a new version of the same to increase its maximum holding force and to simplify the fabrication process. The new clutches are integrated in a wearable interface designed to block elbow joint rotation. This interface is used to train users in a motor activity based on drone teleoperation.

Publication Note: The work presented in this chapter is adapted from:

V. Ramachandran, F. Schilling, A.R. Wu, and D. Floreano, “*Smart textiles that teach: Fabric-based haptic device improves the rate of motor learning*”, in *Advanced Intelligent Systems*, (**under publication**) June 2021

arXiv url: <https://arxiv.org/abs/2106.06332>

3.1 Introduction

Over the past decade, robotic teaching aids have been developed to train people in a variety of motor activities by providing sensory feedback [68, 159, 136, 87, 95, 134, 20]. Motor learning is an error-driven process, and the rate of learning depends on how

sensory feedback is provided during training. Typically, people learn to rectify their errors based on a combination of visual, auditory, and haptic feedback [159]. Motor training by haptic feedback is of particular interest to researchers because it can be applied directly to the part of the body where corrective action is needed [61, 179]. This effectiveness hinges on two critical and intimately linked factors - the haptic interface and the training method [99, 108, 29].

Haptic interfaces should provide reliable, intuitive, and clear feedback when required and be unobtrusive when they are not. Within the scope of motor training, haptic interfaces are generally employed in two fields - rehabilitation and teleoperation [95, 1]. Existing haptic interfaces are mostly grounded i.e., they are fixed to a rigid base, which limits their applicability to tasks that do not require much user displacement, such as object manipulation [52]. With the miniaturisation of electronic components, such as integrated circuits and batteries, wearable interfaces have become a viable alternative because they allow users a greater degree of mobility [116]. This increased mobility has been demonstrated through multiple exoskeletons for gait rehabilitation and robot teleoperation that improve user performance in the specific tasks for which they are designed [111, 78, 38, 125, 173, 5, 90, 4, 119, 7, 141, 140]. However, these interfaces are bulky because of the heavy actuators that they use, such as motors and pumps, which cause user fatigue over prolonged use. In fact, actuators are not always necessary to help users perform motor tasks better. As described in the previous chapter, a recent study shows how a simple, unpowered clutch and spring ankle exoskeleton can increase human walking efficiency by re-purposing their expended energy [27]. Indeed, new lightweight, fabric-based haptic interfaces have been developed in recent years to circumvent the problems associated with using heavy actuators and promote user comfort for continuous usage [88, 179, 6, 90, 30, 131, 120, 177, 16, 59, 85, 181] (Table 3.1). Amongst these fabric-based haptic interfaces, certain interfaces use electrostatic adhesive (EA) clutches to apply kinesthetic feedback through movement braking and passive springs [60, 59, 131, 33, 34]. They operate at low power (~ 1 mW) and are easily integrated into other textile-based wearables, such as clothing. These new types of fabric-based, low-power-consuming haptic interfaces are less complex in mechanical design compared to existing interfaces, which are composed of rigid components. The absence of actuators compels users to rely on the feedback to both identify and correct their errors, which helps them learn the motor task faster.

A fabric-based elbow haptic sleeve for motor training

Textile haptic devices	Year	Feedback type	Power source	Wearable type	Tethering
Bianchi et al. [30]	2014	Tactile	Electric motors	Wrist sleeve	Tethered
Low et al. [22]	2017	Kinesthetic	Pneumatics	Glove	Tethered
Culbertson et al. [31]	2018	Tactile	Magnetics	Forearm sleeve	Tethered
Ramachandran et al. [32]	2018	Kinesthetic	Electrostatics	Elbow joint	Untethered
Park et al. [33]	2019	Tactile	Electrostatics	n/a	Tethered
Wu et al. [34]	2019	Tactile	Pneumatics	Forearm sleeve	Tethered
Carpenter et al. [35]	2019	Kinesthetic	Thermoelectrics	Finger	Tethered
Hinche et al. [36]	2020	Kinesthetic	Electrostatics	Glove	Untethered
Lee et al. [37]	2020	Tactile	Thermoelectrics	Wrist joint	Tethered
Zhu et al. [38]	2020	Tactile	Pneumatics	Forearm sleeve	Tethered
This study	2021	Kinesthetic	Electrostatics	Elbow joint	Untethered

Table 3.1 – Comparison of existing textile-based haptic devices and the one presented in this study.

Furthermore, unlike existing interfaces, these interfaces are not designed for any one specific task alone. Rather, they can be re-purposed to help train users in a variety of motor tasks.

A successful haptic training method ensures that users are immersed in learning the motor activity and are provided timely feedback to improve their performance over the course of training. Existing haptic-based training methods can be broadly divided into two categories - haptic guidance and error amplification [104, 12]. In the former, the haptic system physically guides users to minimize errors they commit during training and accomplish a task. In the latter, the haptic system amplifies user errors to intentionally increase the difficulty of the task [98, 84]. Studies show that haptic guidance increases user performance during training compared to baseline conditions, but that performance levels precipitate when the guidance is not provided [127]. Some have posited that the guidance overly increases user dependency [178]. This dependency curtails both skill retention and skill transfer post-training. On the other hand, error-amplifying systems deliver longer periods of skill retention at the expense of longer training periods [175]. However, some studies state that the comparative effects of haptic guidance and error amplification on motor learning cannot be generalised, because they are subject to the type of motor activity [104, 94]. Nonetheless, there is some consensus that the method of feedback provision and the resulting outcome is dependent on the user skill level [99, 96]. Accordingly, novice users benefit more from haptic guidance, whereas expert users gain more from error

amplification. There is also recent evidence that suggests, allowing users to select the type and magnitude of haptic feedback can accelerate the rate of motor learning [134, 97]. These studies conclusively show that users must actively utilize haptic feedback to rectify their errors and acquire motor skills. However, so far, this active motor learning has only been demonstrated with haptic interfaces made with rigid and bulky devices [134].

This chapter presents a novel haptic interface that promotes active user involvement in rectifying movement errors during motor learning and is composed of only soft, fabric-based components. The interface consists of a programmable elbow sleeve that comprises multiple fabric-based EA clutches, which can rapidly restrict the joint movements of a wearer. In this study, the haptic sleeve is programmed to afford users a margin of error, but provides a motion-blocking feedback to 1) make users aware of their error, and 2) prevent these errors from growing. The haptic feedback operates like a wall that confines the motion range. Through heightened awareness of their errors, users can consciously avoid them in future iterations of the task. This study experimentally shows that the proposed haptic interface increases the training success to learn, retain, and transfer motor skills in a drone teleoperation task.

3.2 Methods

This section describes the key aspects of this study: the manufacture of the updated electroadhesive clutches, the electromechanical characteristics that define the behaviour of the clutches, the simulated environment in which drone teleoperation takes place, and the experimental protocol followed for the human subject study to train user for the drone teleoperation tasks.

3.2.1 Design of the electroadhesive haptic sleeve

The electroadhesive haptic sleeve is a fabric-based exoskeleton that can be programmed to constrain elbow extension and flexion. It is composed of two electroadhesive clutches and three body attachments (Figure 3.1A, Figure 3.2). Each clutch is a parallel plate capacitor composed of overlapping dielectric-coated electrodes. As

mentioned earlier, the EA clutches used in this study are an improved version of the previously described fabric-based clutches to generate higher holding forces [131] (see chapter 2). The higher forces are generated by replacing the fabric-electrodes of the earlier clutches with metallized biaxially-oriented polyethylene terephthalate sheets. This is done to avoid dielectric cracking on the electrode surface, which was observed with the fabric electrode over prolonged usage. Furthermore, surface irregularities and wrinkling are prevented by replacing the fabric electrodes with the metallized plastic sheets.

When a voltage in the order of 100 V is applied across the overlapping electrode plates, they adhere to each other through electrostatic adhesion. As a result, the maximum holding force i.e., the tensile force needed to ply the plates apart longitudinally increases. In this *engaged* state, the magnitude of the holding force is dictated by the applied voltage (Figure 3.1B). When the clutch is *disengaged* by removing the high voltage, it recovers its initial mechanical properties within 40 ms (Figure 3.1C).

The steps involved in the fabrication of the haptic device are as follows:

- Each clutch consists of three pairs of dielectric-coated electrodes that were interleaved in an interdigitated architecture. The electrodes (150 mm × 35 mm) are 15 µm biaxially-oriented polyethylene terephthalate that are metallised on one surface.
- The metallised surface is coated with a 20 µm layer of high- κ dielectric ink, a ferroelectric composition of Barium Titanate and Titanium Dioxide (Luxprint 8153, DuPont).
- The dielectric is oven-cured at 140 °C for 60 min. Post-curing, the solid dielectric that remains is 10 µm thick.
- The non-metallised surface of each electrode is bonded to a 120 µm sheet of polymethyl methacrylate (PMMA).
- Each of the three pairs of interleaved electrodes are overlapped with their dielectric surfaces in contact. By virtue of the interdigitated architecture, one electrode of each pair is maintained at high voltage with respect to its paired electrode that is grounded when the clutch is engaged.

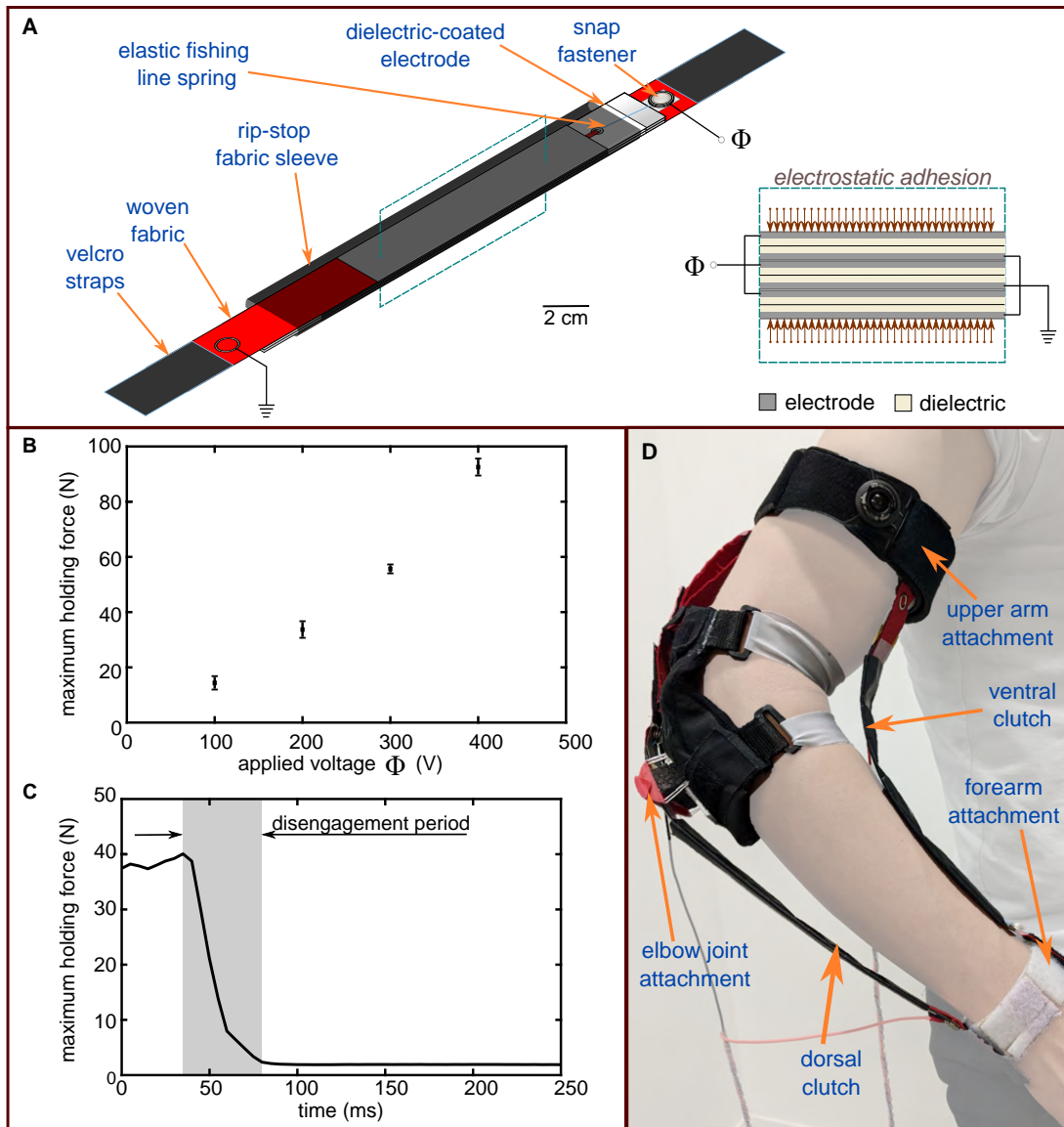


Figure 3.1 – Wearable haptic system to train users for motor activities. (A) Design and composition of the fabric-based electroadhesive clutch. When a high voltage Φ is applied across the dielectric-coated electrode plates, the clutch engages and the clutch plates adhere to each other, thus increasing the maximum holding force. (B) The maximum holding force of the clutch is proportional to the applied voltage. Each data point is the mean value of five measurements trials and the error bars represent one standard deviation from this mean. (C) When the clutch is disengaged by removing the voltage, the adhesion decreases, and the time required for the holding force to drop (gray shading) is measured as the disengagement time. (D) The wearable system is composed of two clutches, one each on the ventral and dorsal faces of the human arm. The clutches are held in place with the help of attachment straps on the forearm, the elbow joint, and the upper arm. The ventral clutch restricts elbow extension and the dorsal clutch restricts elbow flexion.

A fabric-based elbow haptic sleeve for motor training

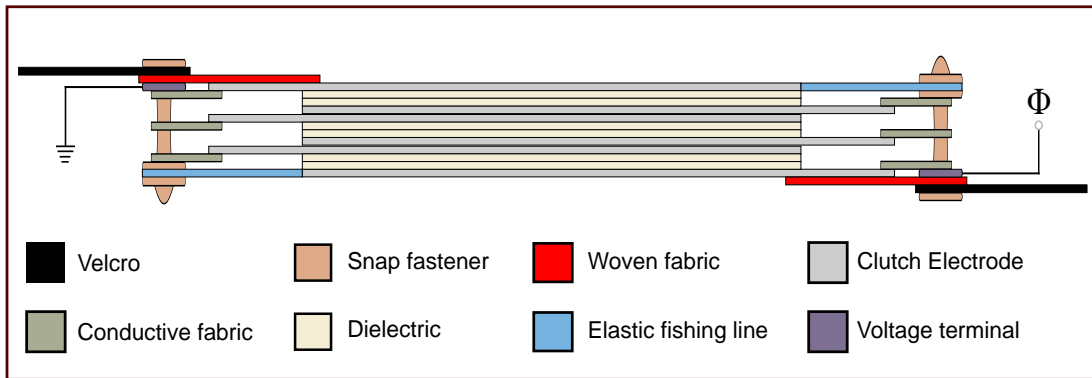


Figure 3.2 – Cross-sectional view of one electroadhesive clutch. Each clutch consists of three pairs of dielectric-coated electrodes that are interleaved in an interdigitated architecture. By virtue of the interdigitated architecture, one electrode of each pair is maintained at high voltage with respect to its paired electrode that is grounded when the clutch was engaged.

- Therefore, the two sets (high voltage and ground) of three electrodes that are maintained at the same voltage are bonded together using electrically conductive copper-plated polyester fabric tape (CN-3190, 3M). Each set is adhered to a strip of woven fabric.
- 50 mm long silicon springs (Zim Fluo 0.6 mm diameter elastic fishing line, Autain Pêche) are attached between one electrode set and the woven fabric strip adhered to the other electrode set via bolted snap fasteners.
- A sleeve of rip-stop fabric is used to ensure that the electrodes plates do not move laterally.
- Hook fastener (Velcro) strips are stitched onto the woven fabric to mount the clutches to the forearm and upper arm body attachments.

The clutches are operated by a customized printed circuit board that can apply high voltages when serial commands are sent via Bluetooth from the computer running the motor learning simulations. The net weight of each clutch is 25 g.

The mechanical and electrical properties of the clutches are characterised to determine the holding force capacity and the time required for the clutches to engage when

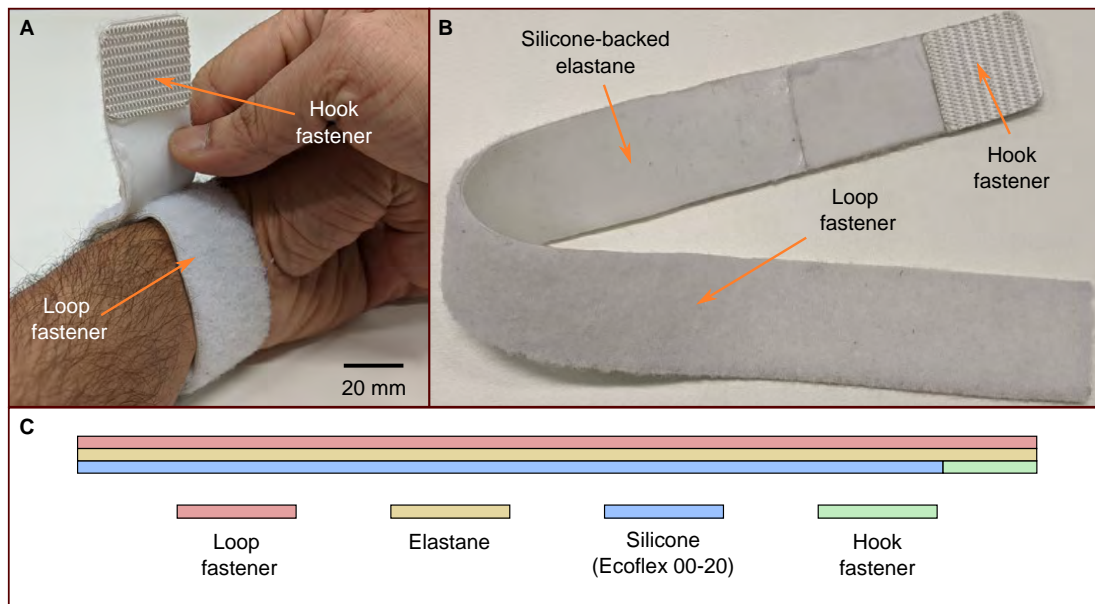


Figure 3.3 – Forearm and upper arm attachments straps. (A) The attachment is wrapped around the arm and tightened by mating the hook and loop fasteners. (B) Each attachment strap is composed of a loop fastener exterior that is bonded to a silicone-backed elastane layer. The silicone layer ensures that the attachment does not slip along the arm. (C) The cross-section of the attachment strap shows its different layers.

A fabric-based elbow haptic sleeve for motor training

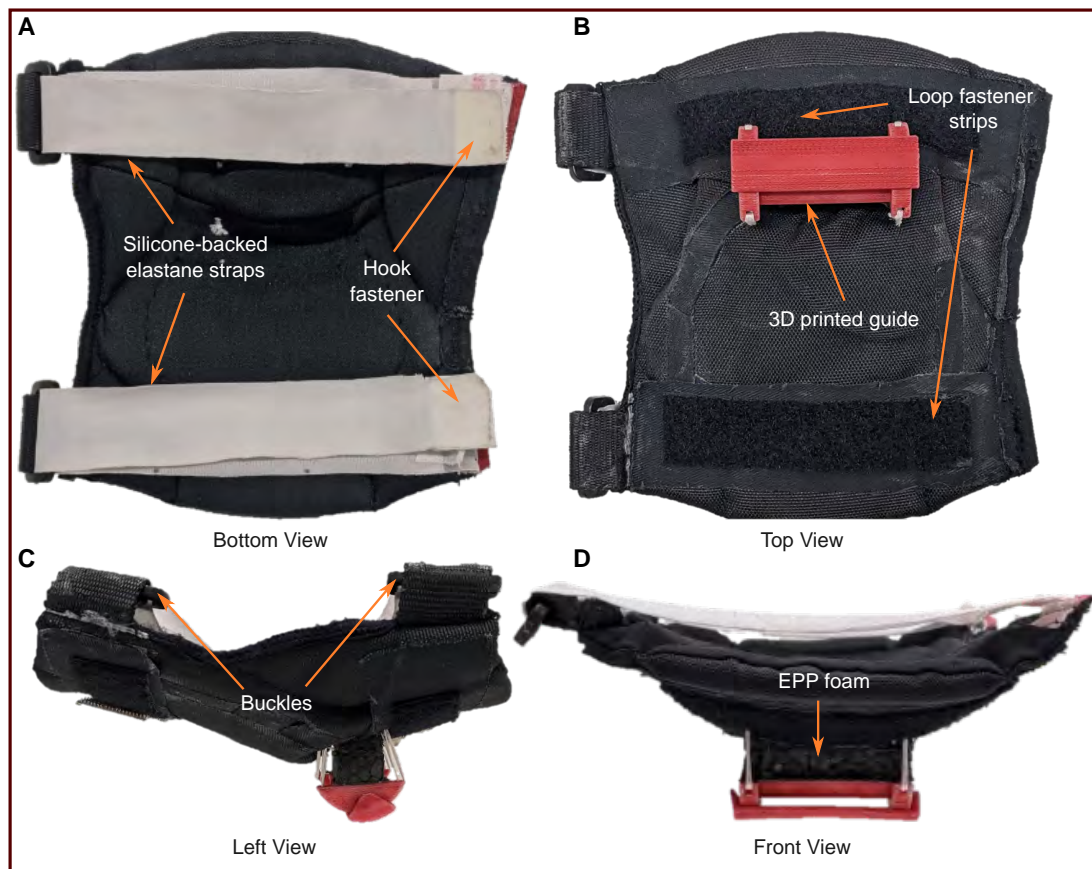


Figure 3.4 – Different views of the foam-padded fabric elbow joint attachment. (A) The interior surface of the elbow attachment, which is in contact with the skin, is fashioned out of an off-the-shelf hockey elbow pad. The silicone-backed elastane straps are wrapped around the forearm and upper arm. (B) A 3D printed guide ensures that the dorsal clutch does not get displaced laterally during elbow extension and flexion. The hook fastener at the end of the silicone-backed elastane straps mates with the loop fastener sewn onto the exterior of the foam-padded attachment. (C) The straps pass through buckles that are sewn on to the sides of the foam-padded attachment. (D) A block of expanded polypropylene (EPP) foam separates the 3D printed guide from the elbow foam-padding to maintain a gap between the forearm and the dorsal clutch.

activated by the printed circuit board. The maximum holding force of each clutch is measured by performing force-displacement tests with a materials testing machine Instron 5965 (Instron, Norwood, MA, USA). The ends of the clutch are fixed to the vices of the tensile tester. Each of the three clutch pairs have an initial dielectric overlap area of $120 \times 35 \text{ mm}^2$. The clutch is engaged at different voltages (100 V, 200 V, 300 V, and 400 V) and loaded in tension at a rate of 10 mm s^{-1} . The maximum holding force is reported for each voltage as an average of five measurement trials. To determine the clutch disengagement time, the clutch is initially fixed between the vices of the tensile tester and then engaged at 250 V. The clutch is loaded in tension until it reached the maximum holding force at which point the clutch is disengaged by setting the applied voltage from the board to zero. At the same time, a serial command is sent to the tensile tester to register the time of disengagement. The disengagement characteristics are reported by averaging the precipitating holding force measurements for three trials. The disengagement time is measured by computing the 90 % drop from the initially measured maximum holding force corresponding to the applied voltage.

The electroadhesive clutches are designed to block the elbow joint. The elbow joint is a hinge-type joint. Hence, the motion of the elbow joint can be blocked in a targeted manner by having one clutch each to block the flexion and extension of the forearm about the upper arm, without affecting the mobility of the remaining body. To block forearm extension and flexion independently, one clutch is attached to the ventral face of the arm and another to the dorsal face, respectively. Each clutch can be extended longitudinally from its rest length by virtue of low stiffness springs, which ensures that the user does not experience any hindrance to natural mobility when haptic feedback is not applied. When the voltage is applied, the electrostatic adhesion prevents further longitudinal extension of the clutch and thus, constrains joint rotation.

The perception of the haptic feedback is quantified by the magnitude of the holding force of the EA clutches. This magnitude is dependent on the dimension of the clutch plates, the dielectric thickness, the number of the clutch pairs and the applied voltage. Perception of the haptic devices can be tuned by changing any of these parameters. The ventral and dorsal clutches are worn by placing them between body attachments that are anchored to the forearm, the elbow joint, and the upper arm (Figure 3.1D). The forearm and the upper arm attachments are made of long strips of elastane bonded

to loop fastener strips (Velcro) on the exterior and a layer of silicone (Ecoflex 00-20, Smooth-On) on the interior (Figure 3.3). Once the clutches are mounted, a custom dial strap with a BOA tightening system (3M ACE Brand, MN, USA) is worn over the upper arm attachment to secure the anchoring. The manufacturing process of the forearm and upper arm attachments involves bonding the elastane to a membrane of cured Ecoflex 00-20 by first, casting an uncured layer of Ecoflex 00-20 on the elastane, then, placing the cured membrane on top of the uncured layer and finally, oven-curing the entire composite. This part of the process was adapted from earlier work carried out by colleagues [166]. The Ecoflex is comfortable and adheres to human skin. The loop fastener on the body attachment mates with the hook fastener of each clutch. The elbow joint attachment is necessary for the functioning of the dorsal clutch. A semi-cylindrical 3D printed guide is sewn onto the pad at the elbow joint to allow for longitudinal extension of the dorsal clutch (Figure 3.4). Two inertial measurement units (IMU, by Xsens Technologies) are attached to the forearm and upper arm body attachments to measure the elbow angle.

3.2.2 Motor learning to teleoperate a drone

The applicability of the EA haptic sleeve is assessed as a teaching aid for drone teleoperation tasks. User errors are used as the performance metric to determine skill retention and transfer. The experiments consist of two drone teleoperation tasks - path following to examine the effect of haptic training on the retention of motor skills, and waypoint navigation to determine the transfer of those skills (Figure 3.5A). Both tasks are frequently used methods in the context of drone teleoperation. Path following is often employed to navigate drones through long, narrow pipelines for maintenance and inspection or navigate through cluttered environments that are inaccessible to humans. Waypoint navigation is commonly used to help drones map areas of interest or carry out aerial monitoring [114]. For the path following motor task, subjects are asked to control the altitude of a drone flying through a cylindrical tube with multiple vertical bends while avoiding collisions with the walls. For the waypoint navigation motor task, subjects are asked to control the altitude of a drone through a series of rings positioned at different heights. The performance of the path following task is computed by measuring the altitude error with respect to the desired centreline

of the tube throughout its length. The performance of the waypoint navigation task is computed by measuring the difference in height between the drone and the centre of each traversed ring. Waypoint navigation is chosen for the skill transfer test because it is similar to path following. Greater task similarity between the skill retention and transfer tests improves the chances of skill transfer. Despite their similarities though, waypoint navigation provides users more freedom in terms of drone movement than path following as the performance is only evaluated at discrete intervals. However, this additional freedom comes at the risk of increased movement errors if the user does not retain and transfer the necessary skills to control the drone.

There is a linear mapping between the elbow angle measured by the IMUs and the altitude of the simulated drone (Figure 3.5C). The IMU readings of the elbow angle are continuous i.e., they are non-discrete. The amplitude limits are determined by initially measuring the elbow angles for each subject at maximum forearm flexion and extension and then, scaling the altitude limits of the drone in the simulated environment to match the elbow angle limits. The path following task consists of three phases - baseline, training, and evaluation, while the waypoint navigation tasks consists of two phases - baseline and evaluation. In chronological order, subjects perform the baseline phase of waypoint navigation, the baseline, training, and evaluation phases of path following, and finally, the evaluation phase of waypoint navigation (Figure 3.5D). The baseline and evaluation phases of both the waypoint navigation and path following tasks consist of three sessions each, during which subjects receive only visual feedback from the drone's camera in first-person view (FPV) via a desktop display. Cubic splines are used to produce the reference trajectories for the baseline and evaluation phases of both tasks. The tubes for the training phase of the path following task are produced with sine curve reference trajectories. This is due to the periodic nature of sine curves, which allow participants to become acclimatized to the nature of the experiment. Since each sine curve is defined by a specific combination of an amplitude and a wavelength, three amplitudes α (0.5 m, 1 m, and 1.5 m) and three wavelengths λ (8 m, 10 m, and 12 m) are used to produce nine distinct tubes. Prior to the commencement of the human subject studies, the chronology of the training sessions is set by randomizing the order of the amplitude and wavelength combinations (Figure 3.5B). This is done to prevent biasing effects due to amplitude or wavelength. This randomization is only performed once, and the chronological order

A fabric-based elbow haptic sleeve for motor training

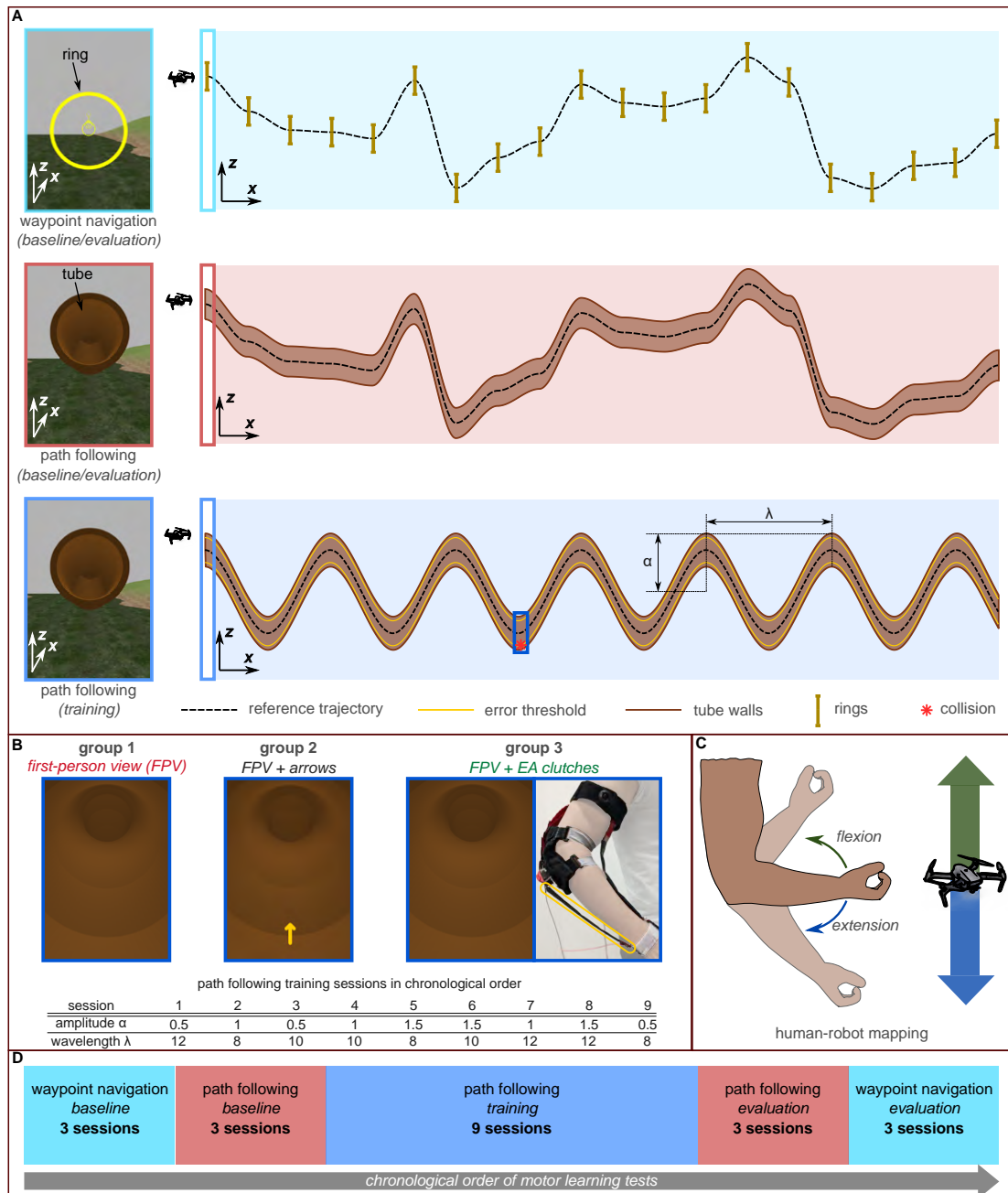


Figure 3.5 – Experimental pipeline for motor learning. (A) Subjects perform two motor tasks - waypoint navigation (rings) and path following (tubes). Cubic splines produce reference trajectories for baseline and evaluation phases of both tasks while sine curves defined by amplitude (α) and wavelength (λ) are used for the training phase of path following. (B) Subjects in each group receive differentiated feedback when they traverse an error threshold within the training phase tubes: first-person view (FPV), FPV + arrows, or FPV + EA clutches. The training sessions are listed chronologically with the α and λ values. (C) A linear mapping is made between the subject's elbow angle and the drone's altitude. (D) The experimental pipeline is shown in chronological order.

is maintained for all subjects. During the training phase, subjects receive additional sensory feedback and are grouped accordingly: group 1 - FPV; group 2 - FPV with yellow arrows indicating corrective action; and group 3 - FPV with EA clutches providing haptic feedback to block elbow joint rotation (Figure 3.5B). An error threshold of 0.4 m is set above and below the centreline of the training tubes, which is not visible to the subject. Whenever subjects in groups 2 and 3 fly the drone past this threshold, they receive the additional sensory feedback (arrows/EA clutches) to prevent them from colliding with the tube wall. For group 2, the arrows point downward when the drone is close to the ceiling, and they point upward when the drone is close to the floor. Similarly, for group 3, the dorsal clutch blocks elbow flexion to prevent ceiling collisions and the ventral clutch blocks elbow extension to prevent floor collisions.

3.2.3 Simulation framework for drone teleoperation

The drone flight tasks are simulated using Gazebo, an open source robotic simulator [79]. Gazebo provides 3D visual scene rendering and simulated on-board sensors, such as RGB cameras. The simulation environment and drone model are based on previous work carried out by colleagues on machine-learning-based multi-drone control [149]. For the flight tasks, single-integrator dynamics are used to move the drone through the environment. The drone flight are restricted within the x-z plane and moved forward at a constant speed of 5 m s^{-1} . For each of the three baseline and evaluation sessions of waypoint navigation, a set of 20 rings of 1 m diameter each are generated in the environment. The rings are spaced at equal intervals of 4 m along the x-axis with the openings facing the drone's direction of travel. For each session, the reference trajectory passing through the ring centres is created using cubic spline, such that the spline slope is zero at the ring centres. Furthermore, the z-position of the ring centres is constrained to remain between 9 m and 11 m above the ground. For the baseline and evaluation sessions of path following, 1 m diameter tubes measuring 76 m in horizontal length are rendered in the same x-z plane as the drone, appearing 4 m in front of it. The centreline of each tube, which is the drone's reference trajectory is also produced using cubic splines. The trough and the peak of the trajectory is constrained to 9 m and 11 m respectively. For the training sessions, 1 m diameter tubes measuring 76 m in horizontal length are produced with tube

centreline reference trajectories as sine curves. To generate nine distinct tubes, nine distinct combinations of amplitude and wavelength are used. The three amplitudes values are 0.5 m, 1 m, and 1.5 m, and the three wavelength values are 8 m, 10 m, and 12 m.

3.2.4 Human subject study

A total of 30 adult subjects (ages between 23 and 42, mean = 29.86, standard deviation = 4.32) are recruited, primarily from the university. Each of the subjects are healthy, have normal hearing and normal or corrected-to-normal vision. None of the subjects have prior knowledge of the tasks they are expected to perform. They are randomly assigned to the three groups with 10 subjects each (6 men, 4 women in each group). The subjects provide written informed consent, and the study is approved by the EPFL Human Research Ethics Commission. Before the motor learning studies are performed, preliminary psychophysical measurements are made to ascertain the Just Noticeable Difference in terms of the holding force needed to constrain their elbow flexion and extension. The applied DC voltage is directly proportional to the maximum holding force. A voltage value of 300 V corresponding to the results of the Just Noticeable Difference is used as the operating voltage for the engagement of the clutches during the experiments. The dimensions of the haptic devices are determined *a priori* by using the anthropometric data collected from 10 individuals, specifically, their forearm length, their upper arm length, and the changes in length on the ventral and dorsal arm faces associated with forearm extension and flexion about the upper arm respectively. While the haptic devices are robust to repeated usage, the elastic fishing line used as the low-stiffness spring can become brittle at the knots, as is often the case with some types of vulcanized rubber. To prevent any deleterious effect as a result of this changing mechanical property, the springs are replaced after every 5 subjects. The clutch plates are operated at a voltage that would not cause electrical shorting. To prevent the accumulation of surface charges on each clutch plate due to the DC voltage operation, the polarity of the clutch plates is reversed for each subject after every session of each experimental phase.

3.2.5 Statistics

All analysis on the data gathered from the simulated flight tasks is carried out in MATLAB 2019b (Mathworks, MA, US). The paired t -test is used when comparing a pair of normally distributed sets of data subjected a single condition, here the effect of the training condition for each group. To compare three or more groups of normally distributed data obtained from different sample populations, an Analysis of Variance (ANOVA) needs to be performed first to ascertain whether there are groups of data that are significantly different from other groups of data. After ascertaining these differences, a post hoc t -test is performed, whereby the pairwise t -test statistics are corrected to avoid minimise the occurrence of false positive results. A repeated measure ANOVA is required when working with multiple sets of data collected for the same population, but subjected to different treatments. A paired-sample t -test is performed to compare the performance errors of baseline and evaluation phases for each group for both path following and waypoint navigation tasks. To compare the differences between groups for the same phase (baseline and evaluation of each task), a one-way ANOVA followed by *post-hoc* Holm-Sidak correction t -test is employed. The same method is used for the analysis of the path following training phase, where statistical comparisons are made between groups for specific amplitude or wavelength values. For the same group, comparisons are performed for changing amplitude or wavelength values by carrying out a repeated measures ANOVA followed by a *post-hoc* Holm-Sidak corrected t -test. [15]. Each of the significance tests are performed by assuming a significance level of $p=0.05$.

3.3 Results

3.3.1 Acquisition and retention of motor skills

Subject performance errors are measured for both teleoperation tasks and the temporal changes in their performance describe the motor learning characteristics of each group (Figure 3.6A). Differences in performance errors between groups for the same task phases reveal the effects of differentiated feedback provision. The performance errors of the path following task are compared to understand how each of the

groups attempt to acquire and retain motor skills specific to this task (Figure 3.6C). Subjects in groups 2 and 3 commit fewer errors (32.89 % and 37.56 % respectively) in the evaluation phase compared to the baseline phase for the path following task. On the other hand, subjects in group 1 commit 12.65 % more errors during the evaluation phase of path following compared to the baseline phase. A paired t -test show that the performance of subjects in group 1 (FPV) deteriorate from baseline to evaluation for the path following task indicating that the training phase between the baseline and evaluation phases do not benefit the subjects and may even be deleterious to them ($t = -2.535$, $p < 0.05$). On the other hand, subjects in group 2 (FPV + arrows) and group 3 (FPV + EA clutches) perform significantly better in the evaluation phase compared to the baseline, which implies that they are able to learn the task over the course of training (group 2: $t = 23.76$, $p < 0.01$; group 3: $t = 10.041$, $p < 0.01$). Indeed, a one-way analysis of variance (ANOVA) followed by a *post-hoc* Holm-Sidak corrected t -test shows that there are no significant differences between the performances of the three groups at baseline ($F_{2,27} = 0.34$, $p = 0.71$). This outcome rules out any biases that might have been introduced by relative differences in subject task expertise prior to training. On the other hand, the same statistical treatment reveal that the performance errors of subjects in group 2 and group 3 are lower than those of subjects in group 1 after evaluation, thus showing the retention of motor skills after training ($F_{2,27} = 84.93$, $p < 0.01$). During the training phase of path following, the subjects of each group receive differentiated feedback as explained earlier. In addition to the received sensory feedback, the performance of each group are subjected to the effects of different amplitude and wavelength combinations that define each tube's reference trajectory (Figure 3.6D). For each group, these effects are resolved by averaging their performance errors of a set of three training sessions. Each set has the same amplitude (0.5 m - sessions 1, 3, 9; 1 m - sessions 2, 4, 7; 1.5 m - sessions 5, 6, 8; Figure 3.6E) or the same wavelength (8 m - sessions 2, 5, 9; 10 m - sessions 3, 4, 6; 12 m - sessions 1, 7, 8; Figure 3.6F). For a given amplitude or wavelength, each comparison is made between groups using a one-way ANOVA followed by a *post-hoc* Holm-Sidak corrected t -test. Groups 2 and 3, which receive augmented visual and haptic feedback, respectively, perform significantly better than group 1 for each training set grouped by amplitude ($\alpha = 0.5$, $F_{2,27} = 20.64$, $p < 0.01$; $\alpha = 1$, $F_{2,27} = 16.6$, $p < 0.01$; $\alpha = 1.5$, $F_{2,27} = 12.33$, $p < 0.01$). Similar results are obtained when comparing the performance errors of

groups 2 and 3 with respect to group 1 for training sets grouped by wavelength ($\lambda = 8$, $F_{2,27}=14.75$, $p < 0.01$; $\lambda = 10$, $F_{2,27}=23.5$, $p < 0.01$; $\lambda = 12$, $F_{2,27}=22.18$, $p < 0.01$). These two results pertaining to the amplitude and wavelength effects on group performance errors show that the additional sensory feedback alerted subjects in groups 2 and 3 in time to switch between extension and flexion before colliding with the tube walls. A repeated measured ANOVA followed by a *post-hoc* Holm-Sidak corrected *t*-test shows that subjects in each group perform progressively worse as the amplitude of the tube reference trajectory increases with observable significant differences (group 1: $F_{2,18}=40.71$, $p < 0.01$; group 2: $F_{2,18}=144.14$, $p < 0.01$; group 3: $F_{2,18}=50.75$, $p < 0.01$). This is expected given the increasing difficulty to alternate between forearm extension and flexion at larger elbow angles. The *post-hoc* Holm-Sidak corrected *t*-test values for pairwise comparisons within-group for different amplitudes are reported. The repeated measures ANOVA did not reveal significant differences in performance for group 1 for varying wavelengths ($F_{2,18}=2.74$; $p=0.09$). However, a repeated measures ANOVA followed by *post-hoc* Holm-Sidak corrected *t*-test reveal that groups 2 and 3 perform significantly better for a wavelength of 12 m compared to 8 m (group 2: $F_{2,18}=4.93$, $p=0.01$; group 3: $F_{2,18}=4.71$, $p=0.02$). The less marked differences in wavelength effects within each group is perhaps due to the chosen drone forward speed. Different drone speeds might have produced more noticeable differences.

3.3.2 Transfer of motor skills

Subjects have to utilize the motor skills garnered during the path following task to improve upon their baseline performance in the waypoint navigation transfer task (Figure 3.6B). A one-way ANOVA with *post-hoc* Holm-Sidak *t*-test corrections establishes no significant differences between the baseline performances of each group, thus reinforcing the absence of expertise bias as shown for the baseline phase results of path following ($F_{2,27}=0.12$, $p=0.88$). While all subjects in each group perform better during the evaluation phase of the waypoint navigation task compared to their baseline, the relative improvement in performance is more pronounced for subjects in group 2 and 3, where the error percentage drop is 42.23 % and 45.64 % respectively, compared to the 9.97 % drop for subjects in group 1. A paired *t*-test shows that the performance errors does not change significantly for subjects in group 1 between the

A fabric-based elbow haptic sleeve for motor training

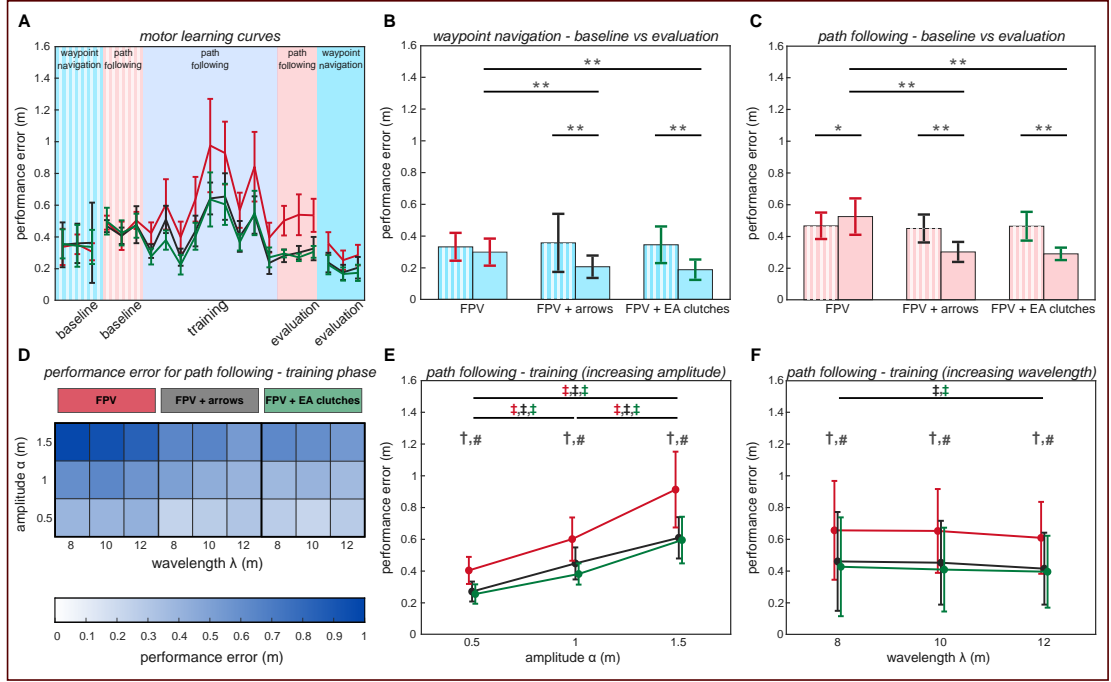


Figure 3.6 – Results from the motor learning human subject study for path following and waypoint navigation. (A) Motor learning curves of each subject group are plotted as a function of mean performance error against experimental phases of both motor tasks in chronological order. Subject groups: group 1 (FPV, red), group 2 (FPV + arrows, black), group 3 (FPV + EA clutches, green); waypoint navigation task - baseline (light blue, striped) and evaluation (light blue, solid) phases; path following - baseline (pink, striped), training (light purple, solid), and evaluation (pink, solid) phases. (B)-(C) Between-group and within-group comparisons of performance errors during baseline and evaluation phases of waypoint navigation and path following tasks, * $p < 0.05$, ** $p < 0.01$. (D) Heat map of group performance errors during the training phase of path following shows the effects of amplitude (α) and wavelength (λ) combinations. (E)-(F) Comparisons between-group and within-group of subject performance during the training phase of path following. Each plotted point is the average performance error of a group for three training sessions with the same amplitude (E) or wavelength (F). † Comparison between group 1 and group 3, $p < 0.01$. # Comparison between group 1 and group 2, $p < 0.01$. ‡ Within-group comparison between different amplitudes or wavelengths colour-coded to match groups, $p < 0.01$. All error bars in this figure show one standard deviation above and below the reported mean performance error.

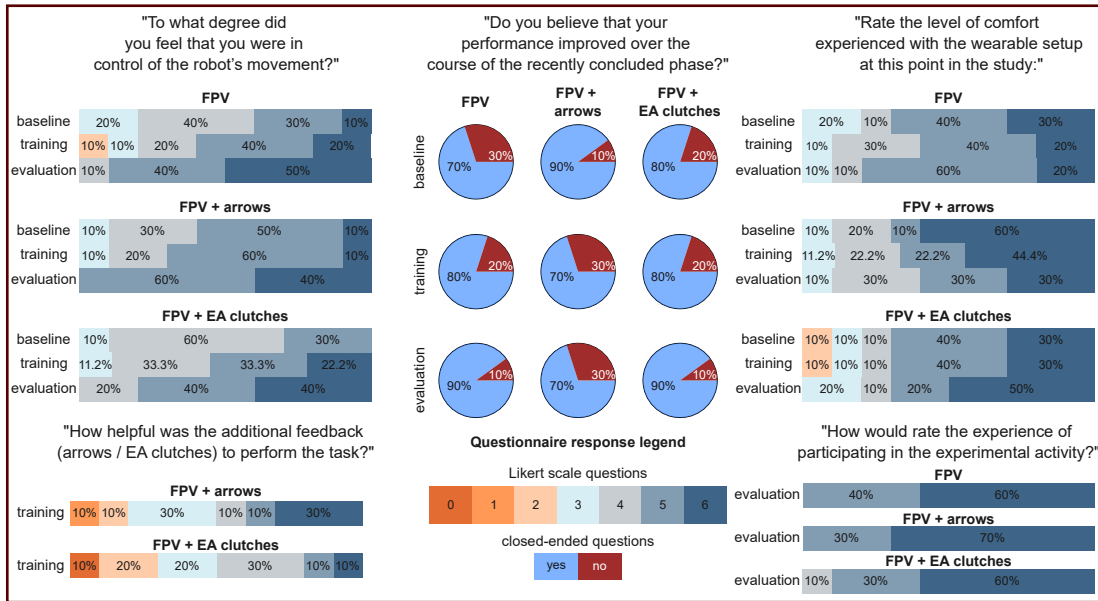


Figure 3.7 – Subject responses to questionnaires filled after the baseline, training, and evaluation phases for path following. Questions posed determine various qualitative aspects of their motor training, including their comfort levels with both the wearable interface and the control of the drone control, as well as their own assessment of performance improvement at the end of each of these phases. At the end of the training phase, subjects in the test groups that receive additional feedback in the form of corrective arrows or EA clutches rate the degree to which this feedback helped them over the course of the phase. Finally, subjects provide an overall rating of their experience in participating in the motor training exercise. With the exception of the yes/no response to the question about their performance self-assessment, responses to all other questions are provided on a 7-point Likert scale between 0 and 6.

baseline and evaluation phases ($t=1.27$, $p=0.23$). This may be attributed to inadequacies in motor skills acquired during the path following task. In the same vein, subjects in groups 2 and 3, who exhibit performance improvement for the path following task, produce similar results for waypoint navigation. There are significant differences between their baseline and evaluation phase performances showing that the skills acquired from path following transfer to waypoint navigation (group 2: $t=3.82$, $p < 0.01$; group 3: $t=7.31$, $p < 0.01$). A one-way ANOVA with *post-hoc* Holm-Sidak *t*-test corrections shows that subjects in groups 2 and 3 perform significantly better during the evaluation phase compared to group 1, thereby showing the relative benefits of having been trained with additional sensory feedback ($F_{2,18}=0.12$, $p < 0.01$).

3.3.3 Subjective assessment of drone teleoperation and sleeve comfort

Each subject's comfort is assessed in learning to control the drone while wearing the haptic sleeve using questionnaires. Since differentiated feedback is only provided during the path following phase, subjects fill three questionnaires, each corresponding to the three phases of path following - *baseline*, *training*, and *evaluation* at the conclusion of each respective phase. Subjects are asked to assess the degree to which they were in control of the drone's movement, their level of comfort with the haptic interface, and a self-evaluation of their performance improvement over the recently concluded phase by indicating a grade on a 7-point Likert scale (0-6). For all groups, at least 80 % of the subjects rate both their degree of control over the drone's movement and their level of comfort with the wearable system between 4 and 6 (both included) for all three phases (Figure 3.7). Subjects of groups 2 and 3 are asked to rate the helpfulness of the additional sensory feedback (arrows and EA clutches) in performing the tasks as part of the training questionnaire. Despite the quantitative results which indicate that subjects in these two groups improve upon their baseline performance, only 50 % of them find the additional sensory feedback (arrows or EA clutches) to be qualitatively helpful. It is interesting that participants do not perceive the feedback as qualitatively helpful and yet, they tend to perform better. The rather counter intuitive response from the subjects may be due to the additional feedback creating sensory overload, but this claim cannot be verified as part of this study. For the self-evaluation of performance improvement subjects could answer "Yes" or "No". For group 1, the percentage of subjects who respond to their self-evaluation of performance improvement as "Yes" increased (70 % - "Baseline"; 80 % - "Training"; 90 % - "Evaluation"). On the other hand, the percentage reduce for group 2 (90 % - "Baseline"; 70 % - "Training" and "Evaluation"). The percentage of affirmative responses increase for group 3 over the phases (80 % - "Baseline" and "Training"; 90 % - "Evaluation"). In the evaluation questionnaire for all groups, subjects are also asked to rate their overall experience in participating in the experimental study. All subjects rate their overall experience between 4 and 6 in participating in the experiments.

3.4 Conclusion

This chapter describes a wearable haptic sleeve that uses fabric-based EA clutches to impart kinesthetic feedback by blocking body joint movement and experimentally show its functionality as a teaching aid for motor activities in drone teleoperation tasks. This study examines and compares the effects of providing haptic feedback for motor training with different forms of visual feedback.

The results show that subjects in the control group, who receive FPV visual feedback do not acquire and retain sufficient motor skills to improve path following performance and subsequently, are unable to perform better in the transfer waypoint navigation task. Instead, subjects who receive either augmented visual feedback in the form of arrows to correct elbow movement or haptic feedback from the electroadhesive haptic sleeve to physically block elbow rotation, display performance improvement from baseline to evaluation for both path following and waypoint navigation. This performance improvement could be attributed to users relying on both types of feedback to determine their errors and consciously learning to avoid them. This conclusion is reinforced by the observable improvement in performance level with respect to the control group immediately after receiving additional haptic/visual feedback. While this additional feedback assists subjects in identifying and avoiding errors during the training phase, their newly acquired motor skills are retained even after the training phase. This shows that the subjects do not become overly dependent on the additional feedback.

The increase in performance errors with the amplitude of tube reference trajectories for all subject groups can be ascribed to the difficulty in rapidly alternating between forearm extension and flexion, especially when approaching the maximum and minimum elbow angle limits. Indeed, the performance errors of specific training sessions on average are higher for all groups than individual sessions within the baseline and evaluation phase due to the training tubes having larger amplitudes. The relatively small differences in performance for all groups with changing tube wavelength may be due to the chosen drone speed. For higher drone speeds, one might expect to see greater performance differences with fewer errors being committed for larger tube wavelengths.

The comparable beneficial effects of haptic feedback and of corrective arrow displays are noteworthy because augmented visual feedback is generally accepted as a benchmark in feedback-based training. Indeed, there are no observable statistically significant differences between the two forms of additional feedback based on the data collected during the subject studies. While the haptic feedback is just as effective as a teaching aid as augmented visual feedback, haptic feedback could be qualitatively more helpful than augmented visual feedback when provided directly to the part of the body responsible for erroneous motion. This is because concentrating the relay of augmented sensory feedback through a single feedback channel (vision) can severely increase the risk of sensory overload over prolonged periods of robot teleoperation [170]. Furthermore, haptic feedback could be used instead of vision when visual feedback from the robot is occluded [170, 91]. Certainly, visual occlusions are not uncommon when operators need to inspect infrastructure, for example maintenance after the occurrence of a natural disaster. In these instances, first-person visual perspective may not reveal concealed structures in the robot's periphery due to a variety of reasons, including insufficient lighting. Another possibility is that visual feedback may be cut off from the operator intermittently due to poor transmission. In addition, haptic feedback can be provided to the visually impaired. In this work, the haptic feedback is binary i.e., either it behaved as a compliant cloth or it blocked the range of motion. In the future, lightweight variable stiffness technologies which use low melting point materials and shape memory materials that can provide a range of blocking forces could also be employed for different training tasks. Furthermore, extension of this technology to other joints, such as the wrist and fingers, could be used for more complex teleoperation and rehabilitation tasks.

4 Multi-joint wearable haptic sleeve for telerobotics with reduced visual feedback

This chapter introduces a wearable haptic sleeve that encompasses both the elbow and the wrist joints. The results presented in the previous chapter show that the wearable elbow sleeve helps users learn path following tasks when they control the altitude of the drone. In the previous study, users receive visual feedback in first-person view from the camera mounted on the drone. In this chapter, users are trained to perform a drone obstacle avoidance task where they control the drone's movement in the horizontal plane using their elbow and wrist joint rotations. The study presented in this chapter examines the effectiveness of the haptic feedback provided by the electroadhesive clutches when the visual feedback is compromised due to poor depth perception.

Publication Note: The work presented in this chapter is adapted from:

V. Ramachandran, M. Macchini, and D. Floreano, "Arm-wrist haptic sleeve for drone teleoperation", in IEEE Robotics and Automation Letters, (**submitted**) June 2021

4.1 Introduction

Robots are becoming a pervasive presence in our everyday lives, ranging from domestic floor cleaners to heavy construction machinery [146]. Drones in particular are used by a variety of people, including hobbyists for adventure photography and

Search-and-Rescue professionals to inspect debris [41, 19]. While robot autonomy is a burgeoning area of research, presently, human operators are still needed to control distally - located robots for most tasks [47]. Indeed, teleoperation is the predominant method of operating drones for civilian applications and conventionally, they are operated using hand-held controllers, such as joysticks [41]. Professional pilots who are able to control drones effectively using these conventional controllers require a considerable amount of training to use them. However, these interfaces are not intuitive for novice users. The growing use of drones by non-professionals mandates more intuitive interfaces [18]. In recent years, researchers have developed wearable interfaces that map natural body movements to drone commands. These interfaces are more intuitive than hand-held controllers, provide a more immersive experience during teleoperation, and require very little time for users to train with [139].

Teleoperation using wearable interfaces, also called wearable teleoperation, of drones is bidirectional. The operator's body movements control drone motion and the robot provides information to the operator about its state and the state of its surroundings through sensory feedback [140, 142]. The sensory feedback is provided as some combination of three channels – visual, auditory, and haptic feedback. Distributing the information from the robot into multiple channels rather than concentrating it through one channel can help lower the cognitive load on the teleoperator [71, 174]. Visual feedback is often treated as the most essential feedback channel that determines the performance of teleoperation. Nonetheless, haptic feedback has specific benefits that can complement and/or supplement visual feedback [159]. For teleoperation training, wearable haptic interfaces, both tactile and kinesthetic, can apply targeted forces at specific parts of the operator's body that are responsible for the control of the robot to guide their body movement. Haptic feedback is vital when visual feedback is obscured either due to visual occlusions in the robot's environment or due to the operator's poor perception of depth [91].

Most haptic interfaces used for telerobotic applications are fixed to the ground [52]. As a result, they only allow users a limited range of motion and consequently, their applicability is limited too. Wearable haptic interfaces circumvent the problem of reduced mobility by being affixed to the user's body. However, several wearable interfaces use heavy actuators to generate force feedback [116]. The bulkiness and

Multi-joint wearable haptic sleeve for telerobotics with reduced visual feedback

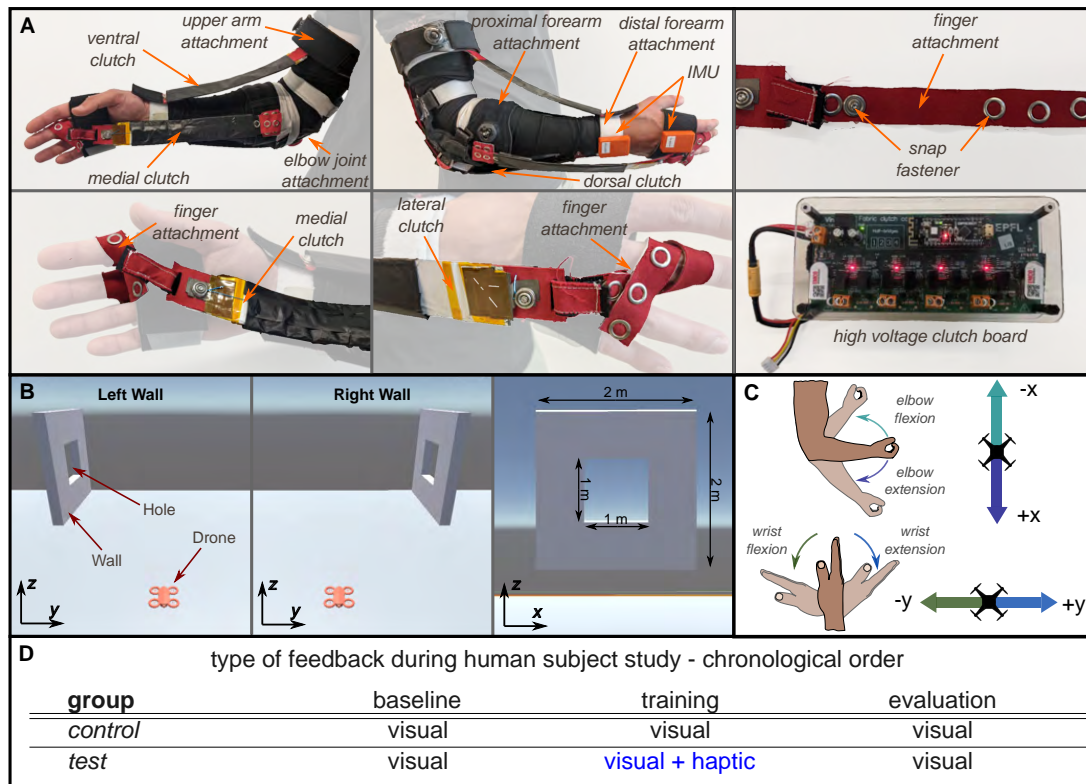


Figure 4.1 – Experimental setup of the elbow and wrist haptic sleeve. (A) The wearable haptic sleeve consists of four electroadhesive clutches to restrict elbow and wrist joint rotations. The clutches are mounted on the user using body attachments. The arm movements are measured using inertial measurement units (IMUs). The clutches are activated independently using a customised printed circuit board. (B) Wearable haptic sleeve to help users to perform obstacle avoidance during drone teleoperation. The obstacles are walls with a hole in the centre. (C) The drone is controlled through a linear mapping between the user's elbow and wrist joint angles and the drone's position in the horizontal plane. (D) The subjects are divided into two groups based on the type of feedback that they receive. There are three experimental phases in the human subject study.

the form factor of these actuators re-introduces mobility problems and can cause fatigue over prolonged use. Actuated haptic interfaces are often used for haptic guidance-based training for teleoperation, a method that has been demonstrated to help users learn motor tasks in previous studies [104, 28]. However, these studies also suggest that trainees can become overly dependent on the haptic guidance. While their performance improves during training when they receive haptic feedback, this elevated performance precipitates when the haptic feedback is removed. In such

cases, the haptic feedback becomes a crutch that curtails motor learning.

Recent studies show the use of lightweight, portable, tactile devices as very effective interfaces to perform teleoperation even when visual feedback is compromised [91, 170]. While these tactile haptic interfaces can indicate to the operator when they are in the vicinity of obstacles, these interfaces are not necessarily capable of completely arresting operator movement to prevent collisions from occurring, whereas kinesthetic haptic interfaces may be capable of doing so [179, 59, 131].

The preceding chapter demonstrates the successful use of a lightweight, fabric-based wearable haptic sleeve that teaches users to perform a drone path following task [132]. The sleeve consists of two electroadhesive clutches attached to the ventral and dorsal faces of the human arm to restrict forearm extension and flexion about the elbow joint, respectively. Free of heavy actuators, the sleeve has a minimal effect on the user's natural mobility. In the study, the users who receive haptic feedback from the sleeve are able to learn and retain motor skills to perform the path following task, whereas the control group of users who only receive visual feedback from the drone's camera are unable to learn the task within the same time. This chapter concludes that due to the absence of actuators, users are compelled to identify and correct their errors by themselves without becoming overly dependent on the feedback.

The chapter demonstrates the use of the wearable haptic sleeve that consists of a network of clutches and attachments to block both the extension and flexion of the wrist and elbow joints. This sleeve is used to train users in a drone obstacle task, where the visual feedback is compromised due to poor depth perception. The sleeve helps users perform better by diminishing the number of obstacle collisions during training and facilitates skill retention in the absence of haptic feedback post-training.

4.2 Methods

This section presents the different parts that constitute the experimental study: the design and operation of the wearable haptic sleeve (Section 4.2.1), the setup of the simulation environment to perform teleoperation (Section 4.2.2), and the human subject study to determine the effects of the haptic sleeve on training users to avoid

obstacles during teleoperation with limited visual feedback (Section 4.2.3).

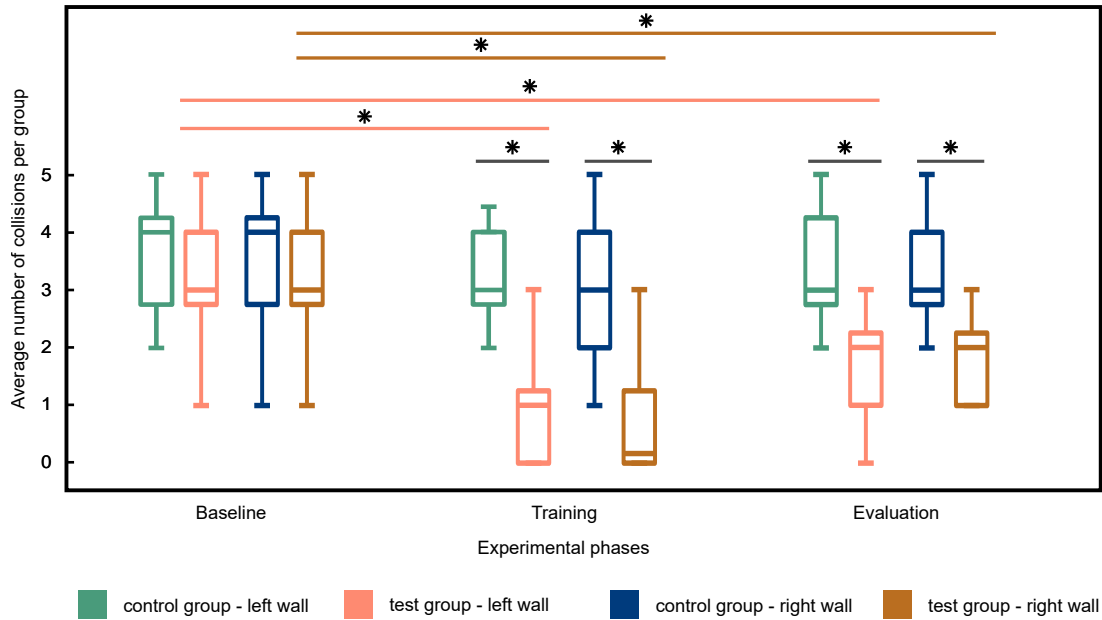


Figure 4.2 – Performance analysis of drone wall collisions for left and right walls. The control and test group performances are measured by computing the median number of collisions that take place per group. These data sets are compared by examining the differences between groups for the same wall in each phase, between walls for the same group in each phase, and between phases for the same group and same wall. $*p < 0.05$

4.2.1 Wearable haptic sleeve

Device design and operation

The sleeve is programmed to restrict the motion of both the elbow and wrist joints. The wearable haptic sleeve consists of four identical electrostatic adhesive clutches - one pair of clutches to restrict the forearm extension and flexion about the elbow joint and a second pair of clutches to restrict the hand extension and flexion about the wrist joint (see Figure 4.1A). This sleeve is an extension of the previously described wearable sleeve that was developed to restrict elbow joint rotation alone. The manufacturing method of the clutches used for the sleeve in this letter are adapted directly from the previous study [132].

Each clutch is a parallel plate capacitor with four interleaved electrode pairs. When a high voltage (~ 300 V) is applied across the electrodes, an electric field is generated between the plates, which causes the plates to adhere to each other. In this state, the clutch is said to be activated. This electrostatic adhesion results in a rapid increase in the tensile stiffness that prevents longitudinal extension. The clutch also consists of a low-stiffness spring in parallel with the interleaved electrodes. When the clutch is deactivated i.e., the applied voltage is set to zero, the interleaved plates can freely slide on top of each other. In this state, the tensile stiffness of the clutch is determined only by the spring stiffness. The electromechanical properties of the clutch are reported in the previous study [132].

The clutches are mounted on the human arm using body attachments (see Figure 4.1A). The elbow clutches require three attachments – distal forearm, upper arm, and elbow joint. The distal forearm and upper arm attachments are used to anchor the ventral and dorsal clutches to block the elbow joint. The elbow joint attachment ensures that the dorsal elbow clutch does not slip out from under the elbow during forearm flexion. The distal forearm attachment and the upper arm attachments are fabricated by coating long strips of elastane on one face with silicone rubber and adhering a strip of loop-type Velcro on the other face. The silicone rubber is used to interface with the human skin because it is comfortable. In addition, an adjustable BOA tightening custom dial strap is used to secure the anchoring of the clutch on the upper arm attachment. The ventral and dorsal clutches have strips of Hook-type fastener that attaches to the Loop-type fastener on the distal forearm attachment and the upper arm attachment.

The wrist clutches, lateral and medial, responsible for restricting the wrist joint, require two attachments – proximal forearm and finger (see Figure 4.1A). The proximal forearm attachment is an adjustable elbow brace with a BOA tightening system and a Loop-type fastener exterior. The finger attachment is a fabric strip coated with the silicone rubber that can be wound around the index finger and adjusted to the length of the user's hand using Hook-and-Loop fasteners and snap fasteners. Both the lateral and medial clutches are fabricated with Hook-type fasteners that mate with the Loop-type fastener exterior on the proximal forearm attachment. The wrist and elbow angles are measured using commercially available inertial measurement units

(Xsens IMUs), which are mounted on the distal forearm attachment and a stretchable Velcro strap that is wrapped around the user's palm.

Driving electronics

Each of the four clutches are activated using a custom designed printed circuit board that requires a 12 V power supply, which is typically provided by a 3-cell Lithium-Ion battery (see Figure 4.1A). The board consists of four H-bridges - well known transistor configurations to drive a bidirectional load from a single power source. Each H-bridge has two independently controlled outputs. Hence, a clutch can be connected either between an output and a ground (for a unidirectional drive) or between two outputs (for a bidirectional drive). When one of the H-bridge outputs is switched on, a high voltage is applied across the clutch to activate it. The high voltage is generated using a commercially available high voltage DC-DC converter. A microcontroller, that operates the H-bridge switching, can be controlled over Bluetooth by means of simple ASCII-based commands ('1', '2', '3', '4') to activate the corresponding clutches. The board is designed to be completely portable, such that users would be free to move unrestricted by cables.

4.2.2 Simulation environment

User are trained to perform a drone-obstacle avoidance task in a simulated environment. For the study, the simulation environment implemented in Unity3D is adapted from recent work carried out by colleagues [91]. Within the environment is a drone that reproduces quadcopter dynamics, which is stabilised using a PID controller (see Figure 4.1B). This drone spawns at an initial height of 1 m above the ground. The user's wrist and elbow joint angles are mapped linearly to the drone's position (see Figure 4.1C). Hand extension and flexion about the wrist joint makes the drone roll to the right and left respectively. Similarly, forearm extension and flexion about the elbow joint pitches the drone forward and backward respectively. The linear scaling factor from the joint angles to the drone's position is chosen such that the user can teleoperate the drone anywhere within the environment. The drone's height is constrained to remain at a constant height above the ground. Each drone is equipped

with orthogonal proximity sensors with a fixed range of 0.7 m. For most inspection tasks in confined spaces, drones need to be navigated around walls and through narrow passages without collisions. The teleoperation task chosen for user training incorporates certain aspects of these inspection tasks. A wall with a hole is placed perpendicular to the line of sight of the user, such that the user is unable to clearly determine the location and dimensions of the hole in the wall (see Figure 4.1B). Shadows are not rendered in the simulation environment to avoid giving fiducial features that might help users ascertain the depth of the wall relative to the location of the drone. The environment has a fixed camera perspective that is relayed to the user as visual feedback during teleoperation. If the drone collides with the wall at any point of time during teleoperation, the wall colour changes to red. If the drone is steered through the hole without colliding with the wall, the wall colour changes to green. Previous psychophysical studies show a relative difference in comfort and strength between hand extension and hand flexion about the wrist joint. Hence, two walls are created - on the left-hand side (*left wall*) and right-hand side (*right wall*) of the user's line of sight to examine any potential differences in their performance. The teleoperation training for one wall is completed before commencing training for the second wall.

4.2.3 Human subject study

A total of 18 adult subjects (ages between 22 and 31; mean = 25.94, standard deviation = 2.79) are recruited for a human subject study to investigate the effect of the wearable haptic sleeve on training users to teleoperate drone through narrow passages with reduced visual feedback. Each of the subjects in this study are healthy, have normal or corrected-to-normal vision, and are right-handed. The subjects provide written informed consent, and the study is approved by the EPFL Human Research Ethics Commission. In chronological order, the task consists of three experimental phases - baseline, training, and evaluation for navigating the drone through the hole in the left wall and the right wall separately using their right-arm's elbow and wrist joint rotations (see Figure 4.1D). The order of the walls, left wall and right wall, is randomized to prevent any biasing effects. Each phase consists of five sessions, which end when the subjects either collides with the wall or passes through the hole. At the commencement of the study, the subjects are explicitly instructed to minimize the

number of collisions during drone teleoperation. The subjects are divided into two groups – control and test. Both groups receive visual feedback from a fixed camera perspective that shows the drone and the wall during all three experimental phases for both the left and right walls. While subjects in both groups don the wearable sleeve during the subject study, only subjects in the test group receive haptic feedback from the sleeve during the training sessions. Subjects in the control group continue to receive only visual feedback from the fixed camera. Haptic feedback is provided to the test group subjects during the training phase when the proximity sensors on the drone detect the presence of the wall. When the wall is detected, only the clutch needed to restrict the specific joint movement to prevent wall collisions is activated. As terminal feedback, the success or failure for each experimental session is indicated by the wall turning green (passage through hole) or red (wall collision) respectively. The subject performance is determined by the average number of drone collisions that occur over the sessions of each phase. In addition, the relative position of the drone with respect to the wall is measured when the drone either passes through the holes or collides with the wall for all phases. A comparative study is made between the test and control groups for each wall as well as for each group between the left and right walls using the aforementioned performance metrics. After performing the teleoperation task phases for each wall, subjects are asked to fill two surveys - one standardised NASA-TLX questionnaire and one customised questionnaire to determine their experience of wearing the haptic sleeve.

4.3 Results

This section summarises the results of the human subject study that examined the effects of haptic feedback as a teaching aid during drone obstacle avoidance tasks when visual feedback was compromised. The section is divided into two parts. Firstly, a comparative performance analysis is provided of the control group and the test group over the experimental phases for each wall (Section 4.3.1). Secondly, the qualitative experiences of subjects in each group are presented based on the data collected from the two questionnaires (Section 4.3.2).

The Shapiro-Wilk statistical test of normality is performed on all the subject data

sets. Since some of these data sets are not normally distributed, non-parametric statistical tests of significance are used to analyse the subject data. Comparisons are made between the subjects' median data using the Kruskal-Wallis test. For each group, comparisons of median data between phases are carried out by the Friedman test. Furthermore, the variances of the data sets of each group for each phase are compared using the Levene test. All the TLX questionnaire responses are compared pairwise using the Kruskal-Wallis test. The null hypothesis for each statistical test of significance is rejected when $p < 0.05$.

4.3.1 Performance analysis of obstacle avoidance

Each subject is required to perform the obstacle avoidance task for five sessions in each experimental phase. Hence, their individual performance for that phase is determined by taking the mean number of collisions over the five sessions. For each wall, the group performance for a particular phase is measured by calculating the median value of the individual performances of that phase (see Figure 4.2). The Friedman test followed by a *post-hoc* Bonferroni correction shows that there is a statically significant difference in the test group's performance between the training and baseline phases as well as between evaluation and baseline phases, but not between the training and evaluation phases for each wall. The same statistical tests show no significant differences in performance between the different phases for the control group for either wall (left wall: $p = 0.88$; right wall: $p = 0.36$). This clearly shows that subjects who receive haptic feedback from the wearable sleeve improve their performance over the course of the training phase and maintain their performance level during the evaluation phase, even in the absence of the haptic feedback. On the other hand, subjects who only receive the visual feedback over the course of all the three experimental phases are unable to correct their errors and their performance do not improve. For both walls, the Kruskal Wallis test shows no statistical differences in baseline performances between the control and test groups for either wall (left wall: $p = 0.46$, right wall: $p = 0.38$). However, the same test reveal statistical differences between the control and test groups for both wall during the training and experimental phases. These results corroborate the earlier observation that the wearable haptic sleeve is a useful aid for operators to avoid drone collisions, especially when the visual feedback is

compromised. There are no measured statistical differences in performance between the left wall and the right wall for either group during any of the phases (baseline, control: $p = 0.94$, test: $p = 0.98$; training, control: $p = 0.84$, test: $p = 0.84$; evaluation, control: $p = 0.93$, test: $p = 0.1$).

The subject data sets are compared for the drone's position along the face of the wall at the time when the drone either collided with it or passed through the hole (see Figure 4.3). The Kruskal Wallis test does not show any significant differences in the median values between the control and test groups for any of the phases in either wall (left wall, baseline: $p = 0.56$, training: $p = 0.5$, evaluation: $p = 0.07$, right wall, baseline: $p = 0.13$, training: $p = 0.06$, evaluation: $p = 0.97$). It does not show significant differences in the median values for the same group and same phase between the left and right walls either (baseline, control: $p = 0.59$, test: $p = 0.64$; training, control: $p = 0.36$, test: $p = 0.64$; evaluation, control: $p = 0.54$, test: $p = 0.24$). The Levene test for comparing variances does not show significant differences in the variance between the control and test groups for the baseline phase for either wall (left wall: $p = 0.43$, right wall: $p = 0.33$; see Figure 4.3A,D). The Levene test shows that there is a significant difference between the groups for both the training and evaluation phases for both walls (see Figure 4.3B,C,E,F). This suggests that not only does the haptic feedback help test group subjects make fewer drone collisions, it also helps them significantly narrow the margin of error as is evident in the smaller spread of data points along the wall compared to their control group counterparts. The Levene test followed by a *post-hoc* Bonferroni correction shows that there is a statically significant difference in the test group's variance between the training and baseline phases as well as between evaluation and baseline phases, but not between the training and evaluation phases for each wall. The Levene test shows that there is no statistically significant difference in the control group's variance between any of the three phases for each wall (left wall: $p = 0.88$, right wall: $p = 0.36$).

4.3.2 Questionnaire responses

The results of the customised questionnaire ascertain the subjects' experiences of comfort in performing the teleoperation task while wearing the haptic sleeve (see Figure 4.4). This questionnaire consists of 6 questions, 5 of which are Likert scale

questions (0 to 6) and 1 is closed question (yes/no). At the end of the experiment, only 66.6 % of the control group subjects feel that they had been in control of the robot's movement for both walls (between 4 and 6) whereas 100 % of the test group subjects feel that they had complete control (see Figure 4.4A). For the left wall, 100 % of the subjects from the test group and 88.8 % from the control group rate the sleeve's level of comfort between 4 and 6 (see Figure 4.4B). However, for the right wall, a relatively lower percent of the subjects rate the sleeve's level of comfort between 4 and 6 (77.7 % test group, 66.6 % control group). The results from both questions allow us to posit that the subjects' ability to control the robot does not necessarily depend upon the location of the wall, but the sleeve appears to cause discomfort when subjects' have to extend their wrist. For the test group subjects, 100 % of the subjects find the haptic feedback helpful (between 4 and 6) for the right wall and 88.8 % find it helpful for the left wall (see Figure 4.4D). At the same time, only 77.7 % of those subjects find the haptic feedback easy to become familiar with for the right wall (between 4 and 6) compared to 88.8 % of them who are able to become familiar with it with the left wall (see Figure 4.4E). Furthermore, 88.8 % and 77.7 % of test group subjects positively assess an improvement in performance over the course of the experimental phases for the left and right walls respectively (see Figure 4.4F). A lower percentage of control group subjects - 66.6 % for left wall and 55.5 % for right wall - positively assess an improvement in their performance. These responses indicate that while tasks that require wrist flexion might be easier to perform than those that require wrist extension, additional haptic feedback could make the task easier to perform for both wrist flexion and wrist extension. Not all test group subjects are able to familiarize themselves with the haptic feedback that they were receiving. Nonetheless, a large percentage of test group subjects feel that their performance had improved as a result of the haptic feedback compared to a lower percentage of control group subjects. Finally, at least 88.8 % of all subjects for both walls positively rate their experience of having participated in the experimental activity (between 4 and 6) (see Figure 4.4C).

The NASA-TLX test is used to assess various qualitative aspects of subjects participating in the study, including the amount of mental, physical, and temporal demands, the amount of effort expended, and the level of frustration experiences (see Figure 4.5). There are no observable significant differences in the amount of mental demand between the control and test groups for the left wall or the right wall as per the Kruskal-

Wallis test (left wall: $p = 0.89$; right wall: $p = 0.53$; see Figure 4.5A). In addition, there are no observable significant differences in the amount of mental demand for each group between the left and right walls (control: $p = 0.53$; test: $p = 0.85$). However, upon comparing the median values, it is worth noting that the control group find the task more mentally demanding when performing the task with the right wall than the left wall. The task is significantly more physically demanding for control group subjects than for test group subjects for both walls (see Figure 4.5B). Neither of the groups find the task with either wall significantly more physically demanding than the other, but similar to the mental demand data, the median value for the control group with the right wall is higher than for the left wall (control: $p = 0.26$; test: $p = 0.68$). There are no significant differences in the temporal demand between the control group and test group for either wall (left wall: $p = 0.65$; right wall: $p = 0.09$, see Figure 4.5C) or for each group between either wall (control: $p = 0.96$; test: $p = 0.19$). The test group subjects expend significantly lesser effort than control group subjects for both walls (see Figure 4.5D). This is indicative of the benefits of the haptic feedback when visual feedback is compromised. Although there are no significant differences in the amount of effort expended by either group between each wall (control: $p = 0.59$; test: $p = 0.24$), the median value is lower for both the control and test groups for the left wall compared to the right. There are no significant differences in the level of frustration experienced between the test and groups for either wall (left wall: $p = 0.75$; right wall: $p = 0.24$; see Figure 4.5E) or for each group between either wall (control: $p = 0.19$; test: $p = 0.82$).

4.4 Conclusions

This chapter presents a wearable haptic sleeve that provides kinesthetic feedback to help users avoid obstacles during a drone teleoperation task when the visual feedback provided to the users is poor. The sleeve reduces errors by blocking the subjects' wrist and elbow joints when the drone is in the vicinity of an obstacle. Test group subjects, who receive the haptic feedback during the training phase of the experiment, make fewer errors than control group subjects. The test group subjects also make fewer errors than the control group subjects during the evaluation phase when the haptic feedback is no longer provided. These results show that subjects trained with the haptic feedback are able to learn the activity and retain the necessary motor skills

without becoming overly dependent on the feedback. While there are no statistically significant differences in the performance for each group between the left and right walls for any of the phases, certain qualitative differences were observed in the questionnaire data. These differences are especially noticeable for the control group subjects who require a higher mental demand and expend a larger amount of effort for performing the task with the right wall than for the left wall. The higher mental demand and effort can be attributed to the relative discomfort in the extension of their wrist compared to flexion. All subjects in the study are right-handed and they use their right arm to don the wearable haptic sleeve and teleoperate the drone.

This work is a demonstration of the scalability of the wearable haptic sleeve to multiple body joints. Each antagonistic clutch pair corresponding to one joint operates independent of the clutch pair for the other joint. The absence of bulky actuators makes this lightweight sleeve both portable and unobtrusive to natural human mobility when haptic feedback is not provided. While the sleeve should be capable of preventing all drone collisions with obstacles, the presence of errors needs to be acknowledged, which are caused due to a combination of hasty subject movement and latencies introduced by drone dynamics. These errors can be further reduced by tuning the controller gains to improve the drone responsiveness to user movement. Further experiments are needed to explore the use of the wearable haptic sleeve to teleoperate multi-agent systems, such as swarms of drones when they pass through narrow spaces without the agents colliding with each other or the surrounding environment.

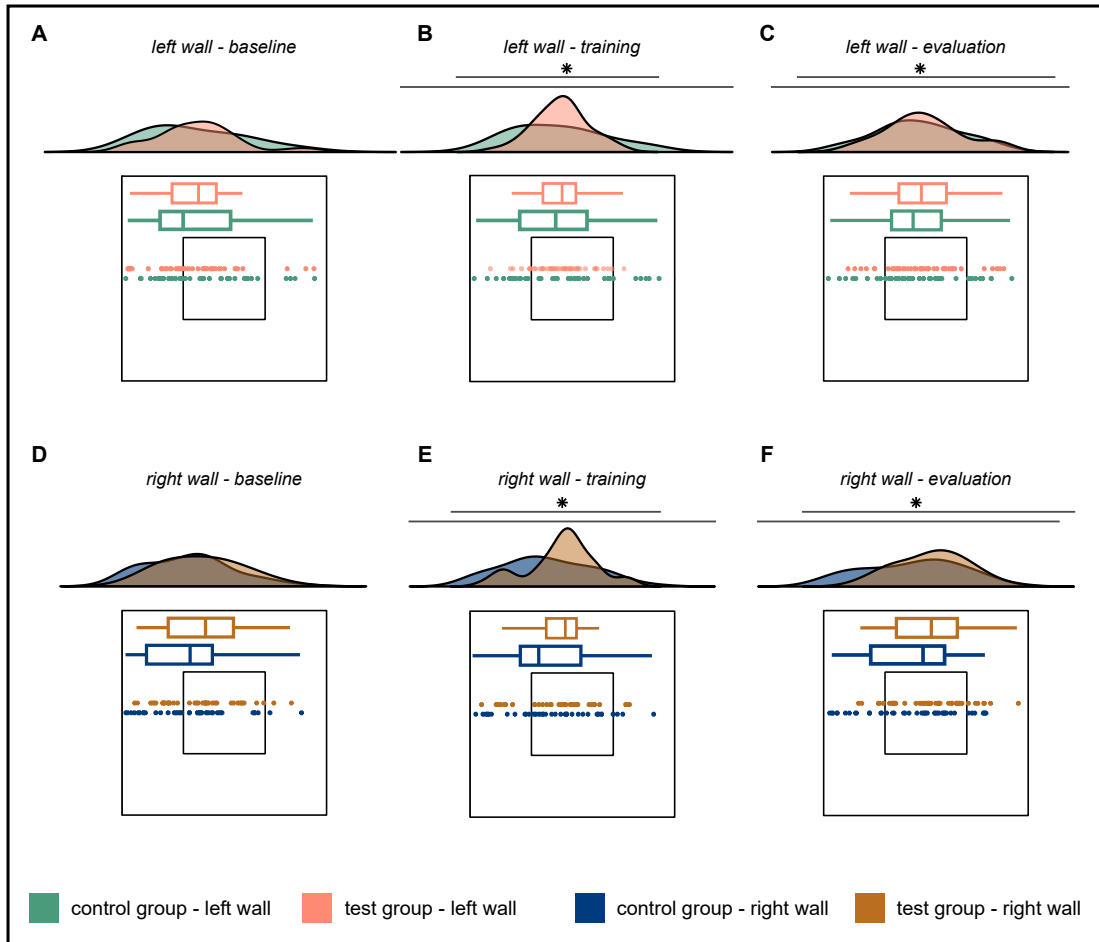


Figure 4.3 – Variance in drone position relative to the walls over the experimental phases. The variances of the drone position relative to the wall are compared at the time instant the drone either collides with the wall or passes through the hole. Comparisons are carried out for the (A-C) left wall and (D-F) the right wall between the control and test groups for the baseline, training, and evaluation phases. * $p < 0.05$

Multi-joint wearable haptic sleeve for telerobotics with reduced visual feedback

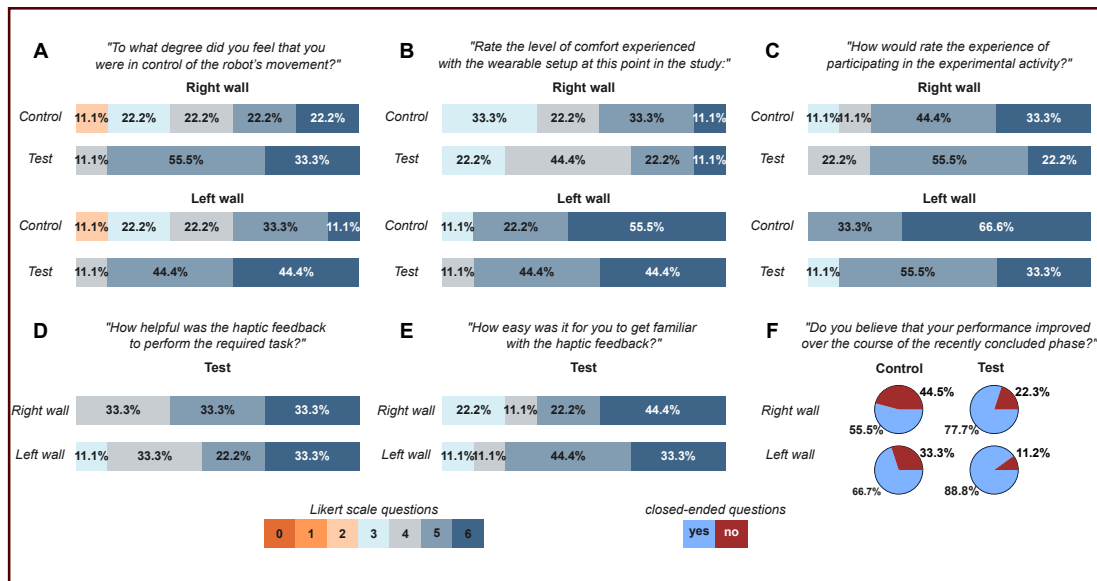


Figure 4.4 – Questionnaire responses pertaining to drone teleoperation and user comfort. Subjects respond to a customised questionnaire that factors in qualitative experiences pertaining to (A) degree of drone control, (B) comfort level with wearable setup, (C) overall participation using a Likert scale. Specific questions were posed to test group subjects to determine the (D) helpfulness and (E) familiarity with the haptic feedback that they received. (F) Subjects in both groups were asked to self-assess their performance improvement in a closed question.

Multi-joint wearable haptic sleeve for telerobotics with reduced visual feedback

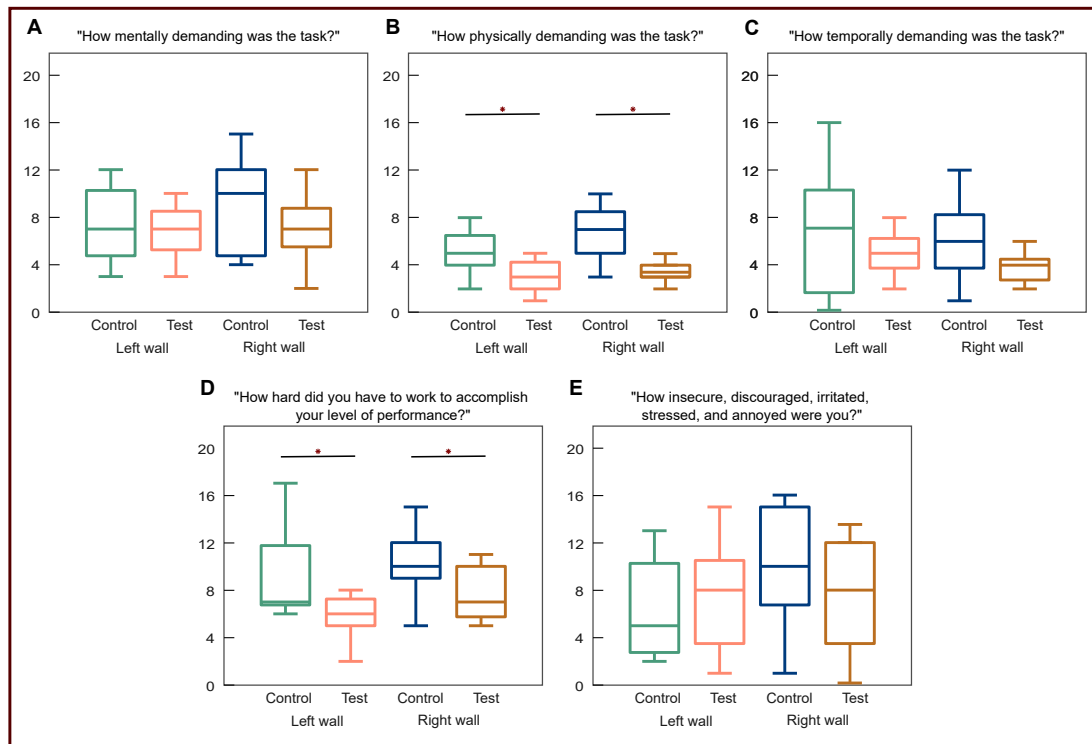


Figure 4.5 – Subject responses to NASA-TLX workload questionnaire that evaluates their work load as a participant through standard metrics. * $p < 0.05$

5 Conclusions

Scientific and technological advancements in human-robot interaction over the past decade has caused a rapid proliferation of robotic applications in our society. A majority of these robotic applications involve humans working with robots with varying degrees of control afforded to the human over the robot's actions. Telerobotics is a catch-all term referring to humans physically controlling the movements of the robot, especially if they are distally located.

Conventional control interfaces, such as joysticks that facilitate robotic teleoperation require users to undergo a considerable amount of training. This is because these interfaces are not intuitive for novice users. As robots become essential for a variety of applications in domains where professionals are not trained to use these conventional control interfaces, new types of intuitive interfaces are required. The advent of wearables in recent years presents a solution to this problem. Wearable control interfaces allow even novice users to teleoperate a robot using intuitive body gestures. Thus, users do not need to spend a considerable amount of time learning to control these wearable interfaces. Wearable interfaces can be bidirectional i.e., enabling two-way communication between the human operator and the robot. Body motion tracking devices, such as IMUs, which can be mounted on the wearable interface can map the operator's body movement and translate them into robot commands. In turn, sensory feedback devices can be integrated into the interfaces to relay information to the operator about the robot's state and its interaction with the environment.

Wearable haptic feedback devices are of particular interest because they are capable

of transmitting forces to the parts of the human body responsible for the robot's actions. This can take the form of physically guiding users during teleoperation when they make errors, and those errors need to be corrected. Here, learning to perform teleoperation is in essence a motor training exercise, wherein the haptic feedback serves as a teaching aid that help the user learn and retain the necessary motor skills after the training is complete. It is worth noting that excessive feedback can have a coddling effect – users become overly dependent on the feedback. In this scenario, their performance improves during training when they receive haptic feedback to physically guide them. However, when the feedback is removed, their performance level precipitates, indicating that they do not retain the required motor skills, and hence, they do not learn the motor task. This can be avoided by adopting a training method that provides impedance to erroneous body movements, but does not physically correct the user. This method makes the user conscious of their movement errors. Since motor learning is highly dependent on users making a concerted effort to correct their own errors, this method of haptic feedback provision can help users learn the motor task of teleoperating robots.

A number of wearable haptic devices are capable of facilitating this training method, but most of them use bulky actuators, which can hinder natural user mobility and can cause user fatigue. Furthermore, a majority of these haptic devices are composed of rigid materials that do not match the compliance of the human body. While there are haptic devices that circumvent the problems of body compliance with soft materials, most of them use silicone-based rubbers, which are not suitable for direct skin mounting because they are not breathable. This thesis presents a wearable haptic interface that addresses these concerns by using a fabric-based wearable haptic sleeve composed of electroadhesive clutches that are lightweight, portable, and consume low power for operation.

An all-fabric wearable haptic device is designed and fabricated using a combination of textiles and textile-based materials. Mechanically, the device is a clutch and spring arranged in parallel to one another. The spring ensures that when the device is not providing haptic feedback, it stretches without greatly affecting the natural compliance of the human body. When feedback needs to be provided, the clutch is engaged, and the device maintains a certain holding force that prevents it from stretching. This

Conclusions

holding force restricts the user's body movement depending upon the location of the device on the body. The clutch operates on the principle of electrostatic adhesion for parallel plate capacitors. The holding force depends on the number of clutch plates, the area of overlap, the dielectric thickness, and the applied voltage.

While the all-fabric clutch is an important milestone is the development of textile-based haptic devices, it is vital to acknowledge the limitations of its low holding force and rather elaborate manufacturing method. Therefore, a newer iteration of the haptic clutches is created, which required changing the materials used to streamline the manufacturing process for adding multiple clutch plate pairs and obtaining higher holding forces. These new fabric-based clutches are integrated in a wearable haptic sleeve that is designed to block elbow joint extension and flexion. The clutches are anchored to the user's body using a set of body attachments on the forearm, upper arm, and the elbow joint. Each the body attachments are also fabricated using textiles. The elbow sleeve is used as a training aid for a human subject study in which users performed a motor task involving drone path following in a simulated environment. Test group subjects who are trained to perform the task with the elbow sleeve exhibit performance improvement and skill retention even after the haptic feedback is removed. This is in contrast with control group subjects who only receive visual feedback from the drone's camera.

This sleeve is extended to encompass multiple body joints i.e., the wrist and elbow joints. In this sleeve, four identical clutches are used to restrict the extension and flexion of the elbow and wrist joints independently. This sleeve is used to train users in a drone obstacle avoidance task when the user's sense of depth perception is intentionally weakened. This is to highlight situations where drone pilots might have occluded vision due to a variety of reasons, including poor lighting, shadows, or intermittent loss of visual feedback. Subjects receive a fixed-camera perspective visual feedback in a simulated environment where fiducial features are absent, which would otherwise help in spatialisation. The human subject study conducted with the wrist-joint wearable haptic sleeve shows that haptic feedback provided using the clutches can greatly reduce collisions with obstacles even when visual feedback is compromised. Moreover, this study also indicates that despite existing qualitative differences between wrist extension and wrist flexion in terms of comfort, the functionality of the sleeve as

a training aid is largely unaffected.

5.1 Future research avenues

This thesis demonstrates the use of the wearable haptic sleeve for training users to teleoperate a single drone under different conditions of visual feedback, nature of task, number of body joints, robot degrees of freedom controlled, and the type of simulated environments. However, there are a considerable number of avenues in which the use of the wearable haptic sleeve can be further investigated.

One avenue is alluded to in chapter 4, section 4.4. The haptic sleeve can be extended by combining it with a haptic hand glove capable of blocking finger joint movement, thus encompassing all the major joints from the fingertip to the elbow (see Figure 5.1). The hand glove is an updated version of the DextrES, which is composed of textile-based electroadhesive clutches [60, 59]. The purpose of developing this new version of the haptic sleeve is to evaluate its effectiveness in training users to teleoperate a swarm of drones in a simulated maze. For this future study, users will control the movement of the drone swarm by mapping the position and orientation of their hand over an infrared motion tracking device (Ultraleap). Therefore, the swarm's collective motion in the horizontal plane is controlled by elbow extension and flexion, and its altitude by wrist extension and flexion. In addition, users can control the contraction and expansion of the swarm relative to its centre of mass by closing and opening their hand. Users receive haptic feedback from specific clutches when one or more drones within the swarm are at a risk of colliding with the environment or each other. Furthermore, this study will also examine the effect of personalising haptic feedback by changing the haptic feedback error threshold for each subject over the course of the training phase. These results will be compared with a control group that only receives visual feedback and another test group that receives haptic feedback with a fixed error threshold.

There is promise in investigating the use of the wearable haptic sleeve for controlling robots apart from drones. The sleeve can also be extended to a full-body suit encompassing more body joints. For instance, the fabric-based electroadhesive clutches can be integrated in clothing-like rehabilitative devices that require intentional body

Conclusions

movement restriction as part of patient therapy. Another field of application is Search-and-Rescue robotics – rescue personnel, who are untrained in robotic teleoperation, can use the full-body haptic suit to control different types of rescue robots using intuitive body gestures and receive feedback in case the robot is at risk of colliding with obstacles. A full-body haptic suit with electroadhesive clutches may also be used for facilitating greater human-human interaction and collaboration between individuals situated in distant locations.

It is worth examining some of the key learnings from the different projects that are described in this thesis. To begin with, the electroadhesive clutches in the literature, including the fabric-based ones presented here are always in one of two states, soft or stiff. When the clutch is not engaged, the clutch plates are free to slide on top of each other and the overall stiffness of the device is determined by the stiffness of the spring in parallel. When a voltage is applied to engage the clutch, the clutch plates adhere to each other. Even so, this stiffness change is largely anisotropic in the direction of longitudinal stretch. As the clutch plates are flexible, they can bend even when they adhere to each other. These mechanical properties have implications for the types of applications that they can be used for. For instance, in both teleoperation tasks that users are trained to perform in this thesis, the presence of an error threshold is necessary. Only when the drone crosses this threshold does the haptic sleeve provide force feedback to prevent further body movement errors. Therefore, the provision of haptic feedback is incumbent upon users making “overshoot” errors.

However, there is a possibility of creating quasi-stiffness tuning haptic devices using electroadhesive clutches. This can be facilitated by powering the clutches with AC high voltage power supplies. The use of AC voltage is more power consuming on average compared to DC voltage because the capacitors of the clutch are charged and discharged continuously with AC voltage whereas they are charged once with DC voltage. The continuous charging and discharging of the clutch plates creates a zipping effect i.e., the plates continue to adhere to each other even when they are plied after. Instead, DC-powered clutch plates exhibit stick-slip behaviour when they are plied apart. This type of stiffness tuning could help make these clutches applicable for haptic training that needs damping forces to be transmitted to users. Moreover, this type of zipping effect can facilitate the provision of gradually increasing haptic

feedback without users having to commit overshoot errors.

It is important to account for the irregularities of the human body morphology and the implications they have on designing wearable interfaces composed of electroadhesive clutches. As these clutches have plates that overlap, slide freely when disengaged and adhere to one another when engaged, it is important to ensure that the overlap does not take place at body joints. This is because when the body joints flex, the joints apply loading on the overlapped plates, which increases the friction between the plates to slide freely when the clutches are not activated. Furthermore, it is more effective to create body joint attachments with “regular” curved geometry, such as spheres and cylinder at joints that have irregular shapes. These body joint attachments with regular geometry can interface with irregular body joints through foam-padded textiles.

While this thesis suggests that textile-based haptic devices can be integrated into regular clothing, it is important to recognise that most clothing that we wear on a daily basis slip on our skin. For the haptic interfaces presented in this thesis, any slippage between the body attachments at anchor points and the skin would result in improper force transmission.

Another important consideration is that this thesis explores the use of rectangular electroadhesive clutch plates that operate on the principle of electrostatics exhibited by parallel plate capacitors. The geometry of these clutches define how they can be integrated into a wearable haptic interface. It is worth exploring other possible geometries, including cylindrical fibres that might be able to produce the same magnitude of holding force, but can be integrated more compactly in a wearable interface.

Finally, it is worth noting that the haptic technologies described in this thesis are “reactive” i.e., they do not produce restoring forces. Rather they provide adequate impedance to match the force produced by a user’s body to generate movement. While the effectiveness of these haptic systems is demonstrated as a teaching for different motor learning tasks, it is important to acknowledge that these tasks have two commonalities – one, the mapping between the user and the robot is position-based, not velocity-based, and two, a clearly defined “forbidden region” is required to indicate user movement errors. For tasks that do not comply with these two requirements, the clutch-based haptic system can be used in conjunction with other wearable

Conclusions

devices that use under-actuated tendon-driven systems with limited actuators. This combination of technologies could allow users to take advantage of the high holding force, low-power-consumption, and lightweight of the clutches while still being able to learn and/or perform a variety of motor tasks that require a restoring force.

5.2 Final thoughts

My personal vision is to enable inclusivity in all spheres of our society. This can only happen by centring social justice. Technological advancements present opportunities for correcting historical injustices that have marginalised several communities in our society. While technology can improve the quality of lives for these communities, it is vital to be aware of the power structures that cause systemic and quotidian oppression. Otherwise, technology will only serve to entrench these power structures and aggravate the suffering of vulnerable communities.

In our present day, robotics is being heralded as a field that can have a democratising effect in our society if it is made easily accessible and affordable. Given the increasing fragmentation of societies globally, the rise of nationalistic xenophobia, and the threat of a looming climate crisis, it is incumbent upon those of us who are afforded societal privileges to contribute towards addressing these problems in our own capacities. For the expansive field of robotics, this might manifest itself in different ways depending upon our own specific areas of interest and expertise. Towards this end, when creating and testing different robotic devices presented in this thesis, I have endeavoured to follow an approach that is grounded in the principles of inclusivity, affordability and most importantly, justice.

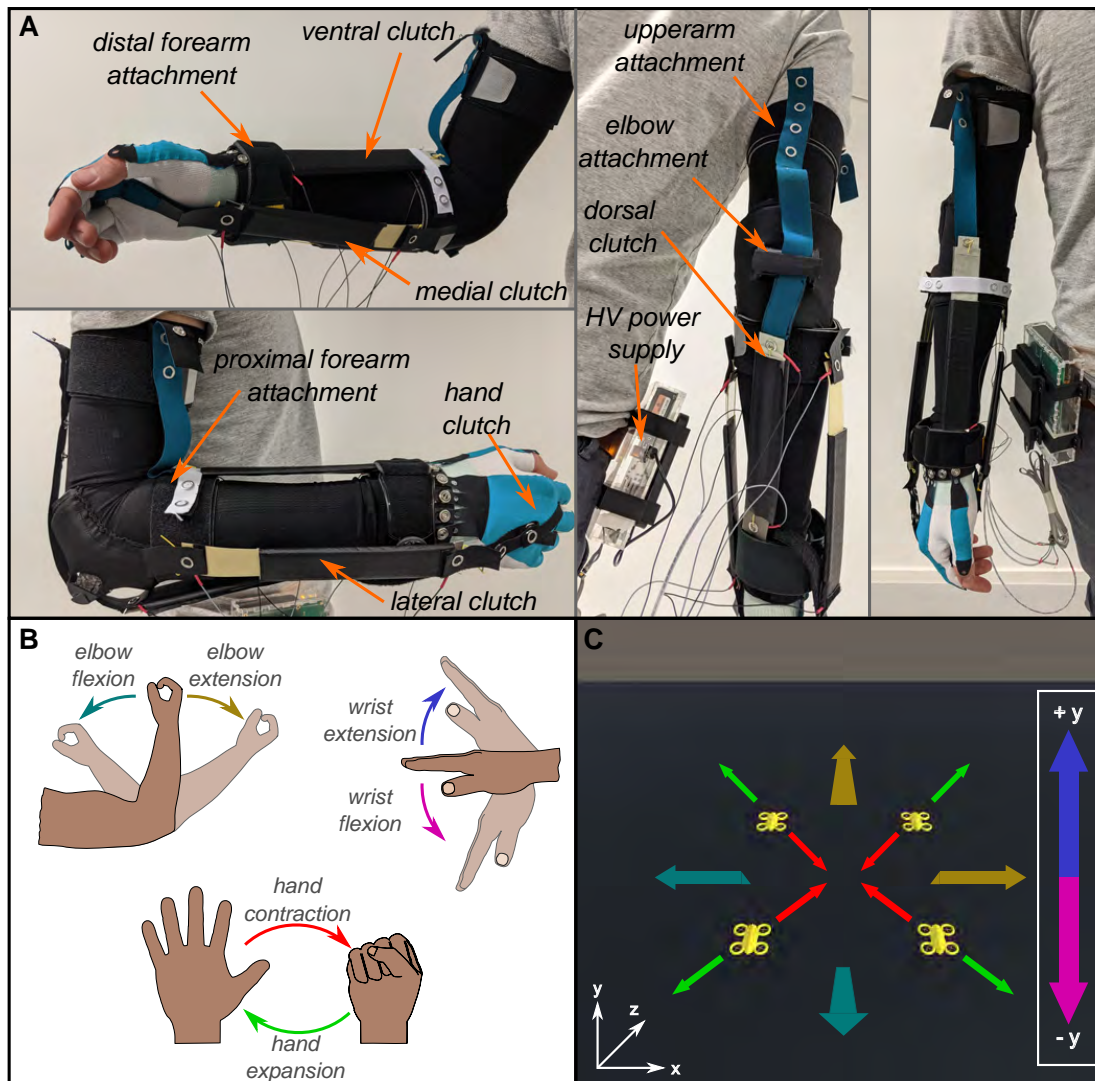


Figure 5.1 – Experimental setup of the hand, wrist, and elbow haptic sleeve. (A) The wearable haptic sleeve consists of four electroadhesive clutches to restrict elbow wrist joint rotations and a hand glove consisting of five clutches to block each of the finger joints. The clutches are mounted on the user using body attachments. All of the clutches are activated independently using a customised printed circuit board. (B) The wearable haptic sleeve is used to help users navigate a drone swarm through a simulated maze. The users control the movement of the swarm by elbow and wrist extension and flexion, and hand expansion and contraction. The arm movements are captured using an Ultraleap infrared motion tracking device. (C) The drone swarm in the Unity environment can be moved as a collective in all three dimensions. Additionally, the individual agents can move inwards and outwards from the swarm centre of mass. The mapping between the human arm and the drone swarm agents are colour coded.

A Clutch holding force derivation

An electric field $\mathbf{E} = E_i \mathbf{e}_i$ is created between the plates of a parallel plate capacitor when a potential difference Φ is applied across its electrodes. Charges flow across the plates until the voltage drop across the capacitor approximately equals Φ (see Figure A.1). The electric field induces Maxwell stress σ with tensor components that can be expressed as:

$$\sigma_{ij} = \kappa \epsilon_0 \left(E_i E_j - \frac{1}{2} \delta_{ij} E^2 \right) \quad (\text{A.1})$$

Here the indices $i, j \in \{1, 2, 3\}$ are subject to Einstein summation convention. Since the electric field is directed normal to the electrode plane, we have $E_1 = 0$, $E_2 = 0$, and $E_3 = \Phi/x$, where x is the dielectric thickness or the separation between the parallel plates. Assuming the edge effects of the electric field to be negligible, and for a given capacitance $C = A\kappa\epsilon_0/x$, the component of the stress tensor normal to the electrode plane is given by:

$$\sigma_{33} = \frac{1}{2} \kappa \epsilon_0 \left(\frac{\Phi}{x} \right)^2 \quad (\text{A.2})$$

while the remaining components are zero. For n engaged clutch plate pairs, the frictional force F in the electrode plane that acts opposite to the direction of loading

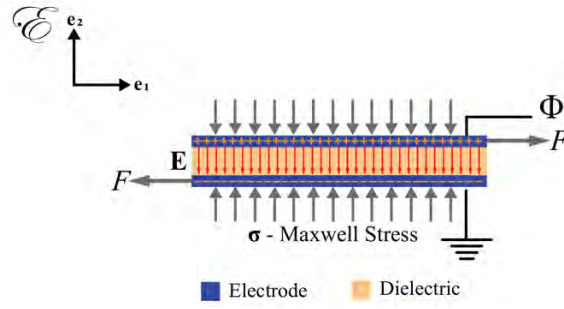


Figure A.1 – Generation of Maxwell stress in capacitors. Voltage Φ applied across a parallel plate capacitor gives rise to charge separation between the electrodes. In the Euclidean space \mathcal{E} , the generated electric field \mathbf{E} induces the Maxwell Stress tensor $\sigma = \sigma_{ij} \mathbf{e}_i \otimes \mathbf{e}_j$ that increases shear resistance to the applied load F .

is given by:

$$F = \mu n A \sigma_{33} = \frac{1}{2} \mu \kappa \epsilon_0 n A \left(\frac{\Phi}{x} \right)^2 \quad (\text{A.3})$$

where μ is the coefficient of static friction between dielectric surfaces.

B Capacitor charging and discharging

In the H-bridge shown in Figure B.1, the two branches, B1 and B2, are RC circuits each consisting of the capacitive load, two transistors, and a measurement resistor: B1 (S1-R-C-S4) and B2 (S2-C-R-S3). Here, the transistors S1, S2, S3, and S4 are identical. Initially, S3 and S4 are closed and S1 and S2 are open. When a 5 V digital signal is sent from the Arduino microcontroller pin D9 to close S1 (and open S3), a high voltage Φ is applied across B1 and current begins to flow through it. Once the voltage is applied, the probes of a digital oscilloscope measure the voltage drop Φ_R across the resistor R , which decays exponentially as a function of time t . The voltage drop Φ_C across the capacitor is obtained by taking the difference between the applied and measured voltages:

$$\Phi_C = \Phi - \Phi_R = \Phi (1 - e^{-t/\tau}) \quad (\text{B.1})$$

where $\tau = RC$ is the time constant. The charging time t_c is calculated as the time required for $\Phi_C = 0.993 \Phi$, which corresponds to $t \approx 5\tau$. The capacitor charging power P_c is dependent on the amount of current flow regulated by R .

$$P_c = \sum_i \left(\frac{\Phi_C(t_i)^2}{R} \right) \quad (\text{B.2})$$

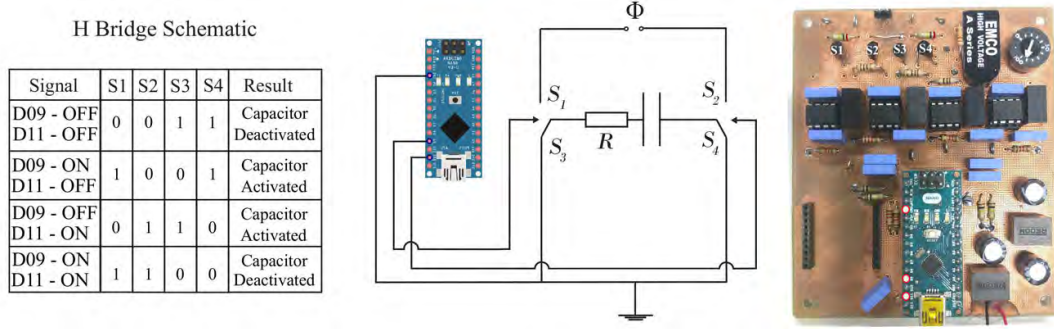


Figure B.1 – Capacitor charging and discharging using a customized H-bridge. The table provides the schematic of the H-bridge operation with regard to clutch activation. The H-bridge consists of two branches, B1 (S1-R-C-S4) and B2 (S2-C-R-S3), each comprised of the capacitor, a measurement resistor and two transistors. The transistors are activated by a 5 V signal sent from the Arduino Nano microcontroller. By default, S3 and S4 are closed.

where i refers to the time index of voltage measurement. Power consumption is computed between t_0 when the voltage is applied and t_c when the capacitor is charged. Capacitor discharge can be instigated in two ways, either shorting the circuit or reversing the polarity of applied voltage for a specific period of time.

Short Circuiting

Capacitor discharge by short circuiting takes place by grounding the two ends of the branch B1 i.e., closing S3 and opening S1 by ceasing the D9 digital signal. The current flow through the circuit reverses and the voltage drop across the capacitor, Φ_C decreases exponentially.

$$\Phi_C = \Phi e^{-t/\tau} \quad (B.3)$$

Capacitor charging and discharging

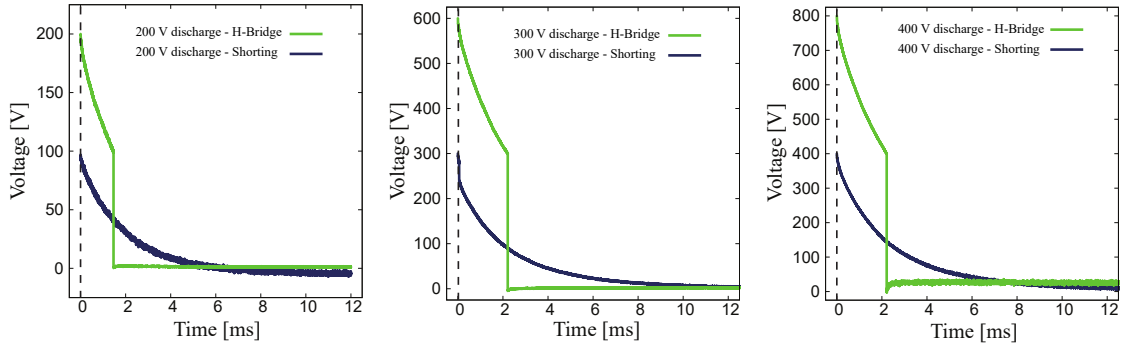


Figure B.2 – Clutch plate discharge characteristics observed measuring the voltage drop across the measurement resistor placed in series with the capacitor. The discharge characteristics are plotted for cases where the clutch was initially engaged at 100 V, 300 V, and 400 V, both by short circuiting and by reversing the voltage polarity using an H-bridge.

Voltage Polarity Reversal

To decrease the discharge time of the charged capacitor, branch B1 is opened and branch B2 is closed simultaneously. Branch B1 is opened by closing S3 and opening S1 i.e., D9 stops sending the 5 V signal. Branch B2 is closed when D11 sends a 5 V digital signal, closing S2 and opening S4. Due to the reversal in voltage polarity, the voltage drop across the resistor increases to 2Φ as soon as B2 is closed. Thereafter, the resistor voltage begins to decay exponentially. The voltage drop across the capacitor Φ_C also decreases exponentially.

$$\Phi_C = \Phi e^{-t/\tau} - \Phi = \Phi(e^{-t/\tau} - 1) \quad (\text{B.4})$$

To discharge the capacitor, it is important that the branch B2 is short-circuited when the voltage drop across the resistor equals Φ i.e., the voltage drop across the capacitor is zero. The duration that Branch B2 is kept closed corresponds to the time required to charge the capacitor when a voltage Φ is applied. Branch B2 is short-circuited by ceasing the digital signal from D11, closing S3 and opening S2.

As shown in Figure B.2, the time required to discharge the capacitor is smaller when

the voltage polarity is reversed compared to when the circuit is shorted.

The discharge time t_d is calculated as time required for $\Phi_C = 0.07 \Phi$. For both cases, the power consumption during discharge is calculated using the following expression:

$$P_d = \sum_i \left(\frac{\Phi_C(t_i)^2}{R} \right) \quad (\text{B.5})$$

Here the power consumption is computed from t_n when the branch B1 is opened until t_d when the capacitor is discharged.

C Mechanics of the clutched-spring

Apart from the voltage Φ across the electrodes, the behaviour of the haptic device is governed by the amount by which the device is stretched. As shown in Figure C.1, the length of the unconstrained knitted fabric and dielectric overlap in the reference (rest) configuration \mathcal{B}'_0 are ℓ_0 and L_0 , respectively. When the module is stretched, the extensible knitted fabric length becomes ℓ and dielectric overlap length reduces to L . The width W of the clutch plate remains invariant in the deformation mapping $\chi_0 : \mathcal{B}'_0 \rightarrow \mathcal{B}_0$. The current configuration \mathcal{B} refers to the case when voltage is applied and the clutch is engaged. We re-write Equation (A.3) in terms of the width W and the length L of dielectric overlap between the electrodes:

$$F = \frac{1}{2} \mu k W L \left(\frac{\Phi}{x} \right)^2 \quad (\text{C.1})$$

From Equation (C.1), it is evident that F is related to the stretch $\lambda = \ell/\ell_0$ due to the reduction in overlap length. The length of the knitted fabric that is constrained by the woven fabric and the textile electrode remains invariant since they are inextensible i.e., $L = L_0 - (\ell - \ell_0)$. We define the dimensionless quantity $\zeta = L/L_0$ that can also be expressed as:

$$\zeta = 1 - (\lambda - 1) \frac{\ell_0}{L_0} \quad \forall \quad \lambda \in \{1, \lambda_{max}\} \quad (\text{C.2})$$

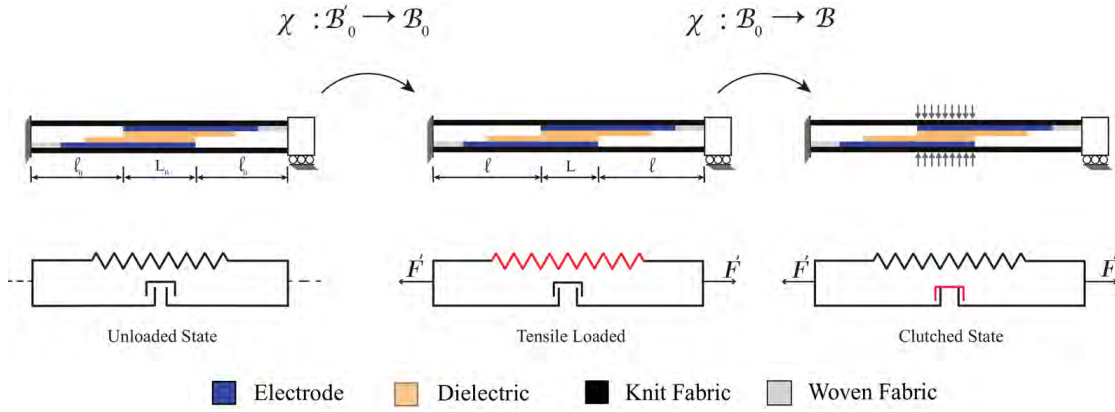


Figure C.1 – Kinematics of the haptic device - in the reference configuration \mathcal{B}'_0 , the device is unloaded. When the device is subjected to a tensile load F' , the device stretches like a spring and the area of dielectric overlap reduces. In the current configuration \mathcal{B}_0 , voltage is applied and the clutch is engaged.

Here, λ_{max} is the maximum extensibility of the knitted fabric. Equation (C.1) and Equation (C.2) allow us to express the voltage in terms of prescribed quantities, provided that the stretch λ is known:

$$\Phi = \sqrt{\frac{x^2 F}{k \zeta W L_0}} \quad (C.3)$$

From Equation (A.3), we know that the maximum holding force of the clutch is dependent on both the overlap area, WL and the voltage applied, Φ . However, only the latter quantity can be controlled. Therefore, the applied voltage needs to account for the changing module length. This could be enabled by using a reliable stretch sensor that can determine the total device length for a changing electrical quantity such as capacitance or resistance. Denoting the total device length as $L_t = L + 2\ell$, we can obtain an expression for the stretch λ from Equation (C.2) in terms of given or measured parameters:

$$\lambda = \left(\frac{L_t - L_0}{\ell_0} \right) - 1 \quad (C.4)$$

D Fabrication method for multi-layered all-fabric clutch

Fabrication method for multi-layered all-fabric clutch

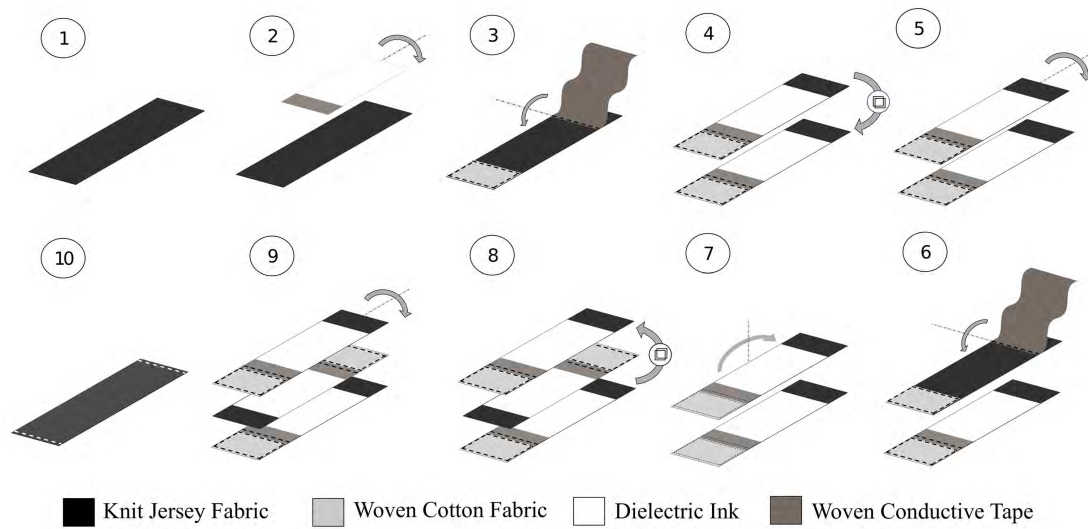


Figure D.1 – Fabrication process to develop the haptic device with two clutch pairs. (1) The substrate knitted fabric is laser cut into rectangular pieces. (2) Copper plated polyester fabric electrodes are coated with a dielectric ink using a thin film applicator. (3) The posterior surface of the electrode is stitched onto the knitted fabric substrate along the end of the coated surface. The electrode is folded to cover the stitched seam and the coated surface is aligned in parallel with the knitted substrate. (4) The uncoated portion of the coated electrode face is stitched onto the substrate. A rectangular woven fabric is stitched onto the substrate surface extending from the uncoated portion of the electrode to the substrate edge. The entire sample is replicated. (5) The first sample is rotated about the longitudinal axis and the unstitched surface of the knitted fabric is used as a substrate. (6) Steps (3) and (4) are repeated, with the exception that the sample is not replicated. (7) The first sample is rotated about the vertical axis until the unstitched portions of the knitted substrates in both samples are at opposite ends. (8) The second sample is replicated. (9) The third sample is rotated about its longitudinal axis until the dielectric surfaces of the first and third samples are in planar contact. (10) Finally, the three samples are stitched along the wider edges. To develop the haptic device with multiple clutch pairs, steps (2)-(4) are repeated.

E Tensile test characteristics of fabric clutches

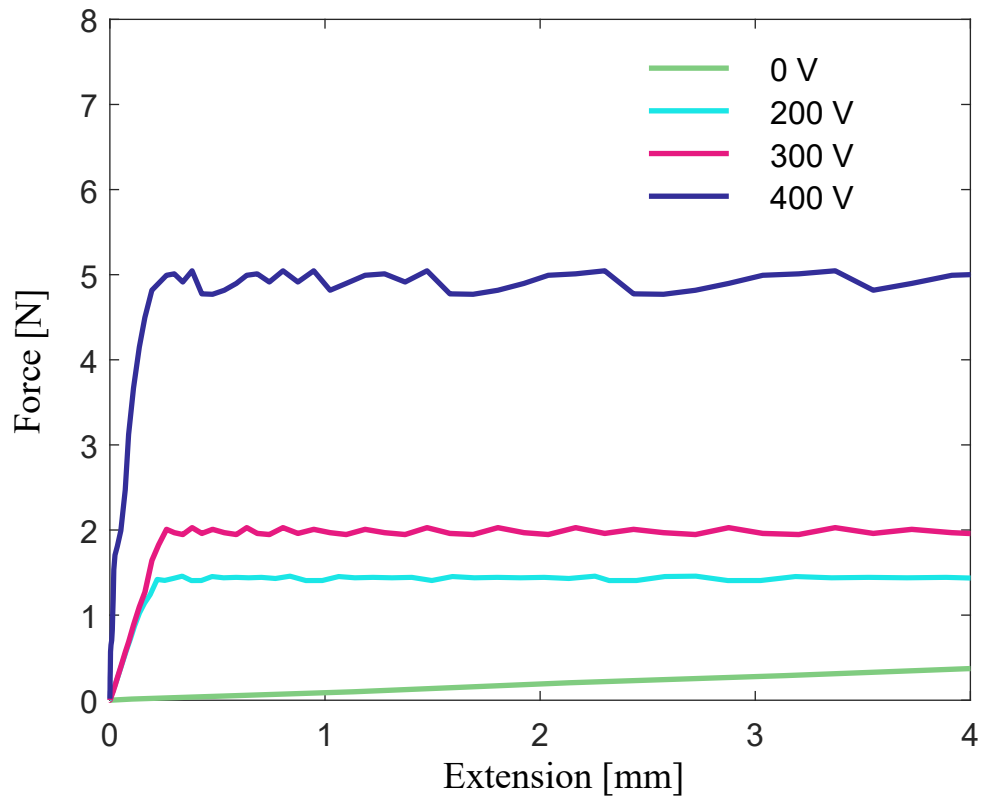


Figure E.1 – Holding force measurements for a pair of clutch plates with a dielectric overlap area of $50 \times 60 \text{ mm}^2$ when the device is operated at 0 V, 200 V, 300 V, and 400 V and loaded at 10 mm/s. As one can observe from the plots, the clutch plates are fully engaged when the device undergoes an extension that is negligible in value compared to the dimensions of the device.

Bibliography

- [1] David A Abbink, Mark Mulder, and Erwin R Boer. “Haptic shared control: smoothly shifting control authority?” In: *Cognition, Technology & Work* 14.1 (2012), pp. 19–28.
- [2] Marco Aggravi et al. “Design and evaluation of a wearable haptic device for skin stretch, pressure, and vibrotactile stimuli”. In: *IEEE Robotics and Automation Letters* 3.3 (2018), pp. 2166–2173.
- [3] Jumpei Arata et al. “A new hand exoskeleton device for rehabilitation using a three-layered sliding spring mechanism”. In: *2013 IEEE International Conference on Robotics and Automation*. IEEE. 2013, pp. 3902–3907.
- [4] Alan T Asbeck et al. “A biologically inspired soft exosuit for walking assistance”. In: *The International Journal of Robotics Research* 34.6 (2015), pp. 744–762.
- [5] Alan T Asbeck et al. “Multi-joint soft exosuit for gait assistance”. In: *2015 IEEE International Conference on Robotics and Automation (ICRA)*. IEEE. 2015, pp. 6197–6204.
- [6] Matteo Bianchi et al. “Design and preliminary affective characterization of a novel fabric-based tactile display”. In: *2014 IEEE Haptics Symposium (HAPTICS)*. IEEE. 2014, pp. 591–596.
- [7] Joao Bimbo et al. “Teleoperation in cluttered environments using wearable haptic feedback”. In: *2017 IEEE/RSJ International Conference on Intelligent Robots and Systems (IROS)*. IEEE. 2017, pp. 3401–3408.
- [8] Ingvars Birznieks et al. “Encoding of direction of fingertip forces by human tactile afferents”. In: *Journal of Neuroscience* 21.20 (2001), pp. 8222–8237.

- [9] J Bodner et al. “First experiences with the da Vinci™ operating robot in thoracic surgery”. In: *European Journal of Cardio-thoracic surgery* 25.5 (2004), pp. 844–851.
- [10] Rares F Boian et al. “Haptic effects for virtual reality-based post-stroke rehabilitation”. In: *11th Symposium on Haptic Interfaces for Virtual Environment and Teleoperator Systems, 2003. HAPTICS 2003. Proceedings.* IEEE. 2003, pp. 247–253.
- [11] Karsten Bormann. “Presence and the utility of audio spatialization”. In: *Presence: Teleoperators & Virtual Environments* 14.3 (2005), pp. 278–297.
- [12] Amy E Bouchard, Hélène Corriveau, and Marie-Hélène Milot. “Comparison of haptic guidance and error amplification robotic trainings for the learning of a timing-based motor task by healthy seniors”. In: *Frontiers in systems neuroscience* 9 (2015), p. 52.
- [13] Eric Brown et al. “Universal robotic gripper based on the jamming of granular material”. In: *Proceedings of the National Academy of Sciences* 107.44 (2010), pp. 18809–18814.
- [14] David Bryson. “Designing smart clothing for the body”. In: *Smart clothes and wearable technology.* Elsevier, 2009, pp. 95–107.
- [15] G Cardillo. “Anovarep: Compute the Anova for repeated measures and Holm-Sidak test for multiple comparisons if Anova is positive”. In: *MATLAB Central File Exchange* (2008).
- [16] Cody W Carpenter et al. “Healable thermoplastic for kinesthetic feedback in wearable haptic devices”. In: *Sensors and Actuators A: Physical* 288 (2019), pp. 79–85.
- [17] Federico Carpi et al. *Dielectric elastomers as electromechanical transducers: Fundamentals, materials, devices, models and applications of an emerging electroactive polymer technology.* Elsevier, 2011.
- [18] Maura Casadio, Rajiv Ranganathan, and Ferdinando A Mussa-Ivaldi. “The body-machine interface: a new perspective on an old theme”. In: *Journal of Motor behavior* 44.6 (2012), pp. 419–433.

BIBLIOGRAPHY

- [19] Jennifer Casper and Robin R. Murphy. “Human-robot interactions during the robot-assisted urban search and rescue response at the world trade center”. In: *IEEE Transactions on Systems, Man, and Cybernetics, Part B (Cybernetics)* 33.3 (2003), pp. 367–385.
- [20] Jacky CP Chan et al. “A virtual reality dance training system using motion capture technology”. In: *IEEE transactions on learning technologies* 4.2 (2010), pp. 187–195.
- [21] Jessie YC Chen, Michael J Barnes, and Michelle Harper-Sciarini. “Supervisory control of multiple robots: Human-performance issues and user-interface design”. In: *IEEE Transactions on Systems, Man, and Cybernetics, Part C (Applications and Reviews)* 41.4 (2011), pp. 435–454.
- [22] Jessie YC Chen, Ellen C Haas, and Michael J Barnes. “Human performance issues and user interface design for teleoperated robots”. In: *IEEE Transactions on Systems, Man, and Cybernetics, Part C (Applications and Reviews)* 37.6 (2007), pp. 1231–1245.
- [23] Xiang-Zhong Chen et al. “Small-Scale Machines Driven by External Power Sources”. In: *Advanced Materials* 30.15 (2018), p. 1705061.
- [24] Corey I Cheng and Gregory H Wakefield. “Introduction to head-related transfer functions (HRTFs): Representations of HRTFs in time, frequency, and space”. In: *Audio Engineering Society Convention 107*. Audio Engineering Society. 1999.
- [25] Inrak Choi et al. “A Soft, Controllable, High Force Density Linear Brake Utilizing Layer Jamming”. In: *IEEE Robotics and Automation Letters* 3.1 (2018), pp. 450–457.
- [26] Matteo Cianchetti et al. “Biomedical applications of soft robotics”. In: *Nature Reviews Materials* 3.6 (2018), pp. 143–153.
- [27] Steven H Collins, M Bruce Wiggin, and Gregory S Sawicki. “Reducing the energy cost of human walking using an unpowered exoskeleton”. In: *Nature* 522.7555 (2015), pp. 212–215.
- [28] Laura Marchal Crespo and David J Reinkensmeyer. “Haptic guidance can enhance motor learning of a steering task”. In: *Journal of motor behavior* 40.6 (2008), pp. 545–557.

- [29] Heather Culbertson, Samuel B Schorr, and Allison M Okamura. “Haptics: The present and future of artificial touch sensation”. In: *Annual Review of Control, Robotics, and Autonomous Systems* 1 (2018), pp. 385–409.
- [30] Heather Culbertson et al. “A social haptic device to create continuous lateral motion using sequential normal indentation”. In: *2018 IEEE Haptics Symposium (HAPTICS)*. IEEE. 2018, pp. 32–39.
- [31] Wang Dangxiao et al. “Haptic display for virtual reality: progress and challenges”. In: *Virtual Reality & Intelligent Hardware* 1.2 (2019), pp. 136–162.
- [32] Myron A Diftler et al. “Robonaut 2-the first humanoid robot in space”. In: *2011 IEEE international conference on robotics and automation*. IEEE. 2011, pp. 2178–2183.
- [33] Stuart Diller, Carmel Majidi, and Steven H Collins. “A lightweight, low-power electroadhesive clutch and spring for exoskeleton actuation”. In: *Robotics and Automation (ICRA), 2016 IEEE International Conference on*. IEEE. 2016, pp. 682–689.
- [34] Stuart B Diller, Steven H Collins, and Carmel Majidi. “The effects of electroadhesive clutch design parameters on performance characteristics”. In: *Journal of Intelligent Material Systems and Structures* 29.19 (2018), pp. 3804–3828.
- [35] Nicola Diolaiti and Claudio Melchiorri. “Teleoperation of a mobile robot through haptic feedback”. In: *IEEE International Workshop HAVE Haptic Virtual Environments and Their*. IEEE. 2002, pp. 67–72.
- [36] Aaron M Dollar and Hugh Herr. “Lower extremity exoskeletons and active orthoses: challenges and state-of-the-art”. In: *IEEE Transactions on robotics* 24.1 (2008), pp. 144–158.
- [37] Xiaoliang Dou et al. “Improved dielectric strength of barium titanate-polyvinylidene fluoride nanocomposite”. In: *Applied physics letters* 95.13 (2009), p. 132904.
- [38] Alexander Duschau-Wicke et al. “Haptic Constraints for Rehabilitation Robots: An Overview”. In: *Biomed Tech* 55 (2010), p. 1.
- [39] Benoni B Edin and Niclas Johansson. “Skin strain patterns provide kinaesthetic information to the human central nervous system.” In: *The Journal of physiology* 487.1 (1995), pp. 243–251.

BIBLIOGRAPHY

- [40] David Feygin, Madeleine Keehner, and R Tendick. “Haptic guidance: Experimental evaluation of a haptic training method for a perceptual motor skill”. In: *Proceedings 10th Symposium on Haptic Interfaces for Virtual Environment and Teleoperator Systems. HAPTICS 2002*. IEEE. 2002, pp. 40–47.
- [41] Dario Floreano and Robert J Wood. “Science, technology and the future of small autonomous drones”. In: *Nature* 521.7553 (2015), p. 460.
- [42] Sean Follmer et al. “Jamming user interfaces: programmable particle stiffness and sensing for malleable and shape-changing devices”. In: *Proceedings of the 25th annual ACM symposium on User interface software and technology*. ACM. 2012, pp. 519–528.
- [43] Cinzia Freschi et al. “Technical review of the da Vinci surgical telemanipulator”. In: *The International Journal of Medical Robotics and Computer Assisted Surgery* 9.4 (2013), pp. 396–406.
- [44] Woon-Seng Gan et al. “Personalized HRTF Measurement and 3D Audio Rendering for AR/VR Headsets”. In: *Audio Engineering Society Convention 142*. Audio Engineering Society. 2017.
- [45] Yang Gao and Steve Chien. “Review on space robotics: Toward top-level science through space exploration”. In: *Science Robotics* 2.7 (2017).
- [46] William W Gaver. “The SonicFinder: An interface that uses auditory icons”. In: *Human–Computer Interaction* 4.1 (1989), pp. 67–94.
- [47] Tricia Gibo. “The\” Shared Control\” Committee [Society News]”. In: *IEEE Systems, Man, and Cybernetics Magazine* 2.2 (2016), pp. 51–55.
- [48] Michael Goldfarb, Brian E Lawson, and Amanda H Shultz. “Realizing the promise of robotic leg prostheses”. In: *Science translational medicine* 5.210 (2013), 210ps15–210ps15.
- [49] Albert Gollhofer, Wolfgang Taube, and Jens Bo Nielsen. *Routledge handbook of motor control and motor learning*. Routledge, 2013.
- [50] Michael A Goodrich, Alan C Schultz, et al. “Human–robot interaction: a survey”. In: *Foundations and Trends® in Human–Computer Interaction* 1.3 (2008), pp. 203–275.

- [51] MA Graule et al. “Perching and takeoff of a robotic insect on overhangs using switchable electrostatic adhesion”. In: *Science* 352.6288 (2016), pp. 978–982.
- [52] Abhishek Gupta and Marcia K O’Malley. “Design of a haptic arm exoskeleton for training and rehabilitation”. In: *IEEE/ASME Transactions on mechatronics* 11.3 (2006), pp. 280–289.
- [53] S Handel and An Listening. *An introduction to the perception of auditory events*. 1989.
- [54] Blake Hannaford. “Task-level testing of the JPL-OMV smart end effector”. In: (1987).
- [55] Aki Härmä et al. “Augmented reality audio for mobile and wearable appliances”. In: *Journal of the Audio Engineering Society* 52.6 (2004), pp. 618–639.
- [56] Vincent Hayward et al. “Haptic interfaces and devices”. In: *Sensor Review* 24.1 (2004), pp. 16–29.
- [57] Claudia Hendrix and Woodrow Barfield. “The sense of presence within auditory virtual environments”. In: *Presence: Teleoperators & Virtual Environments* 5.3 (1996), pp. 290–301.
- [58] Thomas Hermann and Helge Ritter. “Sound and meaning in auditory data display”. In: *Proceedings of the IEEE* 92.4 (2004), pp. 730–741.
- [59] Ronan Hinchet and Herbert Shea. “High Force Density Textile Electrostatic Clutch”. In: *Advanced Materials Technologies* 5.4 (2020), p. 1900895.
- [60] Ronan Hinchet et al. “Dextres: Wearable haptic feedback for grasping in vr via a thin form-factor electrostatic brake”. In: *Proceedings of the 31st Annual ACM Symposium on User Interface Software and Technology*. 2018, pp. 901–912.
- [61] M Hirano, M Sakurada, and S Furuya. “Overcoming the ceiling effects of experts’ motor expertise through active haptic training”. In: *Science Advances* 6.47 (2020), eabd2558.
- [62] Gerd Hirzinger et al. “The DLR-KUKA success story: robotics research improves industrial robots”. In: *IEEE Robotics & Automation Magazine* 12.3 (2005), pp. 16–23.

BIBLIOGRAPHY

- [63] Jie Huang, Noboru Ohnishi, and Noboru Sugie. "Building ears for robots: sound localization and separation". In: *Artificial Life and Robotics* 1.4 (1997), pp. 157–163.
- [64] Arthur S Iberall. *The use of lines of nonextension to improve mobility in full-pressure suits*. Tech. rep. RAND DEVELOPMENT CORP CLEVELAND OH, 1964.
- [65] Hyunki In et al. "Exo-glove: A wearable robot for the hand with a soft tendon routing system". In: *IEEE Robotics & Automation Magazine* 22.1 (2015), pp. 97–105.
- [66] Juan Manuel Jacinto-Villegas et al. "A novel wearable haptic controller for teleoperating robotic platforms". In: *IEEE Robotics and Automation Letters* 2.4 (2017), pp. 2072–2079.
- [67] Kenneth O Johnson. "The roles and functions of cutaneous mechanoreceptors". In: *Current opinion in neurobiology* 11.4 (2001), pp. 455–461.
- [68] Michelle J Johnson. "Recent trends in robot-assisted therapy environments to improve real-life functional performance after stroke". In: *Journal of Neuro-Engineering and Rehabilitation* 3.1 (2006), p. 29.
- [69] Michelle J Johnson et al. "Design and evaluation of Driver's SEAT: A car steering simulation environment for upper limb stroke therapy". In: *Robotica* 21.1 (2003), pp. 13–23.
- [70] Patrik N Juslin and Daniel Västfjäll. "Emotional responses to music: The need to consider underlying mechanisms". In: *Behavioral and brain sciences* 31.5 (2008), pp. 559–575.
- [71] Slava Kalyuga. *Instructional guidance: A cognitive load perspective*. IAP, 2015.
- [72] Soma Kawamura and Ryugo Kijima. "Effect of head mounted display latency on human stability during quiescent standing on one foot". In: *2016 IEEE Virtual Reality (VR)*. IEEE. 2016, pp. 199–200.
- [73] Fakheredine Keyrouz and Klaus Diepold. "Binaural source localization and spatial audio reproduction for telepresence applications". In: *PRESENCE: Teleoperators and Virtual Environments* 16.5 (2007), pp. 509–522.
- [74] Oussama Khatib et al. "Ocean one: A robotic avatar for oceanic discovery". In: *IEEE Robotics & Automation Magazine* 23.4 (2016), pp. 20–29.

- [75] Ali Kilic et al. "Improving electret properties of PP filaments with barium titanate". In: *Journal of Electrostatics* 71.1 (2013), pp. 41–47.
- [76] Munsang Kim et al. "Development of a humanoid robot CENTAUR-design, human interface, planning and control of its upper-body". In: *IEEE SMC'99 Conference Proceedings. 1999 IEEE International Conference on Systems, Man, and Cybernetics (Cat. No. 99CH37028)*. Vol. 4. IEEE. 1999, pp. 948–953.
- [77] Yong-Jae Kim et al. "A novel layer jamming mechanism with tunable stiffness capability for minimally invasive surgery". In: *IEEE Transactions on Robotics* 29.4 (2013), pp. 1031–1042.
- [78] Verena Klamroth-Marganska et al. "Three-dimensional, task-specific robot therapy of the arm after stroke: a multicentre, parallel-group randomised trial". In: *The Lancet Neurology* 13.2 (2014), pp. 159–166.
- [79] Nathan Koenig and Andrew Howard. "Design and use paradigms for gazebo, an open-source multi-robot simulator". In: *2004 IEEE/RSJ International Conference on Intelligent Robots and Systems (IROS)(IEEE Cat. No. 04CH37566)*. Vol. 3. IEEE. 2004, pp. 2149–2154.
- [80] Inwook Koo et al. "Development of A Meal Assistive Exoskeleton made of Soft Materials for polymyositis patients". In: *2014 IEEE/RSJ International Conference on Intelligent Robots and Systems*. IEEE. 2014, pp. 542–547.
- [81] Pontus Larsson, Daniel Vastfjall, and Mendel Kleiner. "Better presence and performance in virtual environments by improved binaural sound rendering". In: *Audio Engineering Society Conference: 22nd International Conference: Virtual, Synthetic, and Entertainment Audio*. Audio Engineering Society. 2002.
- [82] Pontus Larsson et al. "Auditory-induced presence in mixed reality environments and related technology". In: *The Engineering of Mixed Reality Systems*. Springer, 2010, pp. 143–163.
- [83] Corinna E Lathan and Michael Tracey. "The effects of operator spatial perception and sensory feedback on human-robot teleoperation performance". In: *Presence: Teleoperators & virtual environments* 11.4 (2002), pp. 368–377.

BIBLIOGRAPHY

- [84] Jaebong Lee and Seungmoon Choi. “Effects of haptic guidance and disturbance on motor learning: Potential advantage of haptic disturbance”. In: *2010 IEEE Haptics Symposium*. IEEE. 2010, pp. 335–342.
- [85] Jinwoo Lee et al. “Thermo-Haptic Materials and Devices for Wearable Virtual and Augmented Reality”. In: *Advanced Functional Materials* (2020), p. 2007376.
- [86] Huakang Li et al. “A spatial sound localization system for mobile robots”. In: *2007 IEEE Instrumentation & Measurement Technology Conference IMTC 2007*. IEEE. 2007, pp. 1–6.
- [87] Jeff Lieberman and Cynthia Breazeal. “TIKL: Development of a wearable vibro-tactile feedback suit for improved human motor learning”. In: *IEEE Transactions on Robotics* 23.5 (2007), pp. 919–926.
- [88] Su Liu et al. “Textile Electronics for VR/AR Applications”. In: *Advanced Functional Materials* (2020), p. 2007254.
- [89] Tapio Lokki and Matti Grohn. “Navigation with auditory cues in a virtual environment”. In: *IEEE MultiMedia* 12.2 (2005), pp. 80–86.
- [90] Jin Huat Low et al. “Hybrid tele-manipulation system using a sensorized 3-D-printed soft robotic gripper and a soft fabric-based haptic glove”. In: *IEEE Robotics and Automation Letters* 2.2 (2017), pp. 880–887.
- [91] Matteo Macchini et al. “Hand-worn Haptic Interface for Drone Teleoperation”. In: *2020 IEEE International Conference on Robotics and Automation (ICRA)*. IEEE. 2020, pp. 10212–10218.
- [92] Carmel Majidi. “Soft robotics: a perspective—current trends and prospects for the future”. In: *Soft Robotics* 1.1 (2014), pp. 5–11.
- [93] Mariangela Manti, Vito Cacucciolo, and Matteo Cianchetti. “Stiffening in soft robotics: A review of the state of the art”. In: *IEEE Robotics & Automation Magazine* 23.3 (2016), pp. 93–106.
- [94] Laura Marchal-Crespo, Nicole Rappo, and Robert Riener. “The effectiveness of robotic training depends on motor task characteristics”. In: *Experimental brain research* 235.12 (2017), pp. 3799–3816.

- [95] Laura Marchal-Crespo and David J Reinkensmeyer. “Review of control strategies for robotic movement training after neurologic injury”. In: *Journal of neuroengineering and rehabilitation* 6.1 (2009), pp. 1–15.
- [96] Laura Marchal-Crespo et al. “Effect of error augmentation on brain activation and motor learning of a complex locomotor task”. In: *Frontiers in neuroscience* 11 (2017), p. 526.
- [97] Laura Marchal-Crespo et al. “Optimizing learning of a locomotor task: amplifying errors as needed”. In: *2014 36th Annual International Conference of the IEEE Engineering in Medicine and Biology Society*. IEEE. 2014, pp. 5304–5307.
- [98] Laura Marchal-Crespo et al. “The effect of haptic guidance and visual feedback on learning a complex tennis task”. In: *Experimental brain research* 231.3 (2013), pp. 277–291.
- [99] Laura Marchal-Crespo et al. “The effect of haptic guidance, aging, and initial skill level on motor learning of a steering task”. In: *Experimental brain research* 201.2 (2010), pp. 209–220.
- [100] Henrique Martins and Rodrigo Ventura. “Immersive 3-d teleoperation of a search and rescue robot using a head-mounted display”. In: *2009 IEEE conference on emerging technologies & factory automation*. IEEE. 2009, pp. 1–8.
- [101] M.J. Massimino and T.B. Sheridan. “Teleoperator performance with varying force and visual feedback”. In: *Human Factors: The Journal of the Human Factors and Ergonomics Society* 36.1 (1994), pp. 145–157.
- [102] Matjaž Mihelj and Janez Podobnik. *Haptics for virtual reality and teleoperation*. Vol. 67. Springer Science & Business Media, 2012.
- [103] Dwight P Miller. “Evaluation of vision systems for teleoperated land vehicles”. In: *IEEE Control Systems Magazine* 8.3 (1988), pp. 37–41.
- [104] Marie-Hélène Milot et al. “Comparison of error-amplification and haptic-guidance training techniques for learning of a timing-based motor task by healthy individuals”. In: *Experimental brain research* 201.2 (2010), pp. 119–131.
- [105] GJ Monkman. “Dielectrophoretic enhancement of electrorheological robotic actuators”. In: *Mechatronics* 3.3 (1993), pp. 305–313.

BIBLIOGRAPHY

- [106] GJ Monkman, PM Taylor, and GJ Farnworth. "Principles of electroadhesion in clothing robotics". In: *International Journal of Clothing Science and Technology* 1.3 (1989), pp. 14–20.
- [107] Louise Moody, Chris Baber, Theodoros N Arvanitis, et al. "Objective surgical performance evaluation based on haptic feedback". In: *Studies in health technology and informatics* (2002), pp. 304–310.
- [108] Mark Mulder, David A Abbink, and Erwin R Boer. "Sharing control with haptics: Seamless driver support from manual to automatic control". In: *Human factors* 54.5 (2012), pp. 786–798.
- [109] Robin R Murphy et al. "Search and rescue robotics". In: *Springer handbook of robotics* (2008), pp. 1151–1173.
- [110] Anne M Murray, Roberta L Klatzky, and Pradeep K Khosla. "Psychophysical characterization and testbed validation of a wearable vibrotactile glove for telemanipulation". In: *Presence: Teleoperators & Virtual Environments* 12.2 (2003), pp. 156–182.
- [111] Tobias Nef, Matjaz Mihelj, and Robert Riener. "ARMin: a robot for patient-cooperative arm therapy". In: *Medical & biological engineering & computing* 45.9 (2007), pp. 887–900.
- [112] Günter Niemeyer et al. "Telerobotics". In: *Springer handbook of robotics*. Springer, 2016, pp. 1085–1108.
- [113] Allison M Okamura. "Methods for haptic feedback in teleoperated robot-assisted surgery". In: *Industrial Robot: An International Journal* (2004).
- [114] Alena Otto et al. "Optimization approaches for civil applications of unmanned aerial vehicles (UAVs) or aerial drones: A survey". In: *Networks* 72.4 (2018), pp. 411–458.
- [115] Claudio Pacchierotti et al. "Cutaneous haptic feedback to ensure the stability of robotic teleoperation systems". In: *The International Journal of Robotics Research* 34.14 (2015), pp. 1773–1787.
- [116] Claudio Pacchierotti et al. "Wearable haptic systems for the fingertip and the hand: taxonomy, review, and perspectives". In: *IEEE transactions on haptics* 10.4 (2017), pp. 580–600.

- [117] Rebecca Pailles-Friedman. “Electronics and Fabrics: The Development of Garment-Based Wearables”. In: *Advanced Materials Technologies* (2018), p. 1700307.
- [118] Daniel S Pamungkas and Koren Ward. “Tele-operation of a robot arm with electro tactile feedback”. In: *2013 IEEE/ASME International Conference on Advanced Intelligent Mechatronics*. IEEE. 2013, pp. 704–709.
- [119] Fausto A Panizzolo et al. “A biologically-inspired multi-joint soft exosuit that can reduce the energy cost of loaded walking”. In: *Journal of neuroengineering and rehabilitation* 13.1 (2016), pp. 1–14.
- [120] Won-Hyeong Park et al. “Soft haptic actuator based on knitted PVC gel fabric”. In: *IEEE Transactions on Industrial Electronics* 67.1 (2019), pp. 677–685.
- [121] James L Patton et al. “Evaluation of robotic training forces that either enhance or reduce error in chronic hemiparetic stroke survivors”. In: *Experimental brain research* 168.3 (2006), pp. 368–383.
- [122] Joshua M Peschel and Robin R Murphy. “Human Interfaces in Micro and Small Unmanned Aerial Systems”. In: *Handbook of Unmanned Aerial Vehicles*. Springer, 2015, pp. 2389–2403.
- [123] Rebecca M Pierce, Elizabeth A Fedalei, and Katherine J Kuchenbecker. “A wearable device for controlling a robot gripper with fingertip contact, pressure, vibrotactile, and grip force feedback”. In: *2014 IEEE Haptics Symposium (HAPTICS)*. IEEE. 2014, pp. 19–25.
- [124] KnW Plessner. “Ageing of the dielectric properties of barium titanate ceramics”. In: *Proceedings of the Physical Society. Section B* 69.12 (1956), p. 1261.
- [125] Panagiotis Polygerinos et al. “Soft robotic glove for combined assistance and at-home rehabilitation”. In: *Robotics and Autonomous Systems* 73 (2015), pp. 135–143.
- [126] José L Pons. *Wearable robots: biomechatronic exoskeletons*. John Wiley & Sons, 2008.
- [127] Dane Powell and Marcia K O’Malley. “The task-dependent efficacy of shared-control haptic guidance paradigms”. In: *IEEE transactions on haptics* 5.3 (2012), pp. 208–219.

BIBLIOGRAPHY

- [128] Harsha Prahlad et al. “Electroadhesive robots—wall climbing robots enabled by a novel, robust, and electrically controllable adhesion technology”. In: *Robotics and Automation, 2008. ICRA 2008. IEEE International Conference on*. IEEE. 2008, pp. 3028–3033.
- [129] Domenico Prattichizzo et al. “Towards wearability in fingertip haptics: a 3-dof wearable device for cutaneous force feedback”. In: *IEEE Transactions on Haptics* 6.4 (2013), pp. 506–516.
- [130] Gorur Govinda Raju. *Dielectrics in electric fields*. CRC press, 2016.
- [131] Vivek Ramachandran, Jun Shintake, and Dario Floreano. “All-Fabric Wearable Electrode Adhesive Clutch”. In: *Advanced Materials Technologies* 4.2 (2019), p. 1800313.
- [132] Vivek Ramachandran et al. “Smart textiles that teach: Fabric-based haptic device improves the rate of motor learning”. In: *Advanced Intelligent Systems (accepted)* tbd.tbd (2021), tbd.
- [133] Matthias Rath and Davide Rocchesso. “Continuous sonic feedback from a rolling ball”. In: *IEEE MultiMedia* 12.2 (2005), pp. 60–69.
- [134] Georg Rauter et al. “When a robot teaches humans: Automated feedback selection accelerates motor learning”. In: *Science Robotics* 4.27 (2019).
- [135] Joao Rebelo et al. “Bilateral robot teleoperation: A wearable arm exoskeleton featuring an intuitive user interface”. In: *IEEE Robotics & Automation Magazine* 21.4 (2014), pp. 62–69.
- [136] David J Reinkensmeyer, Jeremy L Emken, and Steven C Cramer. “Robotics, motor learning, and neurologic recovery”. In: *Annual review of biomedical engineering* 6 (2004).
- [137] Steven Rich et al. “Liquid Metal-Conductive Thermoplastic Elastomer Integration for Low-Voltage Stiffness Tuning”. In: *Advanced Materials Technologies* 2.12 (2017).
- [138] Shepard Roberts. “Dielectric and piezoelectric properties of barium titanate”. In: *Physical Review* 71.12 (1947), p. 890.

-
- [139] Carine Rognon et al. “FlyJacket: An Upper Body Soft Exoskeleton for Immersive Drone Control”. In: *IEEE Robotics and Automation Letters* 3.3 (2018), pp. 2362–2369.
 - [140] Carine Rognon et al. “Haptic feedback perception and learning with cable-driven guidance in exosuit teleoperation of a simulated drone”. In: *IEEE Transactions on Haptics* 12.3 (2019), pp. 375–385.
 - [141] Carine Rognon et al. “Haptic Guidance with a Soft Exoskeleton Reduces Error in Drone Teleoperation”. In: *International Conference on Human Haptic Sensing and Touch Enabled Computer Applications*. Springer. 2018, pp. 404–415.
 - [142] Carine Rognon et al. “Soft haptic device to render the sensation of flying like a drone”. In: *IEEE Robotics and Automation Letters* 4.3 (2019), pp. 2524–2531.
 - [143] Giulio Rosati et al. “On the role of auditory feedback in robot-assisted movement training after stroke: review of the literature”. In: *Computational intelligence and neuroscience* 2013 (2013).
 - [144] Louis B Rosenberg. “Virtual fixtures: Perceptual tools for telerobotic manipulation”. In: *Virtual Reality Annual International Symposium, 1993., 1993 IEEE*. IEEE. 1993, pp. 76–82.
 - [145] Mordechai Rosner and Michael Belkin. “Video display units and visual function”. In: *Survey of ophthalmology* 33.6 (1989), pp. 515–522.
 - [146] Selma Šabanović. “Robots in society, society in robots”. In: *International Journal of Social Robotics* 2.4 (2010), pp. 439–450.
 - [147] Alan W Salmoni, Richard A Schmidt, and Charles B Walter. “Knowledge of results and motor learning: a review and critical reappraisal.” In: *Psychological bulletin* 95.3 (1984), p. 355.
 - [148] Beatriz Sousa Santos et al. “Head-mounted display versus desktop for 3D navigation in virtual reality: a user study”. In: *Multimedia tools and applications* 41.1 (2009), p. 161.
 - [149] Fabian Schilling et al. “Learning vision-based flight in drone swarms by imitation”. In: *IEEE Robotics and Automation Letters* 4.4 (2019), pp. 4523–4530.

BIBLIOGRAPHY

- [150] Richard Schmidt and Tim Lee. *Motor Learning and performance, 5E with web study guide: from principles to application*. Human Kinetics, 2013.
- [151] GA Schneider and V Heyer. “Influence of the electric field on Vickers indentation crack growth in BaTiO₃”. In: *Journal of the European Ceramic Society* 19.6-7 (1999), pp. 1299–1306.
- [152] Bryan E Schubert and Dario Floreano. “Variable stiffness material based on rigid low-melting-point-alloy microstructures embedded in soft poly (dimethylsiloxane)(PDMS)”. In: *Rsc Advances* 3.46 (2013), pp. 24671–24679.
- [153] F Scribano, M Burns, and ER Barron. *Design, Development and Fabrication of a Personnel Armor Load Profile Analyzer*. Tech. rep. IIT RESEARCH INST CHICAGO IL, 1970.
- [154] Junwon Seo, Luis Duque, and Jim Wacker. “Drone-enabled bridge inspection methodology and application”. In: *Automation in Construction* 94 (2018), pp. 112–126.
- [155] Wanliang Shan, Tong Lu, and Carmel Majidi. “Soft-matter composites with electrically tunable elastic rigidity”. In: *Smart Materials and Structures* 22.8 (2013), p. 085005.
- [156] Sarah Sharples et al. “Virtual reality induced symptoms and effects (VRISE): Comparison of head mounted display (HMD), desktop and projection display systems”. In: *Displays* 29.2 (2008), pp. 58–69.
- [157] Thomas B Sheridan. “Defining our terms”. In: *Presence: Teleoperators & Virtual Environments* 1.2 (1992), pp. 272–274.
- [158] Jun Shintake et al. “Versatile soft grippers with intrinsic electroadhesion based on multifunctional polymer actuators”. In: *Advanced Materials* 28.2 (2016), pp. 231–238.
- [159] Roland Sigrist et al. “Augmented visual, auditory, haptic, and multimodal feedback in motor learning: a review”. In: *Psychonomic bulletin & review* 20.1 (2013), pp. 21–53.
- [160] Cole S Simpson, Allison M Okamura, and Elliot W Hawkes. “Exomuscle: An inflatable device for shoulder abduction support”. In: *2017 IEEE International Conference on Robotics and Automation (ICRA)*. IEEE. 2017, pp. 6651–6657.

- [161] Harshal Arun Sonar and Jamie Paik. “Soft pneumatic actuator skin with piezo-electric sensors for vibrotactile feedback”. In: *Frontiers in Robotics and AI* 2 (2016), p. 38.
- [162] Hong Jun Song, Kirsty Beilharz, and Densil Cabrera. “Evaluation of spatial presentation in sonification for identifying concurrent audio streams”. In: Georgia Institute of Technology. 2007.
- [163] Hao Sun et al. “Microphone array based auditory localization for rescue robot”. In: *2011 Chinese Control and Decision Conference (CCDC)*. IEEE. 2011, pp. 606–609.
- [164] Ana Tajadura-Jiménez et al. “Principles for designing body-centered auditory feedback.” In: (2018).
- [165] Yutaka Tanaka, Hisayuki Yamauchi, and Kenichi Amemiya. “Wearable haptic display for immersive virtual environment”. In: *Proceedings of the jfps international symposium on fluid power*. Vol. 2002. 5-2. The Japan Fluid Power System Society. 2002, pp. 309–314.
- [166] A Tonazzini et al. “Variable stiffness strip with strain sensing for wearable robotics”. In: *2018 IEEE International Conference on Soft Robotics (RoboSoft)*. IEEE. 2018, pp. 485–490.
- [167] Alice Tonazzini et al. “Variable Stiffness Fiber with Self-Healing Capability”. In: *Advanced Materials* 28.46 (2016), pp. 10142–10148.
- [168] Enis Tuncer et al. “Enhancement of dielectric strength in nanocomposites”. In: *Nanotechnology* 18.32 (2007), p. 325704.
- [169] Antonio Vasilijevic, Kristian Jambrosic, and Zoran Vukic. “Teleoperated path following and trajectory tracking of unmanned vehicles using spatial auditory guidance system”. In: *Applied acoustics* 129 (2018), pp. 72–85.
- [170] Julie M Walker and Allison M Okamura. “Continuous Closed-Loop 4-Degree-of-Freedom Holdable Haptic Guidance”. In: *IEEE Robotics and Automation Letters* 5.4 (2020), pp. 6853–6860.
- [171] Albert Wang et al. “The HERMES humanoid system: A platform for full-body teleoperation with balance feedback”. In: *2015 IEEE-RAS 15th International Conference on Humanoid Robots (Humanoids)*. IEEE. 2015, pp. 730–737.

BIBLIOGRAPHY

- [172] Rainer Waser, Tudor Baiatu, and Karl-Heinz Härdtl. “dc Electrical Degradation of Perovskite-Type Titanates: I, Ceramics”. In: *Journal of the american ceramic society* 73.6 (1990), pp. 1645–1653.
- [173] Michael Wehner et al. “A lightweight soft exosuit for gait assistance”. In: *Robotics and Automation (ICRA), 2013 IEEE International Conference on*. IEEE. 2013, pp. 3362–3369.
- [174] Christopher D Wickens. “Multiple resources and mental workload”. In: *Human factors* 50.3 (2008), pp. 449–455.
- [175] Camille K Williams, Luc Tremblay, and Heather Carnahan. “It pays to go off-track: practicing with error-augmenting haptic feedback facilitates learning of a curve-tracing task”. In: *Frontiers in psychology* 7 (2016), p. 2010.
- [176] Daniel M Wolpert, Jörn Diedrichsen, and J Randall Flanagan. “Principles of sensorimotor learning”. In: *Nature Reviews Neuroscience* 12.12 (2011), p. 739.
- [177] Weicheng Wu and Heather Culbertson. “Wearable haptic pneumatic device for creating the illusion of lateral motion on the arm”. In: *2019 IEEE World Haptics Conference (WHC)*. IEEE. 2019, pp. 193–198.
- [178] Gabriele Wulf et al. “Frequent external focus feedback enhances motor learning”. In: *Frontiers in psychology* 1 (2010), p. 190.
- [179] Jessica Yin et al. “Wearable Soft Technologies for Haptic Sensing and Feedback”. In: *Advanced Functional Materials* (2020), p. 2007428.
- [180] Haixia Zhao et al. “Data sonification for users with visual impairment: a case study with georeferenced data”. In: *ACM Transactions on Computer-Human Interaction (TOCHI)* 15.1 (2008), pp. 1–28.
- [181] Mengjia Zhu et al. “Pneusleeve: In-fabric multimodal actuation and sensing in a soft, compact, and expressive haptic sleeve”. In: *Proceedings of the 2020 CHI Conference on Human Factors in Computing Systems*. 2020, pp. 1–12.
- [182] Eberhard Zwicker and Hugo Fastl. *Psychoacoustics: Facts and models*. Vol. 22. Springer Science & Business Media, 2013.

Vivek Ramachandran

PhD Candidate in Robotics, Controls, and Intelligent Systems • MS in Mechanical Engineering

Born: 13 Nov '92 • Address: MED 1 1020, EPFL, 1015 Lausanne, CH • Nationality: Indian

Email: vivekram92@gmail.com; vivek.ramachandran@epfl.ch | Phone: +41 78 667 59 98

Website: <https://www.vivekramachandran.weebly.com>

Education

Laboratory of Intelligent Systems at EPFL

PhD Student (Robotics, Controls, and Intelligent Systems)

[Lausanne, CH](#)

Aug '16 – July '21

Soft Machines Laboratory at Carnegie Mellon University (CMU)

Master's student (Mechanical Engineering), Research Assistant

[Pittsburgh, USA](#)

Aug '14 – May '16

National Institute of Technology Calicut

Bachelor's student (Mechanical Engineering)

[Kozhikode, IN](#)

Aug '10 – May '14

Research

Laboratory of Intelligent Systems at EPFL

[Lausanne, CH](#)

- PhD thesis: Wearable haptic interfaces for human-robot interaction
- Focus: textile-based device prototyping; user-centred design; human subject motor-learning studies

Soft Machines Laboratory at CMU

[Pittsburgh, USA](#)

- MS project: Soft electronics that harness the mechanical instabilities of flexible magnetic materials
- Focus: Mechanics of materials; rapid prototyping; materials science of soft robotic materials

Teaching

Swiss Federal Institute of Technology (EPFL)

[Lausanne, CH](#)

- Teaching Assistant: Basics of mobile robots (Fall '16); Robotics practicals (Spring '17, '18, '19, '20); Introduction to structural mechanics (Spring '19, '20); Legged robots (Fall '19)
- Student supervisor: 12 Master's semester projects, 2 Master's theses, 2 Bachelor's capstone projects
- Established new MAKE interdisciplinary course "Assistive Technologies Challenges" (Spring '21): Curriculum development; Ethical approval (HREC), Academic/Financial support secured from EPFL faculties (STI, SV, IBI)
- Co-facilitated "Make It Awkward" workshops with Siara Isaac (CAPE, EPFL) online and in-person

Carnegie Mellon University (CMU)

[Pittsburgh, USA](#)

- Teaching Assistant: Soft Matter Engineering (Spring '16); Biomechanics and Motor Control (Fall '15)

Volunteering

Swiss Federal Institute of Technology (EPFL)

PhD Student Representative, Doctoral School

Lausanne, CH

May '17 – Sep '19

Hackahealth

Association member

Lausanne, CH

Sep '19 – Present

National Centre for Competence in Research (NCCR) Robotics

Member, Equal Opportunities Committee

Lausanne, CH

May '20 – Present

Carnegie Mellon University (CMU)

Graduate Student Representative, Graduate Student Assembly

Pittsburgh, USA

Feb '15 – May '16

Skills

Software: MATLAB, Python (Jupyter), LaTeX, Inkscape, Adobe Photoshop, SolidWorks

Hardware: CO2 laser cutting, 3D printing, Instron Tensile Tester, Sewing, Thin-film fabrication

Languages: English (native), French (intermediate), German (basic)

Publications

V. Ramachandran, M. D. Bartlett, J. Wissman, and C. Majidi, "Elastic instabilities of a ferroelastomer beam for soft reconfigurable electronics" in *Extreme Mechanics Letters* (2016)

M. Tavakoli, R. Rocha, L. Osorio, A. de A. M. Almeida, **V. Ramachandran**, A. Tabatabai, T. Lu, and C. Majidi, "Carbon doped PDMS: Conductance stability over time and implications for additive manufacturing of stretchable electronics" in *Journal of Micromechanics and Microengineering* (2017)

V. Ramachandran and C. Majidi, "Deformation of Microchannels Embedded in an Elastic Medium" in *Journal of Applied Mechanics* (2018)

V. Ramachandran, J. Shintake, and D. Floreano, "All-Fabric Wearable Electroadhesive Clutch" in *Advanced Materials Technologies* (2018)

A. Tonazzini, J. Shintake, C. Rognon, **V. Ramachandran**, S. Mintchev, and D. Floreano, "Variable stiffness strip with strain sensing for wearable robotics" in *IEEE International Conference on Soft Robotics (RoboSoft)* (2018)

C. Rognon, **V. Ramachandran**, A. R. Wu, A. J. Ijspeert, and D. Floreano, "Haptic feedback perception and learning with cable-driven guidance in exosuit teleoperation of a simulated drone" in *IEEE Transactions on Haptics* (2019)

E. Piskarev, J. Shintake, **V. Ramachandran**, N. Baugh, M. D. Dickey, and D. Floreano, "Lighter and Stronger: Cofabricated Electrodes and Variable Stiffness Elements in Dielectric Actuators" in *Advanced Intelligent Systems* (2020)

V. Ramachandran, F. Schilling, A. R. Wu, and D. Floreano, "Smart textiles that teach: Fabric-based haptic device improves the rate of motor learning" in *Advanced Intelligent Systems* (in press, 2021)

V. Ramachandran, M. Macchini, and D. Floreano, "Arm-wrist haptic sleeve for drone teleoperation" in *IEEE Robotics and Automation Letters* (under review, 2021)